

AD-A144 043

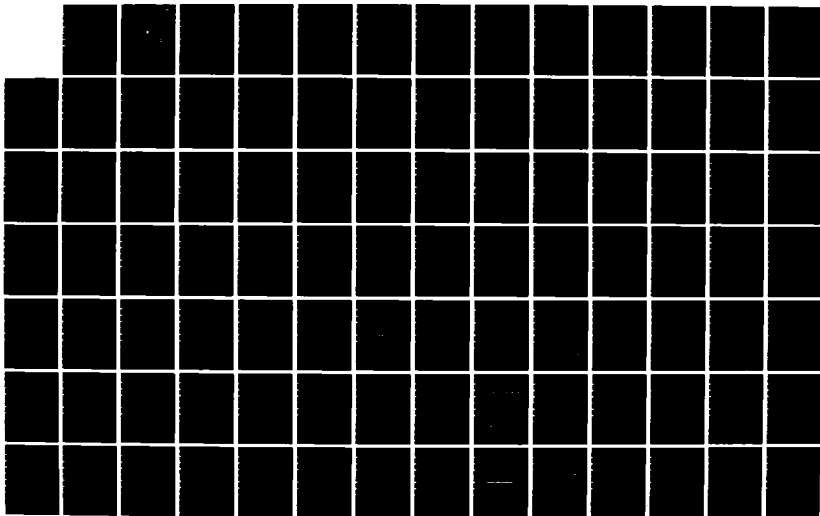
OPTIMAL DIGITAL CONTROL OF A BANK-TO-TURN MISSILE(U)  
NAVAL POSTGRADUATE SCHOOL MONTEREY CA C A VELLOSO  
MAR '84

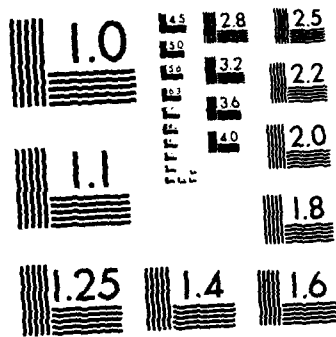
1/2

UNCLASSIFIED

F/G 1/3

NL





MICROCOPY RESOLUTION TEST CHART  
NATIONAL BUREAU OF STANDARDS-1963-A

2

AD-A144 043

# NAVAL POSTGRADUATE SCHOOL

Monterey, California



DTIC  
SELECTED  
AUG 7 1984  
S D

## THESIS

DTIC FILE COPY

OPTIMAL DIGITAL CONTROL  
OF  
A BANK-TO-TURN MISSILE

by

Carlos A. L. Velloso  
March 1984

Thesis Advisor:

Daniel J. Collins

Approved for public release; distribution unlimited

84 08 06 03T

REPORT DOCUMENTATION PAGE		READ INSTRUCTIONS BEFORE COMPLETING FORM
1. REPORT NUMBER	2. GOVT ACCESSION NO. AD-A144643	3. RECIPIENT'S CATALOG NUMBER
4. TITLE (and Subtitle) Optimal Digital Control of a Bank-to-Turn Missile		5. TYPE OF REPORT & PERIOD COVERED Master Thesis March 1984
		6. PERFORMING ORG. REPORT NUMBER
7. AUTHOR(s) Carlos Augusto Leal Velloso		8. CONTRACT OR GRANT NUMBER(s)
9. PERFORMING ORGANIZATION NAME AND ADDRESS Naval Postgraduate School Monterey, California 93940		10. PROGRAM ELEMENT, PROJECT, TASK AREA & WORK UNIT NUMBERS
11. CONTROLLING OFFICE NAME AND ADDRESS Naval Postgraduate School Monterey, California 93940		12. REPORT DATE March 1984
		13. NUMBER OF PAGES 154
14. MONITORING AGENCY NAME & ADDRESS (if different from Controlling Office)		15. SECURITY CLASS. (of this report) Unclassified
		15a. DECLASSIFICATION/DOWNGRADING SCHEDULE
16. DISTRIBUTION STATEMENT (of this Report)  Approved for public release; distribution unlimited		
17. DISTRIBUTION STATEMENT (of the abstract entered in Block 20, if different from Report)		
18. SUPPLEMENTARY NOTES		
19. KEY WORDS (Continue on reverse side if necessary and identify by block number) Guidance and Control Optimal Digital Control Terminal Guidance Law Bank-to-Turn Missile		
20. ABSTRACT (Continue on reverse side if necessary and identify by block number) This work addresses the application of digital optimum control theory to a bank-to-turn missile. A optimal guidance law has been developed and tested in several scenarios using a 2-D model. Effects of sample rate, pitch angle, gravity and approximations for small and large roll excursions are discussed.		

Approved for public release; distribution unlimited.

Optimal Digital Control  
of  
a Bank-to-Turn Missile

by

Carlos A.L. Velloso  
Major, Brazilian Air Force  
B.S., Instituto Tecnológico de Aeronautica, Brasil, 1976

Submitted in partial fulfillment of the  
requirements for the degree of

MASTER OF SCIENCE IN ENGINEERING SCIENCE

from the

NAVAL POSTGRADUATE SCHOOL  
March 1984

Author: \_\_\_\_\_

Approved by: \_\_\_\_\_

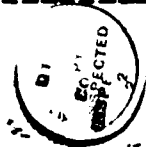
Thesis Advisor

Second Reader

Chairman, Department of Aeronautics

Dean of Science and Engineering

Accession For	
NTIS GRA&I	<input checked="" type="checkbox"/>
DTIC TAB	<input type="checkbox"/>
Unannounced	<input type="checkbox"/>
Justification	
By _____	
Distribution/	
Availability Codes	
Dist	Avail and/or Special
A1	



## ABSTRACT

This work addresses the application of digital optimum control theory to a bank-to-turn missile.

A optimal guidance law has been developed and tested in several scenarios, using a 2-D model. Effects of sample rate, pitch angle, gravity and approximations for small and large roll excursions are discussed.

## TABLE OF CONTENTS

I.	INTRODUCTION . . . . .	11
II.	MODEL OF THE SYSTEM . . . . .	13
	A. INTRODUCTION . . . . .	13
	B. ASSUMPTIONS . . . . .	13
	C. THE CONTINUOUS MODEL . . . . .	13
	D. THE DISCRETE MODEL . . . . .	17
	1. Introduction . . . . .	17
	2. Calculation of the Matrices $A(k)$ , $B(k)$ and $E(k)$ . . . . .	19
III.	THE OPTIMAL CONTROLLER . . . . .	29
	A. DERIVATION OF THE OPTIMAL CONTROLLER . . . . .	29
	B. EXTENSION OF THE MODEL FOR LARGE ROLL ANGLES . . . . .	36
	1. Effects on the Miss Distance of the Extension of the Model . . . . .	42
	C. SIMULATION . . . . .	44
	D. COMMENTS AND CONCLUSIONS . . . . .	45
	1. Results . . . . .	45
	2. Comments . . . . .	47
IV.	ANALYSIS OF GAINS, SAMPLE RATE AND PITCH ANGLE . . . . .	82
	A. ANALYSIS OF THE GAINS . . . . .	82
	B. EFFECT OF THE SAMPLE RATE . . . . .	84
	C. EFFECT OF THE INITIAL PITCH ANGLE . . . . .	85
	D. EFFECT OF TIME TO INTERCEPT . . . . .	88
V.	FINAL CONCLUSIONS AND COMMENTS . . . . .	130

APPENDIX A: PORTRAN PROGRAM . . . . .	132
LIST OF REFERENCES . . . . .	153
INITIAL DISTRIBUTION LIST . . . . .	154

LIST OF TABLES

I.	Results From Tests . . . . .	81
II.	Results from Biased Control . . . . .	96
III.	Results for Different Sample Periods . . . . .	105
IV.	Results Using Pitch Angle . . . . .	120
V.	Effect of Time to Intercept . . . . .	129

## LIST OF FIGURES

2.1	Reference Frames . . . . .	27
2.2	Reference Frames . . . . .	28
3.1	Representation of the System . . . . .	51
3.2	Variation of Commands with Initial Roll Angle . . . . .	52
3.3	Variation of Roll Angle - Small Angles . . . . .	53
3.4	Variation of Roll Angle - Large Angles . . . . .	54
3.5	Ideal Initial Roll Angles . . . . .	55
3.6	Scenarios for Simulation . . . . .	56
3.7	Commanded Acceleration- Case 0 . . . . .	57
3.8	Commanded Roll Rate- Case 0 . . . . .	58
3.9	Miss Distance in Z Direction- Case 0 . . . . .	59
3.10	Miss Distance in Y Direction- Case 0 . . . . .	60
3.11	Roll Angle- Case 0 . . . . .	61
3.12	Commanded Acceleration- Case 1 . . . . .	62
3.13	Commanded Roll Rate- Case 1 . . . . .	63
3.14	Miss Distance- Case 1 . . . . .	64
3.15	Roll Angle- Case 1 . . . . .	65
3.16	Commanded Acceleration- Case 2 . . . . .	66
3.17	Commanded Roll Rate- Case 2 . . . . .	67
3.18	Miss Distance- Case 2 . . . . .	68
3.19	Roll Angle- Case 2 . . . . .	69
3.20	Commanded Acceleration- Case 3 . . . . .	70
3.21	Commanded Roll Rate- Case 3 . . . . .	71
3.22	Miss Distance- Case 3 . . . . .	72
3.23	Roll Angle- Case 3 . . . . .	73
3.24	Commanded Acceleration- Case 4 . . . . .	74
3.25	Commanded Roll Rate- Case 4 . . . . .	75

3.26	Miss Distance- Case 4 . . . . .	76
3.27	Roll Angle- Case 4 . . . . .	77
3.28	Corrected Model . . . . .	78
3.29	Boundary of the Commanded Acceleration . . . . .	79
3.30	Corrections on the Roll Angle . . . . .	80
4.1	Gains affecting the commanded acceleration . . . . .	90
4.2	Gains Affecting the Commanded Roll Rate . . . . .	91
4.3	Commanded Acceleration-Case 5 . . . . .	92
4.4	Commanded Roll Rate-Case 5 . . . . .	93
4.5	Miss Distance-Case 5 . . . . .	94
4.6	Roll Angle-Case 5 . . . . .	95
4.7	Commanded Acceleration-Case 6 . . . . .	97
4.8	Commanded Roll Rate-Case 6 . . . . .	98
4.9	Miss Distance-Case 6 . . . . .	99
4.10	Roll Angle-Case 6 . . . . .	100
4.11	Commanded Acceleration-Case 7 . . . . .	101
4.12	Commanded Roll Rate-Case 7 . . . . .	102
4.13	Miss distance-Case 7 . . . . .	103
4.14	Roll Angle-Case 7 . . . . .	104
4.15	Effect of Initial Pitch Angle . . . . .	106
4.16	Scenarios With Pitch Angle . . . . .	107
4.17	Commanded Acceleration-Case 8 . . . . .	108
4.18	Commanded Roll Rate-Case 8 . . . . .	109
4.19	Miss Distance-Case 8 . . . . .	110
4.20	Roll Angle-Case 8 . . . . .	111
4.21	Commanded Acceleration-Case 9 . . . . .	112
4.22	Commanded Roll Rate-Case 9 . . . . .	113
4.23	Miss Distance-Case 9 . . . . .	114
4.24	Roll Angle-Case 9 . . . . .	115
4.25	Commanded Acceleration-Case 10 . . . . .	116
4.26	Commanded Roll Rate-Case 10 . . . . .	117
4.27	Miss Distance-Case 10 . . . . .	118
4.28	Roll Angle-Case 10 . . . . .	119

4.29	Commanded Acceleration-Case 11 . . . . .	121
4.30	Commanded Roll Rate-Case 11 . . . . .	122
4.31	Miss Distance-Case 11 . . . . .	123
4.32	Roll Angle-Case 11 . . . . .	124
4.33	Commanded Acceleration-Case 12 . . . . .	125
4.34	Commanded Roll Rate-Case 12 . . . . .	126
4.35	Miss Distance-Case 12 . . . . .	127
4.36	Roll Angle-Case 12 . . . . .	128

## ACKNOWLEDGEMENT

To my wife, Rosy, for her constant encouragment, support and love.

To my children, Ana, Antonio, Chica, Joao and Rita, for yours smiles and love.

Without you this work would be impossible.

## I. INTRODUCTION

Because of threats from highly maneuverable high performance aircrafts and the need for increase standoff ranges, major improvements are needed in guidance and control capabilities of missiles.

The high maneuverability of targets, has led to defense missiles capable of develop higher lift accelerations and to more complex control laws, able to improve performance over well know laws as proportional navegation.

In order to accomplish these new requirements with large standoff ranges, propulsion systems using airbreathing engines has been studied and developed in recent years.

The advent of airbreathing engines leads natural to a consideration of bank-to-turn missiles in order to minimize the angle of attack of the inlets.

The necessity of more complex control laws, leads in a general way, to the application of modern control and estimation theory, since more complete informations of the states of missile and target are necessary than those states informed by sensors commonly in use in missiles today. This leads to the use of a airborne computer.

The present work adresses the design and evaluation of a optimal digital control for application to terminal guidance in a bank-to-turn missiles.

One continuous two dimensional model was adopted, in the following form:

$$\dot{X}(t) = A(t) x(t) + B(t) u(t) + E g \quad (1.1)$$

where the effect of gravity appears explicitly in the third term on the right hand side of expression 1.1.

After the development of a equivalent discrete model, the optimal control problem has been solved, using a modified Ricatti equation due to the existence of the third term representing to the gravity effect.

Next, several analysis has been made in order to check the effects of small and large roll excursions, the effect of the sample rate on the system, and the effect of the initial pitch angle, in order to check the validity of such two dimensional model, when applied in some scenarios of interest.

## II. MODEL OF THE SYSTEM

### A. INTRODUCTION

In the present work the problem of terminal guidance for long range, bank-to-turn missiles with ramjet engines, using a digitalized system has been investigated.

The model developed in reference 1 is used as the base for this work. After the digitalization of that model, an optimal control law was developed.

### B. ASSUMPTIONS

Keeping the same assumptions as in ref.1, one has:

The missile is limited to  $-2g$ 's and  $+15g$ 's of commanded acceleration in the pitch plane, with zero lag. Also its yaw auto pilot has zero lag, yaw regulator maintains zero sideslip.

Missile thrust exactly cancels drag.

The angle of attack is assumed to be very small, which leads to the commanded acceleration acting normal to the velocity vector.

The missile will not have to roll through a large angle. (Further considerations will give to this at the end of the derivation of the control law).

### C. THE CONTINUOUS MODEL

Using the same reference frames as in ref.1, one assumes:

-Body frame with  $x_b$  axis parallel to the longitudinal missile axis, positive  $y_b$  axis out of the left wing, and positive  $z_b$  axis upward. (see fig.2.1)

-Flight path axis with  $x_r$  axis parallel to the velocity vector, positive  $z_r$  axis pointing upwards and  $y_r$  axis pointing to the left. (see fig. 2.2)

In fig 2.1 and 2.2, the angles  $\phi$  and  $\theta$  are the Eulerian roll and pitch angles.

The state vector is given as

$$\underline{\dot{x}} = \left[ y_r, \dot{y}_r, Aty, z_r, \dot{z}_r, Atz, \Delta\phi \right]^T \quad (2.1)$$

where  $y_r$  and  $z_r$  are the components of the relative target position,  $\dot{y}_r$  and  $\dot{z}_r$  are the relative target velocity,  $Aty$  and  $Atz$  are the components of target acceleration, which is exponentially decaying with a time constant  $\tau$ .

$$\Delta\phi = \phi - \phi_0 \quad (2.2)$$

where  $\phi_0$  is the initial roll angle (at  $t=0$ ).

The control vector is given as:

$$\underline{u} = \left[ Ac, Pc \right]^T \quad (2.3)$$

where  $Ac$  is the commanded acceleration and  $Pc$  is the commanded roll rate.

The nonlinear plant equation is

$$\underline{\dot{x}} = f(\underline{x}, \underline{u}) + \underline{g} \quad (2.4)$$

or

$$\dot{\underline{x}} = \begin{bmatrix} \dot{y}_F \\ Aty + Ac \sin \phi \\ -Aty/G \\ \dot{z}_F \\ Atz - Ac \cos \phi \\ -Atz/G \\ \rho_c \end{bmatrix} + \begin{bmatrix} 0 \\ 0 \\ 0 \\ 0 \\ -g \cos \theta \\ 0 \\ 0 \end{bmatrix} \quad (2.5)$$

where  $g$  is gravity's acceleration and  $\theta$  is the pitch angle as seen in fig.2.2

Linearizing and setting

$$\underline{G} = \underline{E} \underline{g} \quad (2.6)$$

one has

$$\dot{\underline{x}} = \begin{bmatrix} \dot{y}_F \\ Aty + A'c(\cos \phi_0) \Delta \phi \\ -Aty/G \\ \dot{z}_F \\ Atz + A'c(\cos \phi_0) \Delta \phi \\ -Atz/G \\ 0 \end{bmatrix} + \begin{bmatrix} 0 & 0 \\ \sin \phi_0 & 0 \\ 0 & 0 \\ 0 & 0 \\ -\cos \phi_0 & 0 \\ 0 & 0 \\ 0 & 0 \end{bmatrix} \quad (2.7)$$

where

$$\underline{z} = \begin{bmatrix} 0 & 0 & 0 & 0 & -\cos\theta & 0 & 0 \end{bmatrix}^T \quad (2.3)$$

in eqn. 2.7, we have set

$$\cos\phi = \cos(\phi_0 + \Delta\phi) = \cos\phi_0 \cos\Delta\phi - \sin\phi_0 \sin\Delta\phi$$

$$\sin\phi = \sin(\phi_0 + \Delta\phi) = \sin\phi_0 \cos\Delta\phi + \cos\phi_0 \sin\Delta\phi$$

and expanded in  $\Delta\phi$  which is considered small.

Now assuming that  $\dot{A}c$ , which is actually the desired control  $A_c$ , can be expressed in the form of:

$$\dot{A}c = A_{c0} \left[ 1 - \frac{t}{T_i} \right] \quad (2.9)$$

with  $A_{c0} = A_c$  at  $t=0$ , one has

$$\dot{\underline{x}} = \underline{A} \underline{x} + \underline{B} \underline{u} + \underline{E} \underline{g} \quad (2.10)$$

where

$$\underline{A} = \begin{bmatrix} 0 & 1 & 0 & 0 & 0 & 0 & 0 \\ 0 & 0 & 1 & 0 & 0 & 0 & A_{c0} \left[ 1 - \frac{t}{T_i} \right] \cos\phi_0 \\ 0 & 0 & -1/\beta & 0 & 0 & 0 & 0 \\ 0 & 0 & 0 & 0 & 1 & 0 & 0 \\ 0 & 0 & 0 & 0 & 0 & 1 & A_{c0} \left[ 1 - \frac{t}{T_i} \right] \sin\phi_0 \\ 0 & 0 & 0 & 0 & 0 & -1/\beta & 0 \\ 0 & 0 & 0 & 0 & 0 & 0 & 0 \end{bmatrix} \quad (2.11)$$

(2.12)

$$\underline{B} = \begin{bmatrix} 0 & 0 \\ \sin \phi_0 & 0 \\ 0 & 0 \\ 0 & 0 \\ -\cos \phi_0 & 0 \\ 0 & 0 \\ 0 & 1 \end{bmatrix}$$

$$\underline{E} = \begin{bmatrix} 0 & 0 & 0 & 0 & -\cos \theta & 0 & 0 \end{bmatrix}^T \quad (2.13)$$

$$\underline{g} = g \quad (2.14)$$

#### D. THE DISCRETE MODEL

##### 1. Introduction

With the introduction of a digital computer to control the continuous-time system, one has to have some kind of interface in order to take care of the communication between the discrete and continuous-time systems. In this case it will be considered, A-to-D and D-to-A converters as samplers and zero-order holders as in reference 2.

In such case, considering the system:

$$\dot{\underline{x}}(t) = \underline{A}(t) \underline{x}(t) + \underline{B}(t) \underline{u}(t) + \underline{E}(t) \underline{z}(t) \quad (2.15)$$

one can write the state of the system at time  $t(k+1)$  as :

$$\begin{aligned}
 x(t_{k+1}) = & \phi(t_{k+1}, t_k) x(t_k) + \int_{t_k}^{t_{k+1}} \phi(t_{k+1}, \eta) B(\eta) d\eta u(t_k) \\
 & + \int_{t_k}^{t_{k+1}} \phi(t_{k+1}, \eta) E(\eta) d\eta g(t_k)
 \end{aligned} \quad (2.16)$$

where  $\phi(t, t_0)$  is the transition matrix of the system represented by eqn. 2.13.

Furthermore, we will consider that the sampling instants are equally spaced, or:

$$t_{k+1} - t_k = T \quad (2.17)$$

$$t_{k+1} = kT + T \quad (2.18)$$

so one can replace

$$t_k = kT$$

thus,

$$x(kT+T) = \phi(kT+T) x(kT) \quad (2.19)$$

$$\begin{aligned}
 & + \int_{kT}^{kT+T} \phi(kT+T, \eta) B(\eta) d\eta u(kT) \\
 & + \int_{kT}^{kT+T} \phi(kT+T, \eta) E(\eta) d\eta g(kT)
 \end{aligned}$$

or in a simplified notation:

$$x(k+1) = A_d(k) x(k) + B_d(k) u(k) \quad (2.20)$$

$$+ E_d(k) g(k)$$

where,

$$A_d(k) = \phi(kT+T, kT) \quad (2.21)$$

$$B_d(k) = \int_{kT}^{kT+T} \phi(kT+T, \eta) B(\eta) d\eta \quad (2.22)$$

$$E_d(k) = \int_{kT}^{kT+T} \phi(kT+T, \eta) B(\eta) d\eta \quad (2.23)$$

## 2. Calculation of the Matrices A(k), B(k) and E(k)

It is straightforward to show, using the sparseness of the matrix A(t), that the transition matrix of equation 2-19 is :

$$\phi(kT+T) = \begin{bmatrix} 1 & T & Ad_{13} & 0 & 0 & 0 & Ad_{17} \\ 0 & 1 & Ad_{23} & 0 & 0 & 0 & Ad_{27} \\ 0 & 0 & e^{-T/5} & 0 & 0 & 0 & 0 \\ 0 & 0 & 0 & 1 & T & Ad_{46} & Ad_{47} \\ 0 & 0 & 0 & 0 & 1 & Ad_{56} & Ad_{57} \\ 0 & 0 & 0 & 0 & 0 & e^{-T/5} & 0 \\ 0 & 0 & 0 & 0 & 0 & 0 & 1 \end{bmatrix} \quad (2.24)$$

where:

$$A_{d_{1,3}} = A_{d_{4,6}} = \bar{c} T - \bar{c}^2 (1 - e^{-T/\bar{c}})$$

$$A_{d_{2,3}} = A_{d_{5,6}} = (1 - e^{-T/\bar{c}})$$

For the calculation of the others terms one may make use of the property of the transition matrix that:

$$\frac{d\phi(t_2, t_1)}{dt_2} = A(t_2) A_d(t_2, t_1)$$

so,

$$\frac{dA_d(kT+T, kT)}{d(kT+T)} = A(kT+T) A_d(kT+T, kT)$$

FOR A (2,7) :

$$\frac{dA_{d_{2,7}}(kT+T, kT)}{d(kT+T)} = A_{d_{2,7}}(kT+T) = A_{c0} \left[ 1 - \frac{t}{T_i} \right] \cos \phi_0 \Big|_{kT+T}$$

$$\frac{dA_{d_{4,7}}(kT+T, kT)}{d(kT+T)} = A_{c0} \left[ 1 - \frac{kT+T}{T_i} \right] \cos \phi_0$$

$$A_{d_{2,7}} = A_{c0} \cos \phi_0 \int_{kT}^{kT+T} \left[ 1 - \frac{kT+T}{T_i} \right] d(kT+T)$$

$$A_{d_{2,7}} = A_{c0} \cos \phi_0 \left[ T - \left[ \frac{2k+1}{2T_i} \right] T^2 \right]$$

FOR A (1,7) :

$$\frac{dA_{d_{1,7}}(kT+T, kT)}{d(kT+T)} = A_{d_{2,7}}(kT+T, kT)$$

$$A_{d_{1,7}}(kT+T, kT) = \int_{kT}^{kT+T} A_{d_{2,7}} d(kT+T)$$

$$A_{d_{4,7}} = \left[ T^2 - \left[ \frac{2k+1}{2T_i} \right] T^3 \right] A_{c0} \cos \phi_0$$

Doing the same process for  $A_d(5,7)$  and  $A_d(4,7)$  one has:

$$A_{d_{4,7}} = A_{c0} \sin \phi_0 \left[ T^2 - \left[ \frac{2k+1}{2T_i} \right] T^3 \right]$$

$$A = A_{c0} \sin \phi_0 \left[ T - \left[ \frac{2k+1}{2T_i} \right] T^2 \right]$$

For the derivation of the matrix  $B_d(k)$  one needs according to eqn. 2-22

$$\phi(kT+T) B(\eta) = A_d(kT+T, \eta) B(\eta)$$

where,

$$A_d(kT+T, \eta) = \begin{bmatrix} 1 & A_{\eta_{1,2}} & A_{\eta_{1,3}} & 0 & 0 & 0 & A_{\eta_{1,7}} \\ 0 & 1 & A_{\eta_{2,3}} & 0 & 0 & 0 & A_{\eta_{2,7}} \\ 0 & 0 & A_{\eta_{3,3}} & 0 & 0 & 0 & 0 \\ 0 & 0 & 0 & 1 & A_{\eta_{4,5}} & A_{\eta_{4,6}} & A_{\eta_{4,7}} \\ 0 & 0 & 0 & 0 & 1 & A_{\eta_{5,6}} & A_{\eta_{5,7}} \\ 0 & 0 & 0 & 0 & 0 & A_{\eta_{6,6}} & 0 \\ 0 & 0 & 0 & 0 & 0 & 0 & 1 \end{bmatrix}$$

where  $A_\eta$  represents  $A_d(kT+T, \eta)$ , and

$$B(\eta) = \begin{bmatrix} 0 & 0 \\ \sin \phi_0 & 0 \\ 0 & 0 \\ 0 & 0 \\ -\cos \phi_0 & 0 \\ 0 & 0 \\ 0 & 0 \end{bmatrix}$$

thus

$$A_d(kT+T, \eta) B(\eta) = \begin{bmatrix} A\eta_{1,2} \sin \phi_0 & A\eta_{1,7} \\ \sin \phi_0 & A\eta_{2,7} \\ 0 & 0 \\ -A\eta_{4,5} \cos \phi_0 & A\eta_{4,7} \\ -\cos \phi_0 & A\eta_{5,7} \\ 0 & 0 \\ 0 & 0 \end{bmatrix}$$

where

$$A\eta_{1,2} = kT+T - \eta = A\eta_{4,5}$$

$$A\eta_{2,7} = \left[ kT+T - \frac{(kT+T)^2}{2Ti} - \eta + \frac{\eta^2}{2Ti} \right] A\cos \phi_0$$

$$A\eta_{1,7} = \left[ T(kT+T) - \left[ \frac{2k+1}{2Ti} \right] (kT+T) T^2 - \right. \\ \left. - T\eta + \left[ \frac{2k+1}{2Ti} \right] T^2 \eta \right] A\cos \phi_0$$

$$A\eta_{4,7} = \left[ T(kT+T) - \left[ \frac{2k+1}{2Ti} \right] (kT+T) T^2 - \right. \\ \left. - T\eta + \left[ \frac{2k+1}{2Ti} \right] T^2 \eta \right] A\sin \phi_0$$

$$A\eta_{5,7} = \left[ kT+T - \frac{(kT+T)^2}{2Ti} - \eta + \frac{\eta^2}{2Ti} \right] A\cos \phi_0$$

and for  $B_d(k)$ :

$$B_d = \begin{bmatrix} B_{d_{1,1}} & B_{d_{1,2}} \\ \sin \phi_0 & B_{d_{2,2}} \\ 0 & 0 \\ B_{d_{4,1}} & B_{d_{4,2}} \\ -\cos \phi_0 & B_{d_{5,2}} \\ 0 & 0 \\ 0 & T \end{bmatrix} \quad (2.25)$$

where

$$B_{d_{1,1}} = \int_{kT}^{kT+T} (kT+T-\eta) d\eta \sin \phi_0 = -\frac{T^2}{2} \sin \phi_0$$

$$B_{d_{4,1}} = -\frac{T^2}{2} \cos \phi_0$$

$$B_{d_{2,2}} = \int_{kT}^{kT+T} A \eta_{2,7} d\eta$$

which after some algebraic work has been found

$$B(k) = \left[ \frac{T^2}{2} - \frac{(kT+T)^3}{3Ti} - \frac{(kT+T)^2 kT}{2Ti} - \frac{(kT)^2}{6Ti} \right] \text{Acc} \cos \phi_0$$

and

$$B_{d_{1,2}}(k) = \int_{kT}^{kT+T} A \eta_{1,7} d\eta$$

which can be found to be:

$$B_{d_{4,2}}(k) = \left[ \frac{T^3}{2} - \frac{1}{2} - \left[ \frac{-2k+1}{2Ti} \right] T \right] A \cos \phi$$

thus

$$B_{d_{4,2}}(k) = \left[ \frac{T^3}{2} - \frac{1}{2} - \left[ \frac{-2k+1}{2Ti} \right] T \right] A \cos \phi$$

$$B_{d_{5,2}}(k) = \left[ \frac{T^2}{2} - \frac{(kT+T)^3}{3Ti} + \frac{(kT+T)^2}{2Ti} kT - \frac{(kT)^2}{6Ti} \right] A \cos \phi$$

In the same way:

$$\phi(kT+T, \eta) E(\eta) = \begin{bmatrix} 0 \\ 0 \\ 0 \\ -T \cos \theta \\ -\cos \theta \\ 0 \\ 0 \end{bmatrix}$$

thus  $\underline{E}(k)$  is equal to

$$\underline{E} = \left[ 0 \ 0 \ 0 \ 0 \ -\frac{T^2}{2} \cos \theta \ -T \cos \theta \ 0 \ 0 \right]$$

where we have considered  $\theta$  as a constant angle. (Further comments on this after development of the control law).

Notice that throughout this work, the commanded acceleration has been considered an unknown and the assumption has been made that it will be in the form of eqn.2.9. One will need in further developments to consider the control  $A_c$  as a known  $A_c(k)$ , which will be a constant between  $kT$  and  $kT+T$ . With such assumptions, the discrete representation of the system is easily found to be :

$$\underline{x}(k+1) = \underline{A}(k) \underline{x}(k) + \underline{E}(k) \underline{u}(k) + \underline{E} g$$

(2.26)

where

$$A_d = \begin{bmatrix} 1 & T & A_{d_{1,3}} & 0 & 0 & 0 & A_{d_{1,7}} \\ 0 & 1 & A_{d_{2,3}} & 0 & 0 & 0 & A_{d_{2,7}} \\ 0 & 0 & e^{-T/\tau} & 0 & 0 & 0 & 0 \\ 0 & 0 & 0 & 1 & T & A_{d_{4,6}} & A_{d_{4,7}} \\ 0 & 0 & 0 & 0 & 1 & A_{d_{5,6}} & A_{d_{5,7}} \\ 0 & 0 & 0 & 0 & 0 & e^{-T/\tau} & 0 \\ 0 & 0 & 0 & 0 & 0 & 0 & 1 \end{bmatrix} \quad (2.27)$$

with

$$A_{d_{1,3}} = \tau T - \tau^2 (1 - e^{-T/\tau}) = A_{d_{4,6}}$$

$$A_{d_{2,3}} = \tau (1 - e^{-T/\tau}) = A_{d_{5,6}}$$

$$A_{d_{1,7}} = -\frac{T^2}{2} AC \cos \phi_0$$

$$A_{d_{2,7}} = T AC \cos \phi_0$$

$$A_{d_{4,7}} = -\frac{T^2}{2} AC \sin \phi_0$$

$$A_{d_{5,7}} = T AC \sin \phi_0$$

and

$$B_d(k) = \begin{bmatrix} \frac{T^2}{2} \sin \phi_0 & \frac{T^3}{6} A_c \cos \phi_0 \\ T \sin \phi_0 & \frac{T^2}{2} A_c \cos \phi_0 \\ 0 & 0 \\ -\frac{T^2}{2} \cos \phi_0 & \frac{T^3}{6} A_c \sin \phi_0 \\ -T \cos \phi_0 & \frac{T^2}{2} A_c \sin \phi_0 \\ 0 & 0 \\ 0 & T \end{bmatrix}$$

and

$$E_d(k) = \begin{bmatrix} 0 \\ 0 \\ 0 \\ -\frac{T^2}{2} \cos \theta \\ -T \cos \theta \\ 0 \\ 0 \end{bmatrix}$$

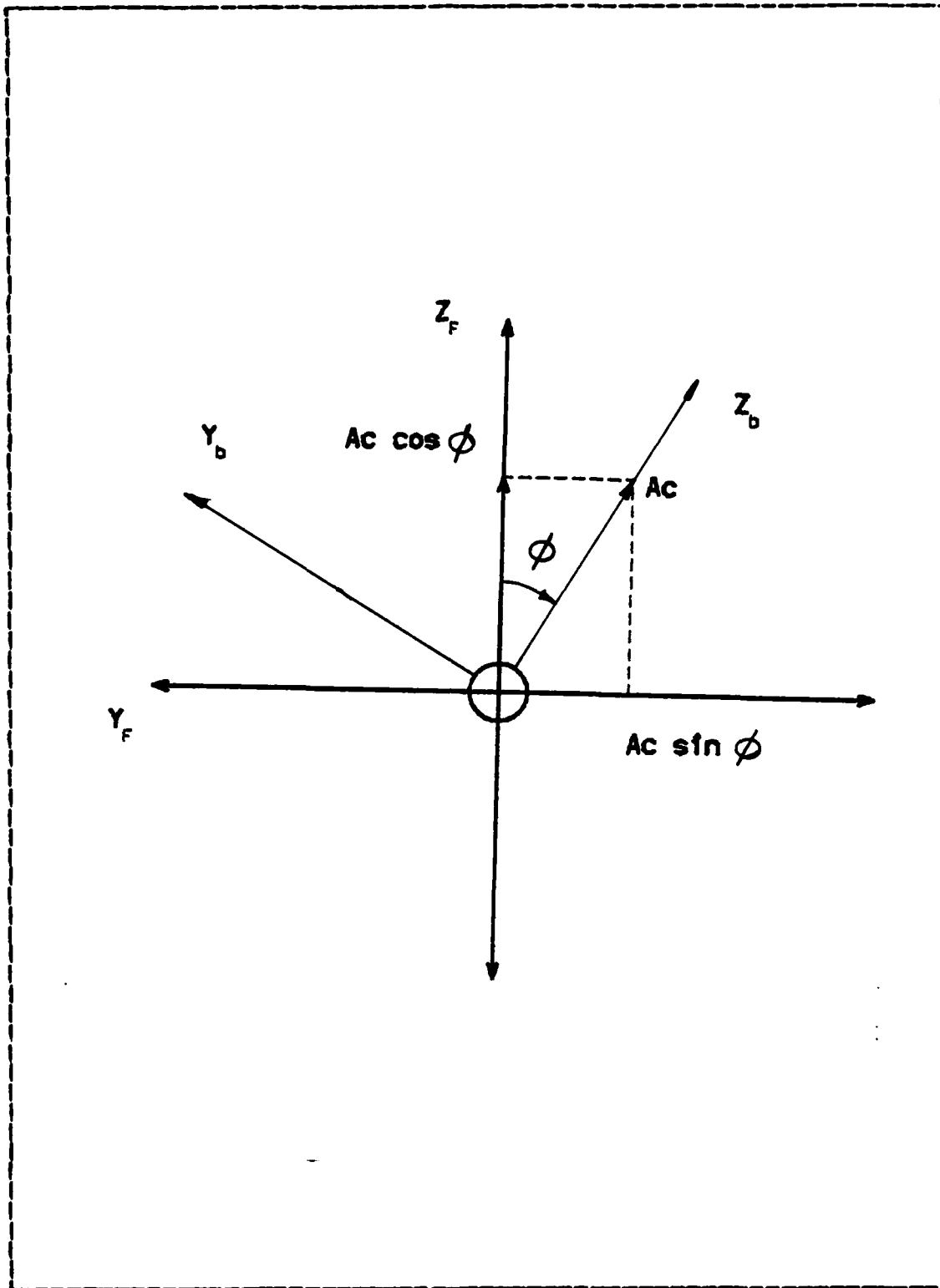


Figure 2.1 Reference Frames.

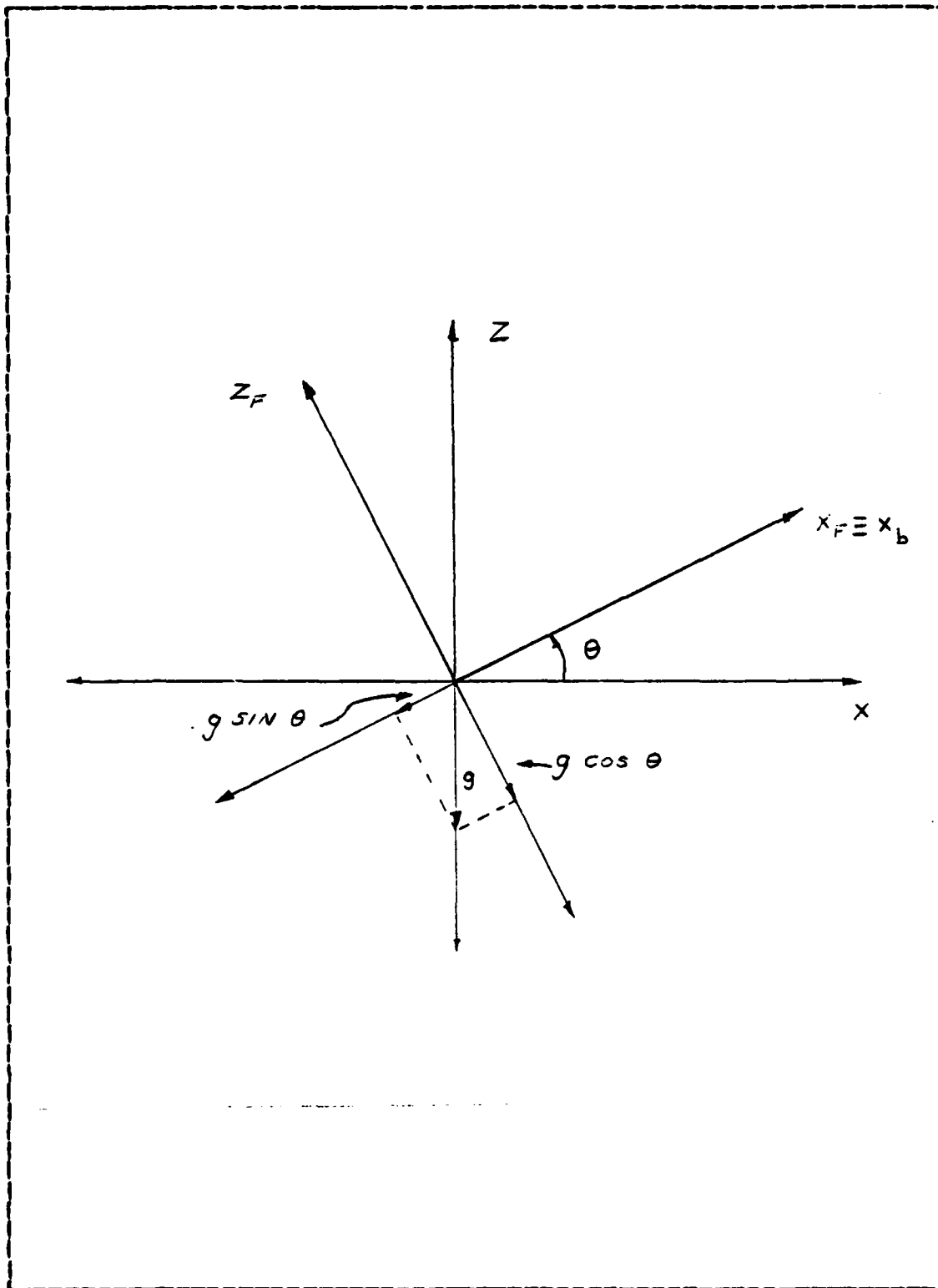


Figure 2.2 Reference Frames.

### III. THE OPTIMAL CONTROLLER

#### A. DERIVATION OF THE OPTIMAL CONTROLLER

In order to have a suitable guidance law to implement the control commands, we will minimize the following performance index:

$$J = \frac{1}{2} x^T(N) W(N) x(N) + \sum_{k=0}^{N-1} \frac{1}{2} u^T(k) Q(k) u(k) \quad (3.1)$$

where  $x(N)$  is the final state at  $t=T_1$

As we want to minimize the final miss distance, the weighting matrix  $W(N)$  is taken as

$$\begin{bmatrix} 1 & 0 & 0 & 0 & 0 & 0 & 0 \\ 0 & 0 & 0 & 0 & 0 & 0 & 0 \\ 0 & 0 & 0 & 0 & 0 & 0 & 0 \\ 0 & 0 & 0 & 1 & 0 & 0 & 0 \\ 0 & 0 & 0 & 0 & 0 & 0 & 0 \\ 0 & 0 & 0 & 0 & 0 & 0 & 0 \\ 0 & 0 & 0 & 0 & 0 & 0 & 0 \end{bmatrix} \quad (3.2)$$

and  $Q(k)$  is a two by two positive definite symmetric weighting matrix to be chosen.

In the derivation of the solution, reference 3 has been followed keeping in mind that the state equation has the form:

$$\underline{x}(k+1) = \underline{A}(k) \underline{x}(k) + \underline{B}(k) \underline{u}(k) + \underline{E} g \quad (3.3)$$

or

$$\underline{x}(k+1) = f(\underline{x}(k), \underline{u}(k), g) \quad (3.4)$$

where the third term, which represents the effect of the gravity has been considered constant.

Considering that the performance index is in the form:

$$J = \phi[x(N)] + \sum_{k=0}^{N-1} L(k) [x(k), u(k), g(k)] \quad (3.5)$$

we need to find a sequence of  $u(k)$  that minimizes  $J$ .

Adjoin the system equation to  $J$  with a multiplier  $\lambda(k)$

$$J = \phi[x(N)] + \sum_{k=0}^{N-1} \left\{ L(k) [x(k), u(k), g] + \lambda^T(k+1) \left\{ f_k[x(k), u(k), g] - x(k+1) \right\} \right\} \quad (3.6)$$

and defining a scalar sequence  $H(k)$

$$H(k) = L(k) [x(k), u(k), g] + \lambda^T(k+1) f_k [x(k), u(k), g] \quad (3.7)$$

$k=0, 1, 2, \dots, n-1$

one has:

$$J = \phi [x(N)] - \lambda^T(N) x(N) + \quad (3.8)$$

$$+ \sum_{k=1}^{N-1} [H(k) - \lambda^T(k) x(k)] + H(0)$$

Considering differential changes in J:

$$dJ = \left[ \frac{\partial \phi}{\partial x(N)} - \lambda^T(N) \right] dx(N) + \quad (3.9)$$

$$+ \sum_{k=1}^{N-1} \left\{ \left[ \frac{\partial H(k)}{\partial x(k)} - \lambda^T(k) \right] dx(k) + \right.$$

$$\left. + \frac{\partial H(k)}{\partial u(k)} du(k) \right\} + \frac{\partial H(0)}{\partial x(0)} dx(0) +$$

$$+ \frac{\partial H(0)}{\partial u(0)} du(0)$$

choosing the multiplier  $\lambda(k)$  so that

$$\lambda^T(k) - \frac{\partial H(k)}{\partial x(k)} = 0 \quad (3.10)$$

thus

$$\frac{\partial L(k)}{\partial x(k)} + \lambda^T(k+1) \frac{\partial f_k}{\partial x(k)} = \lambda^T(k)$$

and

$$\frac{\partial H(k)}{\partial u(k)} = 0 \quad (3.11)$$

with boundary condition

$$\lambda^T(N) = \frac{\partial \phi}{\partial x(N)} \quad (3.12)$$

we obtain the minimization of the performance index.

In the present case we have:

$$J = \frac{1}{2} x^T(N) W(N) x(N) + \sum_{k=0}^{N-1} u^T(k) Q(k) u(k) + \lambda^T(k+1) [A(k)x(k) + B(k)u(k) + E g - x(k+1)] \quad (3.13)$$

and  $H(k)$  :

$$H(k) = \frac{1}{2} u^T(k) Q(k) u(k) + \lambda^T(k+1) [A(k)x(k) + B(k)u(k) + E g] \quad (3.14)$$

then in order to minimize  $J$ :

$$\frac{\partial H(k)}{\partial u(k)} = u^T(k) Q(k) + \lambda^T(k+1) B(k) = 0 \quad (3.15)$$

or considering that  $Q^T(k) = Q(k)$

$$Q(k) u(k) = - B^T(k) \lambda(k+1)$$

and

$$\lambda^T(k) = \frac{\partial H(k)}{\partial x(k)} \quad (3.16)$$

$$\lambda^T(k) = \lambda^T(k+1) A(k)$$

and

$$\lambda^T(N) = x^T(N) W(N) \quad (3.17)$$

Notice that we are not weighting the states in the performance index, except the last state. A more general form could be obtained, with all states being weighting, if we change the eqn 3.16 to:

$$\lambda^T(k) = \lambda^T(k+1) A(k) + x^T(k) W1(k) \quad (3.18)$$

where  $W1(k)$  is the weighting matrix of the states.

With equations 3.15, 3.16 and 3.17 one is able to find the sequence of  $u(k)$  that will give the minima controls.

Such set of equations can be solved by the sweep method as in ref.2 .

We will look for a solution of the form:

$$u(k) = -F(k)x(k) - FG(k)g(k) \quad (3.19)$$

what means that the commanded acceleration and roll rate, will have a correction due to the effect of gravity.

Placing:

$$\lambda(k) = S(k) x(k) + SG(k) g(k) \quad (3.20)$$

from eqn. 3.15

$$Q(k) u(k) = -B^T(k) [S(k+1) x(k+1) + SG(k+1) g(k+1)]$$

from eqn. 3.3

$$Q(k) u(k) = -B^T(k) S(k+1) [A(k) x(k) + B(k) u(k) + E g] - B^T(k) SG(k+1) g(k+1) \quad (3.21)$$

so

$$\begin{aligned} [Q(k) + B^T(k) S(k+1) B(k)] u(k) = \\ -B^T(k) S(k+1) A(k) x(k) - B^T(k) S(k+1) E g(k) - \\ -B^T(k) SG(k+1) g(k+1) \end{aligned}$$

considering that g is a constant

$$u(k) = - [Q(k) + B^T(k) S(k+1) B(k)]^{-1} \quad (3.22)$$

$$\begin{bmatrix} B^T(k) & S(k+1) & A(k) & x(k) + \\ + [B^T(k) & S(k+1) & E + B^T(k) & SG(k+1)] & g \end{bmatrix}$$

so:

$$u(k) = -F(k)x(k) - FG(k)g$$

where

$$F = [Q(k) + B^T(k) S(k+1) B(k)]^{-1} \quad (3.23)$$

$$\cdot B^T(k) S(k+1) A(k)$$

$$FG = [Q(k) + B^T(k) S(k+1) B(k)]^{-1} \quad (3.24)$$

$$[B^T(k) S(k+1) E + B^T Sg(k+1)]$$

from eqn. 3.16 and 3.19

$$\begin{aligned} \lambda(k) &= A^T(k) \lambda(k+1) = A^T(k) [S(k+1)x(k+1) + SG(k+1)g(k+1)] = \\ &= A^T(k) S(k+1) A(k) x(k) + A^T(k) S(k+1) B(k) u(k) \\ &+ A^T(k) S(k+1) Eg + A^T(k) SG(k+1) g(k+1) \end{aligned}$$

from eqn. 3.19

$$\begin{aligned} \lambda(k) &= A^T(k) S(k+1) A(k) x(k) + A^T(k) S(k+1) B(k) \cdot \\ &\cdot [-F(k)x(k) - FG(k)g] + A^T(k) S(k+1) Eg + \\ &+ A^T(k) SG(k) g(k+1) \end{aligned}$$

so, as  $g$  is a constant:

$$S(k)x(k) + SG(k)g = [A^T(k)S(k+1)A(k) - A(k)S(k+1)B(k)F(k)] +$$

$$+ \left[ A^T(k) S(k+1) E - A^T(k+1) B(k) FG(k) + A(k) SG(k+1) \right] g$$

thus

$$S(k) = A^T(k) S(k+1) A(k) - A^T(k) S(k+1) B(k) F(k) \quad (3.25)$$

and

$$SG(k) = A^T(k) S(k+1) E - A^T(k) S(k+1) B(k) FG(k) + A^T(k) SG(k+1) \quad (3.26)$$

These equations, 3.25, 3.26, 3.23 and 3.24 can be solved backwards with the final condition:

$$S(N) = W(N)$$

$$SG(N) = 0$$

Notice that this satisfies our previous boundary condition in eqn. 3.17 where:

$$S(N) = W(N) x(N)$$

$$S(N) x(N) = W(N) x(N)$$

so

$$S(N) = W(N)$$

## B. EXTENSION OF THE MODEL FOR LARGE ROLL ANGLES

Up to this point, one has to take into account that throughout the development of this work, the angle has been considered small, it is necessary to relax this restriction.

In order to do that, the system has been broken in two blocks as in figure 3.1.

The first block is a representation of the algorithm which will calculate the optimal commands. The algorithm has contain with itself an exact model of the system or missile. The model of the missile is initialized from the information on the initial states, the initial input command  $A_{c0}$  and initial roll angle (at  $t=0$ ); and computes the optimal gains and further the optimal commands which will be feed to the missile.

The method adopted in computing the optimal commands is more easily understood if one considers figure 3.2.

In figure 3.2, the lines numbered as 0 in the graph for  $A_c$  and for  $P_c$  are the optimal commands for a given initial roll angle ( $\phi_0$ ). Lines number 1 are the commands for a second initial roll angle ( $\phi_1$ ) larger than  $\phi_0$ , and so on. Thus in figure 3.2 one has a family of optimal commands for any initial roll angle.

Notice that the upper line of the graph of  $A_c$  represents the accelerations of a missile which had at  $t=0$  a correct initial roll angle in order to hit the target with no comands in roll rate.

In the present method the computer performs the calculation of the commands only for the first step of time and then feeds these commands to the missile. The missile is then driven to the next state ( $x(k+1)$ ) and feed-backs to the computer the information on the roll angle at that step. The roll angle feed-backs from the missile is considered by the algorithm as the initial roll angle at  $t=0$  and the next commands are calculated. Notice that at this second step the algorithm will feed to the system the second command (at  $t=t_1$ ). This process is then repeated until  $t$  is equal to the intercepted time.

It is important to realize that with this method of calculation, since the algorithm was developed with the assumption of small roll excursions some error is expected due to the fact that in computing the gains by solving a Ricatti equation backwards, as has been done, it is necessary to update the system from  $t=0$  to  $t=T_i$  at each step, and in this process the roll angle is not small. Notice however that we are applying the commands only in one step, and if one expects that the roll rate will decrease to zero, as we are increasing in time, the variation of the roll angle will tend to decrease, so, we can expect that the error will decrease as the time increases.

Another important point to be studied is how the missile itself (second block in fig. 3.2) has to be implemented in order to be valid for small and large roll excursions.

It is considered that one has the perfect knowledge of the commands, thus the missile is modeled as a state variable system as in eqn 2.26 with the initial roll angle being update at each step. In this way the system will take the initial roll angle as the summation of all previous initial roll angles. (see fig 3.4)

From the original variables one has for the state  $\Delta\phi$ , the following:

$$\Delta\phi(k+1) = \Delta\phi(k) + P_c(k) T \quad (3.27)$$

which is show in figg. 3.3, where the initial roll angle is kept constant and  $\Delta\phi$  is update each step.

Notice however that considering large roll excursions (see fig. 3.4) and keeping in mind that the angle  $\phi$  has been defined as

$$\phi = \phi_0 + \Delta\phi$$

the expression 3.27 is not valid, since in modeling the system it was assumed that  $\Delta\phi$  would be small.

This leads to a change in the expression for the variation of  $\Delta\phi$  as in fig. 3.4. In fig. 3.4, the angle  $\Delta\phi$  is updated at each step, so one has:

$$\Delta\phi(k+1) = P_c(k) T \quad (3.28)$$

By consideration of the equation 2.27 it can be seen that by setting the element  $A(7,7)$  to zero, one can obtain equation 3.28.

Thus the missile model for large roll excursions will be represented by the following equation.

$$x(k+1) = A(k) x(k) + B(k) u(k) + E g$$

where

$$A(k) = \begin{bmatrix} 1 & T & A_{1,3} & 0 & 0 & 0 & A_{1,7} \\ 0 & 1 & A_{2,3} & 0 & 0 & 0 & A_{2,7} \\ 0 & 0 & e^{-T/c} & 0 & 0 & 0 & 0 \\ 0 & 0 & 0 & 1 & T & A_{4,6} & A_{4,7} \\ 0 & 0 & 0 & 0 & 1 & A_{5,6} & A_{5,7} \\ 0 & 0 & 0 & 0 & 0 & e^{-T/c} & 0 \\ 0 & 0 & 0 & 0 & 0 & 0 & A_{7,7} \end{bmatrix} \quad (3.29)$$

where  $A(7,7)=0$  , for large roll excursions

$A(7,7)=1$  , for small roll excursions

$$B = \begin{bmatrix} \frac{T^2}{2} \sin \phi_0 & \frac{T^3}{6} A_c \cos \phi_0 \\ T \sin \phi_0 & \frac{T^2}{2} A_c \cos \phi_0 \\ 0 & 0 \\ -\frac{T^2}{2} \cos \phi_0 & \frac{T^3}{6} A_c \sin \phi_0 \\ -T \cos \phi_0 & \frac{T^2}{2} A_c \sin \phi_0 \\ 0 & 0 \\ 0 & T \end{bmatrix} \quad (3.30)$$

$$E = \begin{bmatrix} 0 \\ 0 \\ 0 \\ -\frac{T^2}{2} \cos \theta \\ -T \cos \theta \\ 0 \\ 0 \end{bmatrix} \quad (3.31)$$

We will redefine the states  $x_1$ , as the relative position,  $x_2$  as the relative velocity in the Y direction and  $x_3$  as the target acceleration in Y direction. The states  $x_4$ ,  $x_5$  and  $x_6$  has the same meaning, but in the Z direction and

$x_1$  is  $\Delta\phi$ . In this representation of the system,  $x_1(k)$  is equal to the component of the miss distance along the Y direction and:

$$x_1(k+1) = y_p(k+1) = y_p(k) + \dot{y}_p(k) T + \quad (3.32)$$

$$+ \left[ \zeta T - \zeta^2 (1 - e^{-T/\zeta}) \right] \Delta y(k) + \frac{T^2}{2} A_c(k) \cos\phi_0 \Delta\phi(k) \\ + \frac{T^2}{2} \sin\phi_0 A_c(k) + \frac{T^3}{6} A_c(k) \cos\phi_0 P_c(k)$$

The first three terms in the RHS of eqn.3.32, are easily seen as the contribution to the miss distance of respectively the previous miss distance, relative velocity and target acceleration. The following two terms represents the contribution of the commanded acceleration and the last term represents the effect of coupled  $A_c$  and  $P_c$ , and tends to be small due to the cube of the sample period.

For the component of miss distance in the Z direction, one has:

$$x_4(k+1) = z_p(k+1) = z_p(k) + \dot{z}_p(k) T + \\ + \left[ \zeta T - \zeta^2 (1 - e^{-T/\zeta}) \right] \Delta z(k) + \frac{T^2}{2} A_c(k) \sin\phi_0 \Delta\phi(k) - \\ - \frac{T^2}{2} \cos\phi_0 A_c(k) + \frac{T^3}{6} A_c(k) \sin\phi_0 P_c(k) - \frac{T^2}{2} \cos\theta g$$

where its terms have the same physical meaning as in the expression for  $x(k+1)$ , with the effect of the gravity added to the expression.

Since one can notice that in the representation of the miss distance in Y direction appear two terms as a function of  $\cos\phi_0$ , and in the representation of the miss distance in Z direction appear two terms as function of  $\sin\phi_0$ , it is

interesting to verify that the fourth term in the RHS of both expressions acts like a correction for the fifth term. Referring to fig. 3.4b, one can see that at any step of time, the commanded acceleration is actually,

$$Ac \cos \phi_0 - \Delta Ac$$

and considering small angles:

$$\begin{aligned} \Delta Ac &= Ac \cos \phi_0 - Ac \cos(\phi_0 + \Delta \phi) = \\ &= Ac \cos \phi_0 - Ac [\cos \phi_0 \Delta \phi - \sin \phi_0 \sin \Delta \phi] = \\ &= Ac \sin \phi_0 \Delta \phi \end{aligned}$$

The same idea can be applied to the expression for  $x(k+1)$ .

The terms  $x_2$  and  $x_3$ , represent the relative velocity, and are:

$$\begin{aligned} x_2(k+1) &= \dot{y}_r(k) + \zeta (1 - e^{-T/\tau}) Aty(k) + Ac(k) \cos \phi_0 T \\ &+ Ac(k) \sin \phi_0 T + \frac{T^2}{2} Ac(k) \cos \phi_0 Pc(k) \end{aligned}$$

$$\begin{aligned} x_3(k+1) &= \dot{z}_r(k) + \zeta (1 - e^{-T/\tau}) Atz(k) + Ac(k) \sin \phi_0 T - \\ &- Ac(k) \cos \phi_0 T + \frac{T^2}{2} Ac(k) \sin \phi_0 Pc(k) - T \cos \theta g \end{aligned}$$

Where the two first terms in the RHS represents the effect of the velocity and acceleration at a previous step, and the other three terms has the same meaning as previously stated.

The terms  $x_3$  and  $x_4$  are the target accelerations, in this model being exponentially decaying.

#### 1. Effects on the Miss Distance of the Extension of the Model

In previous subsection, a extension of the model for large roll excursions has been performed. Notice that there are two models of the system being used. The first one, used

in the algorithm is valid only for small roll excursions, and a second model, valid for small and large roll excursions used as a representation of the missile.

The algorithm with the first model, as explained before, is initialized at each step with the actual roll angle of the missile, and performs the calculation of the commands.

In order to check the effect of the extension of the model on the miss distance, one can define a ideal initial roll angle ( $\phi_{o,ideal}$ ), as the roll angle at  $t=0$  in order to have the commanded acceleration vector pointing to the projected final target's position. This means that the missile would not have to roll to hit the target (see fig 3.5), thus the commanded roll rate calculated by the algorithm will be equal to zero. This implies that from that point ahead, the roll angle is constant and equal to  $\phi_{o,ideal}$ , and that the time history of the control  $A_c$  will be a straight line.

The fact that the roll angle will tend to this limit deserves an investigation. Notice that, as show in fig. 3.2, at the moment the missile reaches its maximum roll angle, the control  $A_c$  will be the required acceleration to hit the target if the missile initial roll angle was  $\phi_{o,ideal}$ . This means that the control  $A_c$  computed would be correct only if the missile would have turned immediately to this angle.

For very small angles, the previous comment would be acceptable, but in a normal situation, as showed in figure 3.5, the missile will only reach the ideal initial roll angle after some time, and due to the vertical component of the acceleration, when this occurs the missile would be in a position above the ideal trajectory, which means that it would follow a course parallel to the ideal trajectory to intercept.

One can see that such problem will lead to a large miss distance, in the case that the target acceleration it is not small. Thus, some correction is necessary in order to improve the missile performance.

Figure 3.5b shows the missile at some point of its trajectory where it has reached its maximum roll angle, thus it is at a parallel course with its ideal trajectory to intercept. At this point, since all the states are known, it is possible to recompute a new  $\phi_{ideal}$ . So, if at this point the computer is fed with the states at this point it will compute the commands in order to drive the missile to the new  $\phi_{ideal}$ , which will introduce the desired correction. Notice that such correction can be made during all the flight, from  $t=0$ , to  $t=T_i$ .

In the present work this method has been accomplished by feeding-back to the computer the roll angle and all the states of the missile. With this information the computer is able to perform the calculation of the corrected commands at each step of time. However as the states are being updated, it is also necessary to update the time to intercept, which has been done using the time to go to intercept, or:

$$T_i(k) = T_i - k T$$

where  $T_i$  is the nominal time to intercept.

### C. SIMULATION

In order to keep the same assumptions as reference 1, the matrix  $Q$  (weighting the control) has been put as suggested in such reference or:

$$\begin{bmatrix} b_1 & 0 \\ 0 & b_2 \end{bmatrix}$$

(3.33)

with

$$b_1 = 5.78 \cdot 10^3$$

$$b_2 = 5.0 \text{ meters}$$

Five different cases were run:

Case 0, tested with one simple model valid only for small roll angles begins with missile and target on parallel courses to the inertial x axis, the target 100 meters above the missile and with an evasive manoeuvre exponentially decaying with time constant of 20 seconds. The initial acceleration of target was  $-0.5 \text{ g's}$  in y direction. (see fig. 3.6)

Case 1, with the same scenarios as case 0, but was run using the algorithm for large roll excursions.

Case 2, is the same scenario as in case 1, except that the initial acceleration of target was  $-1.0 \text{ g's}$  in the y direction. (Same as case 1 in ref. 1).

Case 3, the same as case 2, with target acceleration of  $-4 \text{ g's}$ . (Same as case 2 in the reference 1)

Case 4, same as case 3 but with target at initial position 600 meters below the missile. (Same as case 3 in reference 1.)

#### D. COMMENTS AND CONCLUSIONS

##### 1. Results

In case 0, the missile begins its trajectory commanding  $26.5 \text{ m/sec}^2$  and the time history of the control  $A_c$  follows exactly a straight line in the form suggested in

ref. 1, as seen in fig.3.7 The control  $P_c$ , beginning at .35 rad per second, is decaying and reaches zero at  $k=80$  (see fig.3.8). Figures 3.9 and 3.10 show the miss distance, where one can see that the missile is crossing the target with a CG-to-CG distance of 1.5 meters.

Figure 3.11, shows the time history for the roll angle, which as expected, reaches a constant value, with the missile crossing target at  $t=T_i$ , with a bank of .44 radians.

In case 1, which was run with the model for large roll excursions, the missile kept the same  $A_{c0}$ , but there is a very small increase in further commanded acceleration in order to correct the effect of the roll angle on the vertical component of the control  $A_c$ , as seen in fig.3.12, and table I.

Figure 3.13 shows that the roll rate decreases almost as before, and the final roll angle is .42 rds, as shown in fig.3.15 and table I. Referring to figure 3.14 there is a change in the final miss distance, which is better than case 0, due to a improvement in its Z component (see table I). This results in a final CG-to-CG miss distance of .65 meters.

In case 2, the missile has the same  $A_c$  at  $t=0$ , but with the correction for roll angle being increased due to the increase of target acceleration (see fig.3.16), the commanded  $A_c$  reaches a larger peak value.

The initial value of the commanded roll rate is .69 radians, which is larger than case 1, due to the increase in the target acceleration. In figure 3.18, there is no noticeable change in the shape of the curve for Z direction, and in the Y direction the final distance is about the same as in case 1. The CG-to-CG distance at  $t=T_i$  is .73 meters. The larger roll rate leads to larger roll angles as seen in fig. 3.19, where the final roll angle is .72 radians.

The effect of target acceleration can be easily seen in case 3, where one can see that with the same  $A_{co}$ , the accelerations are largely increased from this point, and the missile begins its trajectory with very high roll rate (see figures 3.20 and 3.21). There is a change in the Z component of the miss distance, that decreases its final value to .05 meters, but now the miss distance in Y direction is made worse as shown in figure 3.22, which leads to a final CG-to-CG distance of 1.5 meters. In fig. 3.23 one can see that the missile crosses the target with a bank angle of 1.26 radians.

In case 4, due to the position of target 600 meters under the missile, the initial commanded acceleration is negative and reaches the limit of -2 g's. The initial roll rate begins at a smaller value than in case 3 but increases during the initial part of the flight reaching its peak value at 1.75 seconds when again as in the previous cases begins to decay. As the missile banks to roll angles larger than 90 degrees, the acceleration goes to positive values, as seen in figures 3.24 and 3.25. Figure 3.26, shows the worse case among these in respect to the miss distance, mainly in the Z direction, and in the final cg-to-cg distance, which is equal to 4.43 meters. Also the final roll angle of 3.0 radians is the largest among all these cases, as seen in fig. 3.27.

## 2. Comments

Defining the projected zero effort miss distance (ZEM) as the miss distance the missile cross the target with no commands. It can be calculated at  $t=0$  as the initial distance between target and missile plus the miss distance due to the gravity or:

$$ZEM = z(0) + \frac{1}{2} g t^2 \quad (3.34)$$

which is equal in all the three first cases.

In the first three cases, the initial missile's commanded acceleration is the same as seen in table 3.1. Considering that the control  $A_c$  necessary to correct the initial miss distance can be calculated as:

$$A_{c_{ZEM_0}} = \left\{ \frac{ZEM_z}{\frac{T_i^2}{2} - \frac{T_i^2}{6}} \right\} = 26.7 \quad (3.35)$$

which is close to the initial control  $A_c$ .

This suggests that the initial  $A_c$ , would be that one necessary to correct the initial ZEM in Z direction, which agrees with reference 1. Notice however that in all cases the initial  $A_c$  is less than the calculated value of  $A_{c_0}$ , which agrees with the previous statement that some error was expected in the initial part of the computations.

Considering the ideal initial roll angle as defined before, one has:

$$\phi_{o,ideal} = \tan^{-1} \left[ \frac{ZEM_y}{ZEM_z} \right] \quad (3.36)$$

From table I, and figures showing roll angles, it can be verified that the missile is banking to reach angles larger than  $\phi_{o,ideal}$ , in order to correct its trajectory to hit the target.

Therefore, in all cases, the missile begins its trajectory with an  $A_{c_0}$  (discussed before), and a roll rate

which is proportional to the target acceleration in the Y direction. As the missile rolls at decreasing roll rates, the commanded acceleration is changed in order for to compensate the effect of the roll angle on its Z direction component. At some time when the control  $P_c$  is zero or near zero, the control  $A_c$  begins to follow a linear law, as suggested in eqn. 2.7:

$$A_c = A_{c0} \left[ 1 - \frac{t}{T_i} \right]$$

Notice however that the term  $A_{c0}$  in this equation is no more the actual initial commanded acceleration, but that one the missile would have if its initial roll angle was equal to the final .

Such behavior defines a boundary in the control  $A_c$  which is clearly seen in 3.29, where the commanded acceleration is bounded by the curve of the control  $A_c$  the missile would have if its initial  $\phi_0$  was equal to  $\phi_{0,ideal}$  (or, if no commanded roll was necessary to reach the target).

Although the missile commands roll angles larger than the ideal initial roll angle, it is possible to do a prediction- with no no computer work- of an approximation for the maximum acceleration the missile would experience during its flight, as following (see fig. 3.32):

$$A_c = \left[ \frac{ZEM_z}{\frac{T_i^2}{2} - \frac{T_i^2}{6}} \right] \frac{1}{\cos \phi_{0,ideal}} \quad (3.37)$$

where  $\phi_{0,ideal}$  comes from eqn. 3.50, and  $A_c$  is a straight line as in fig 3.32.

Other interesting point is that the missile is commanding to reach roll angles about twice of  $\phi_{0,ideal}$  when the target is at small accelerations, and when at large

accelerations, the missile is making a small correction on its roll angle, as shown in table I.

One can see from the figures showing miss distance, that the relative position of missile to target is about the same in all three initial cases. Thus, the new  $\phi_{ideal}$  at each point is the same. As the  $\phi_{o,ideal}$  computed at  $t=0$  is smaller when the target is at small accelerations, the correction has to be larger in order to hit the target, as seen in figure 3.30.

In table I, one can see the final miss distances, the final miss distance cg to cg and the final roll angle. Such results show that with this digitalized model, good results has been obtained.

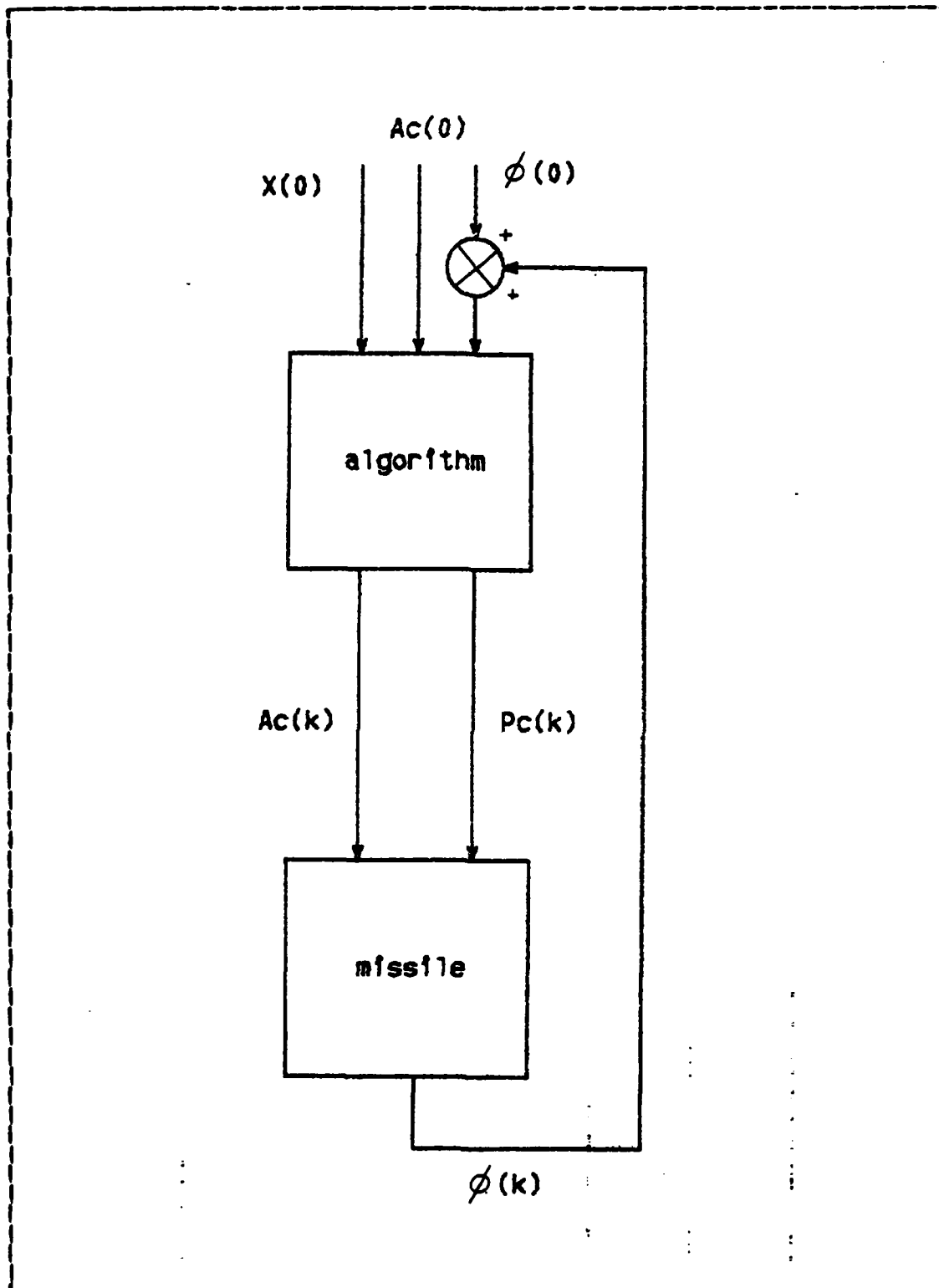


Figure 3.1 Representation of the System.

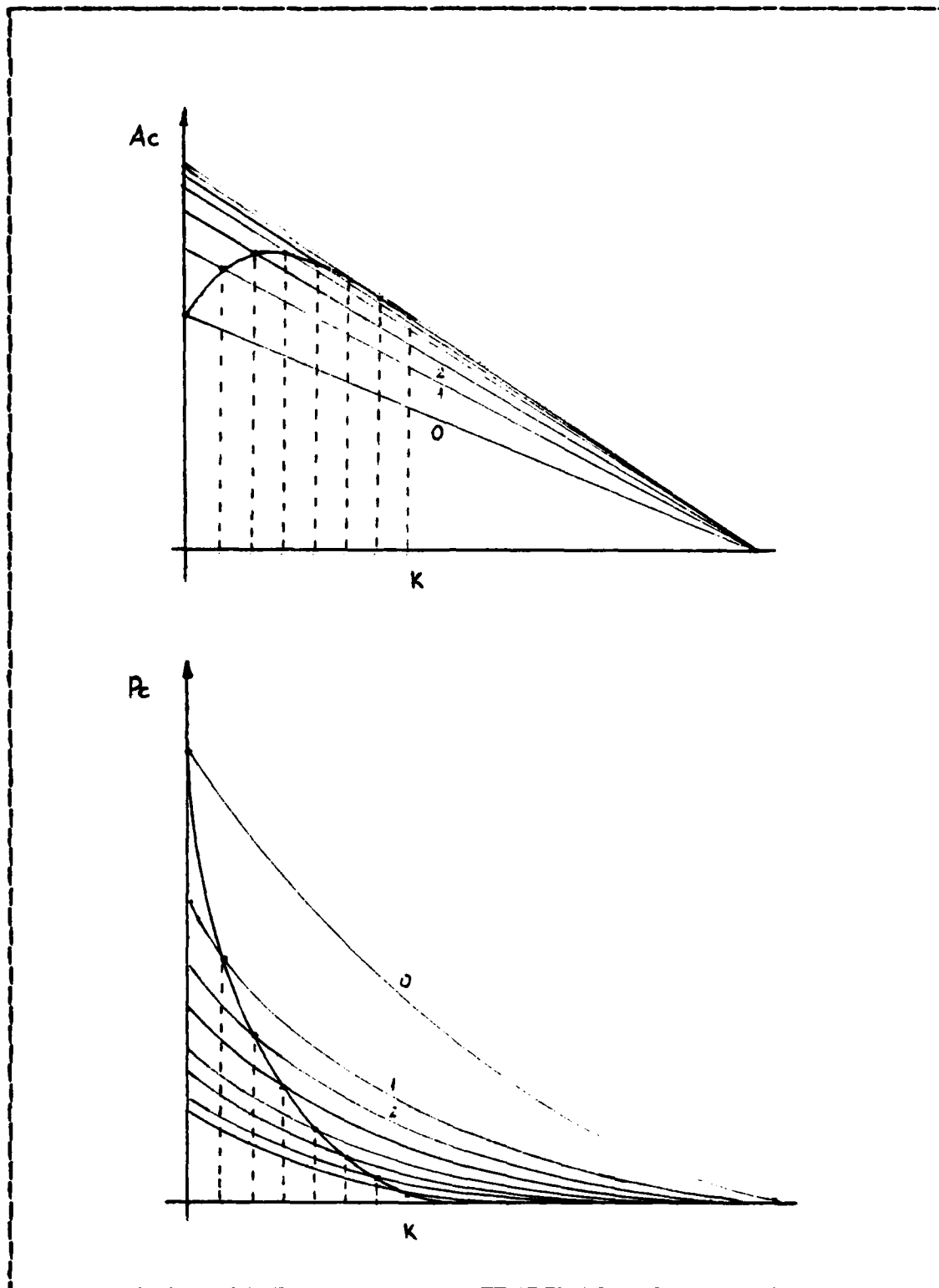


Figure 3.2 Variation of Commands with Initial Roll Angle.

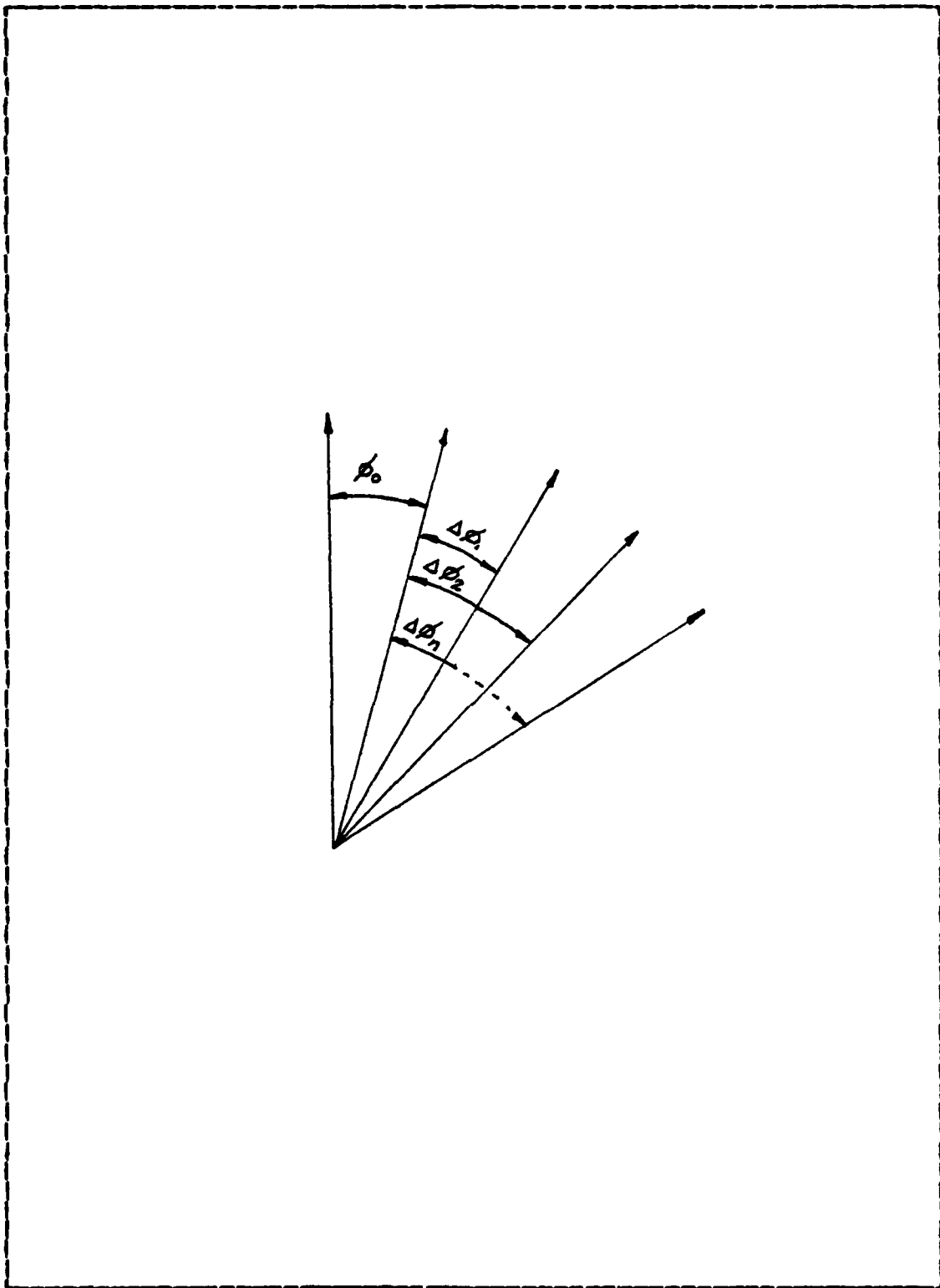


Figure 3.3 Variation of Roll Angle - Small Angles.

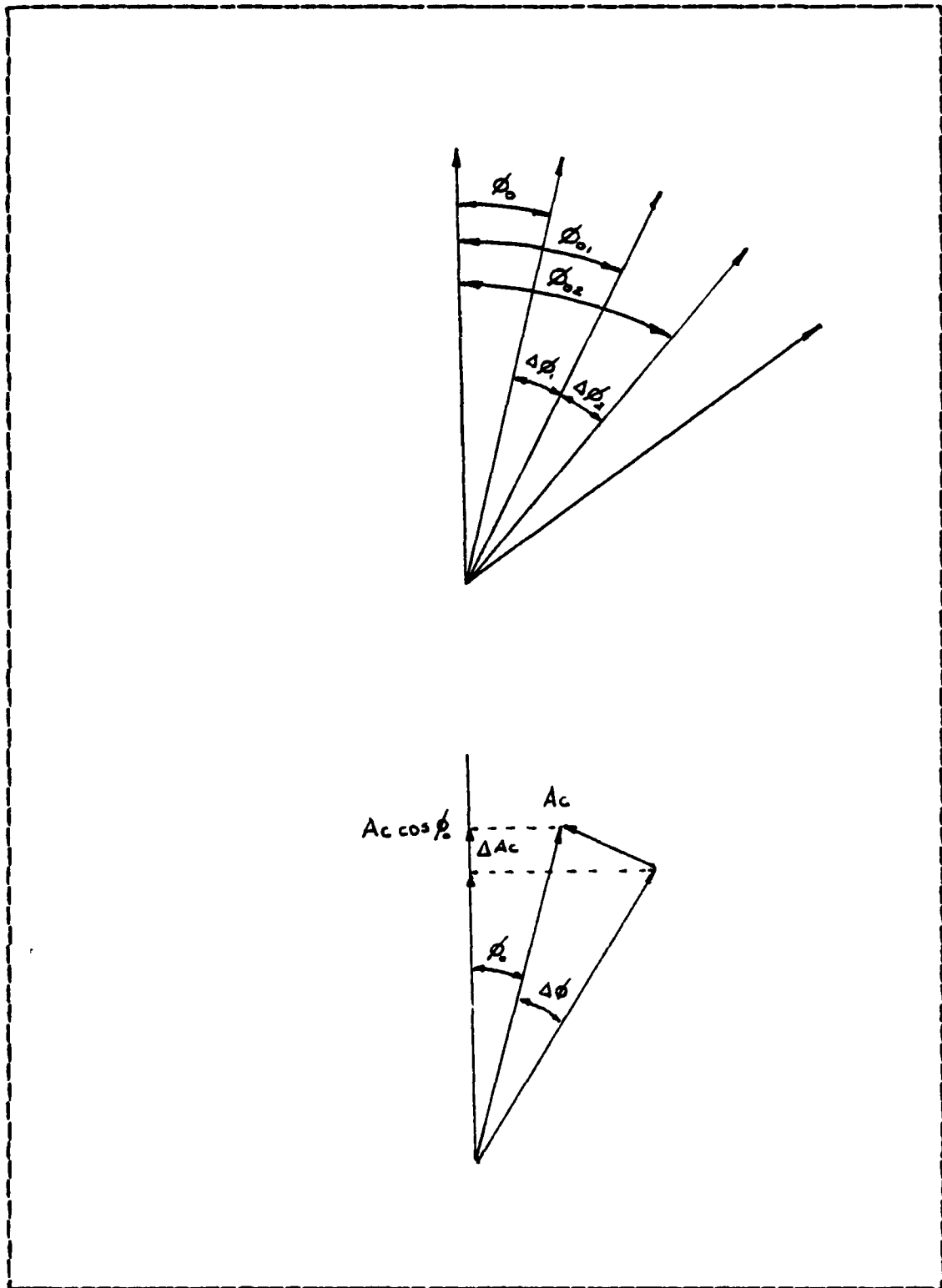


Figure 3.4 Variation of Roll Angle - Large Angles.

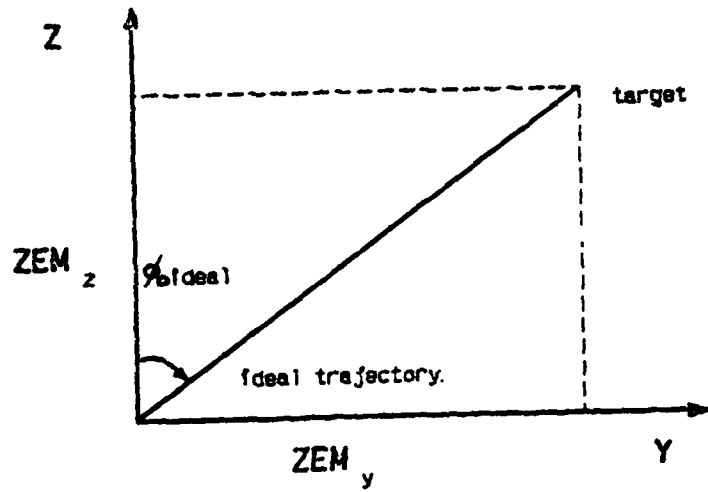


Figure 3.5a

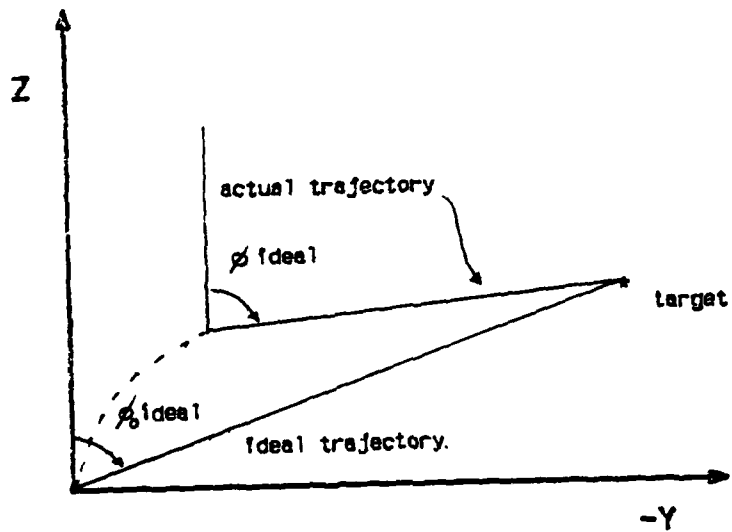


Figure 3.5b

Figure 3.5 Ideal Initial Roll Angles.

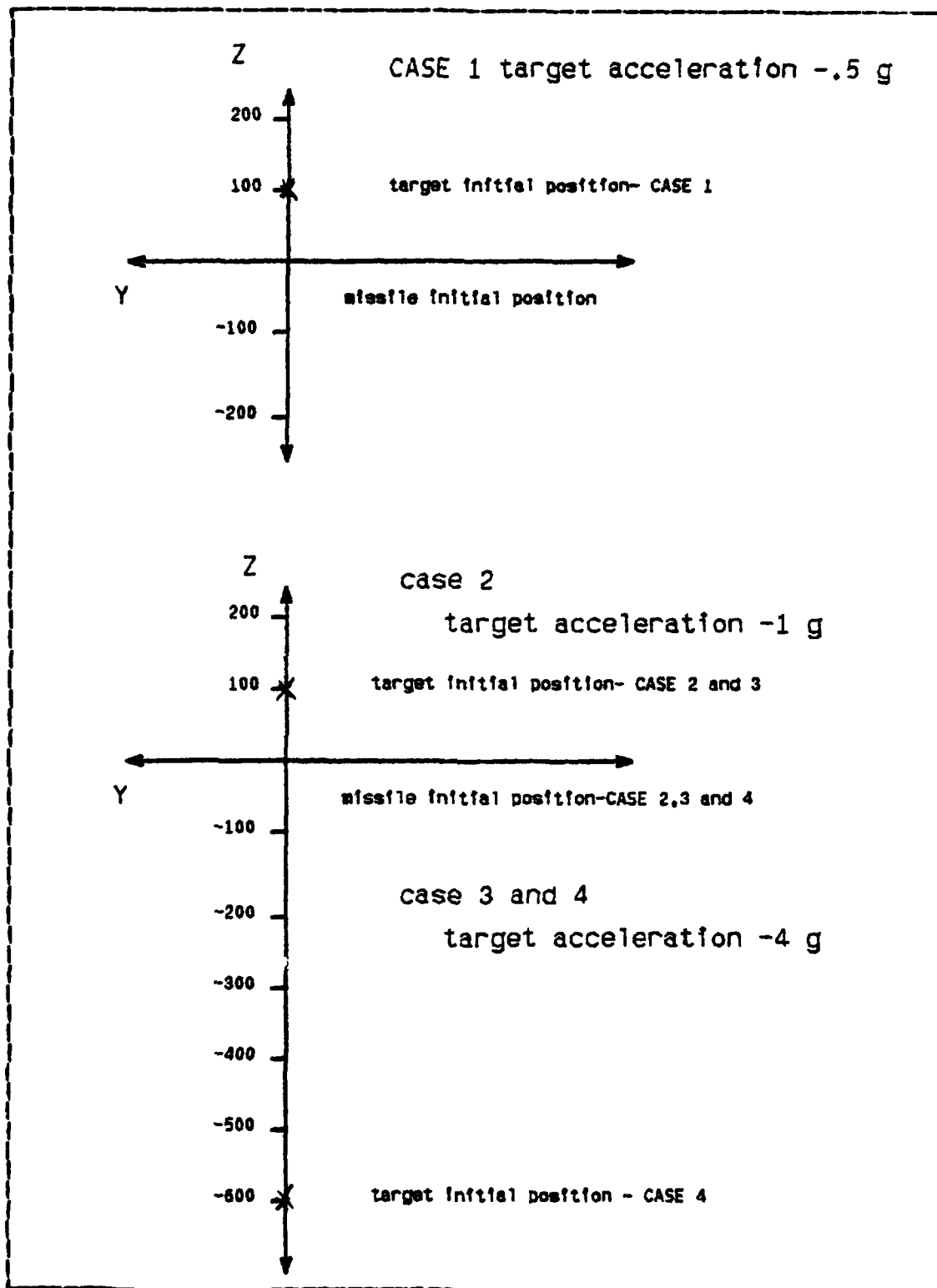


Figure 3.6 Scenarios for Simulation.

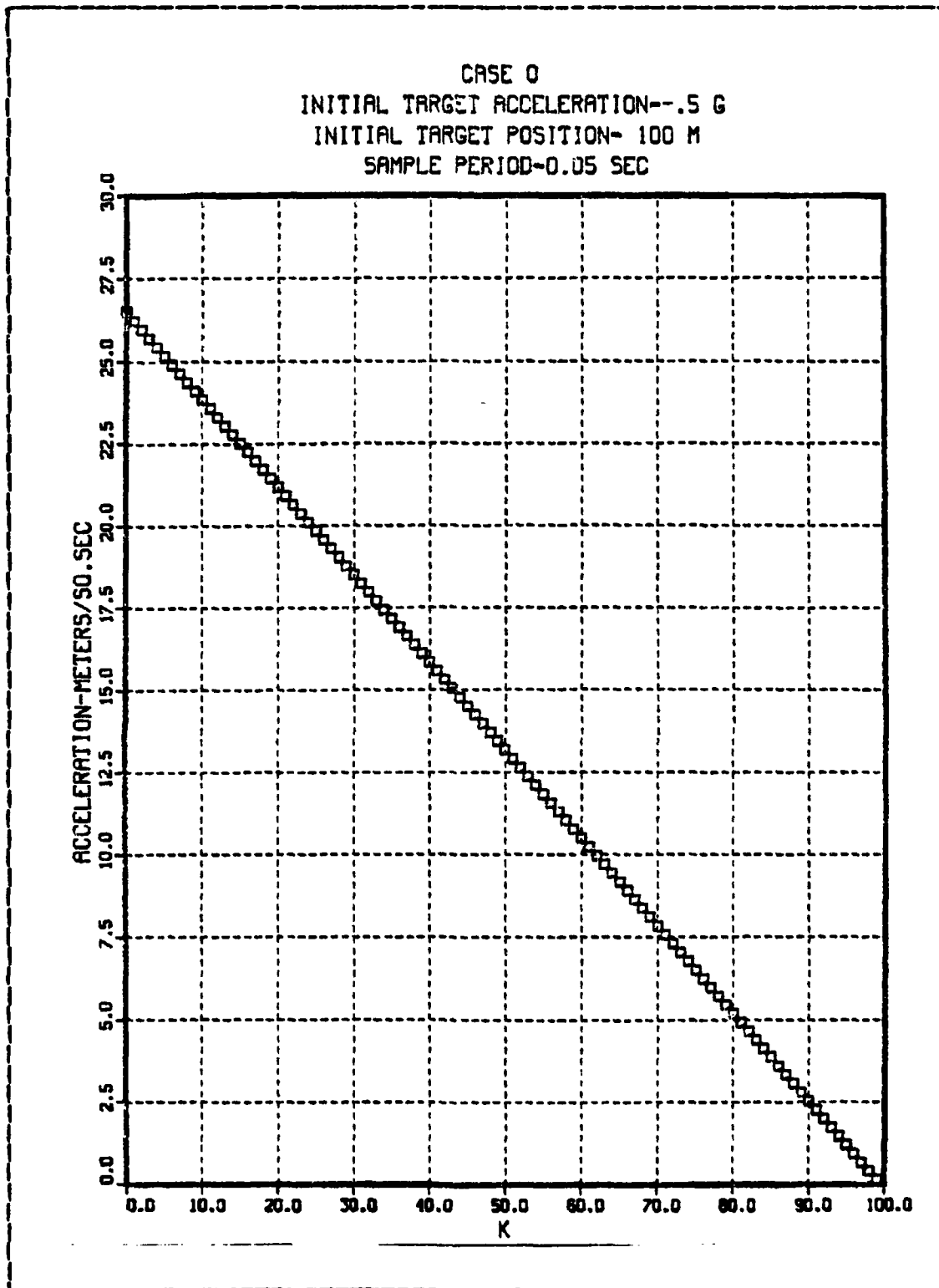


Figure 3.7 Commanded Acceleration- Case 0.

CASE 0  
INITIAL TARGET ACCELERATION--.5 G  
INITIAL TARGET POSITION- 100 M  
SAMPLE PERIOD-0.05 SEC

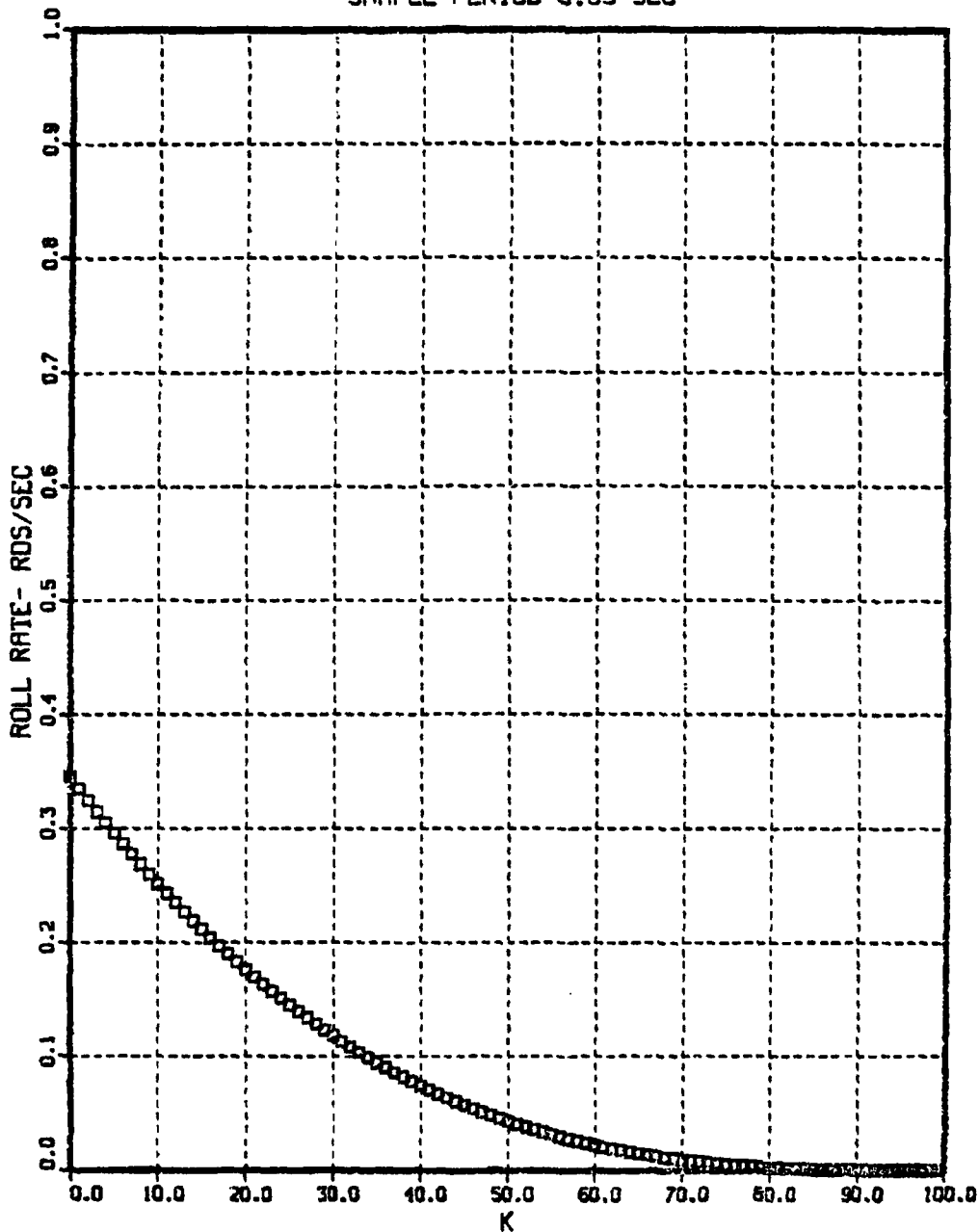


Figure 3.8 Commanded Roll Rate- Case 0.

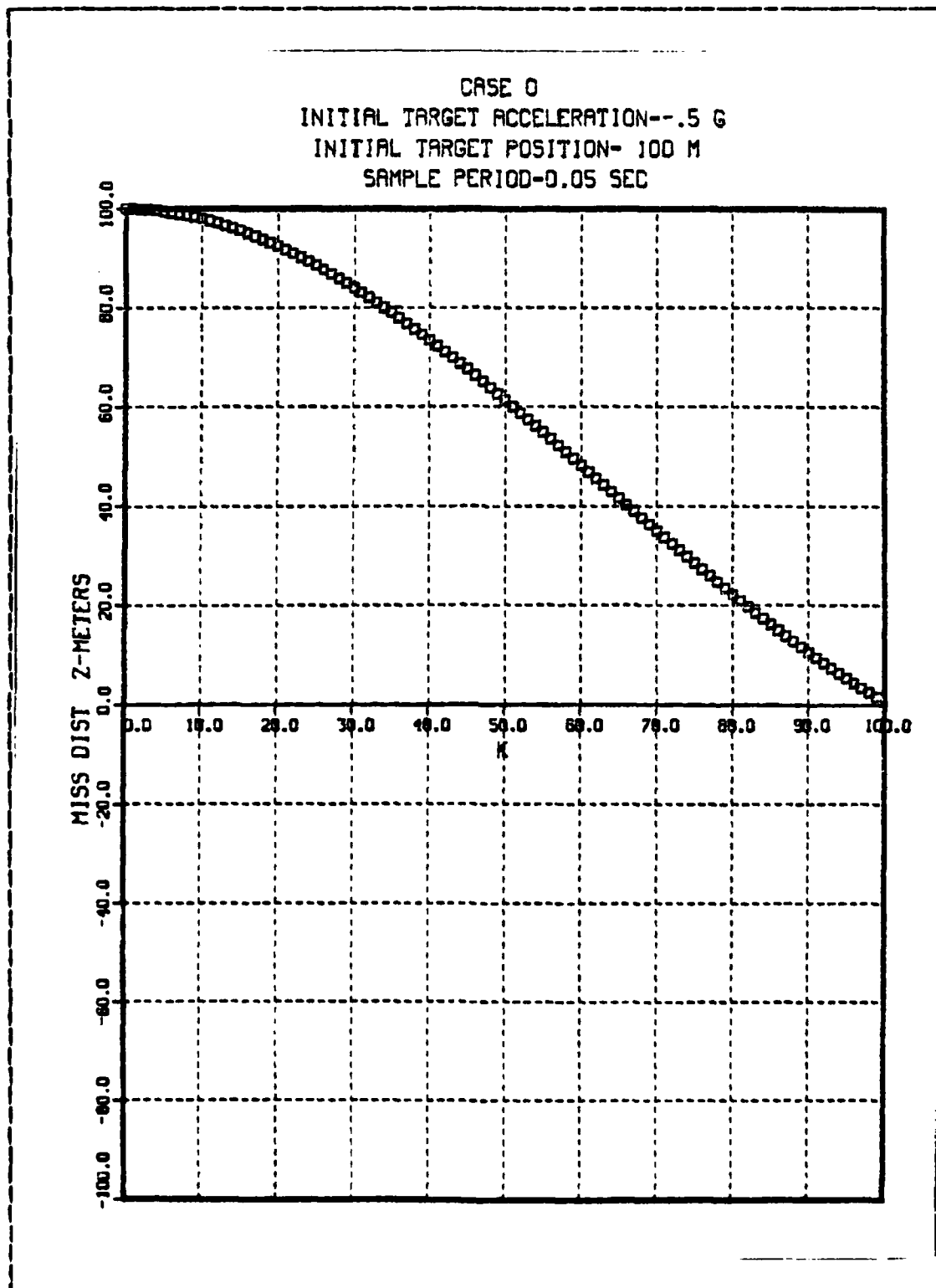


Figure 3.9 Miss Distance in Z Direction- Case 0.

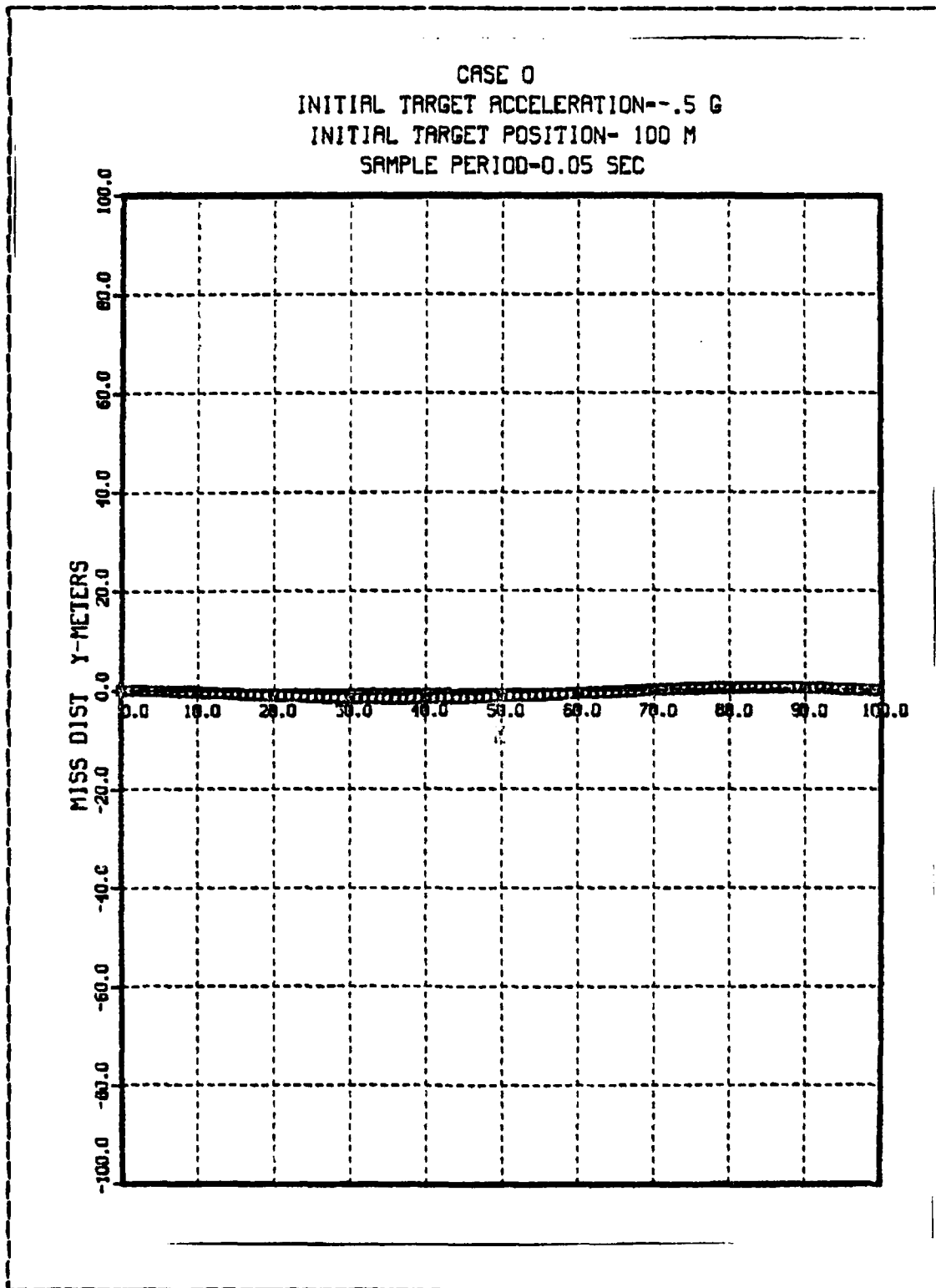


Figure 3.10 Miss Distance in Y Direction- Case 0.

CASE 0  
INITIAL TARGET ACCELERATION--.5 G  
INITIAL TARGET POSITION- 100 M  
SAMPLE PERIOD-0.05 SEC

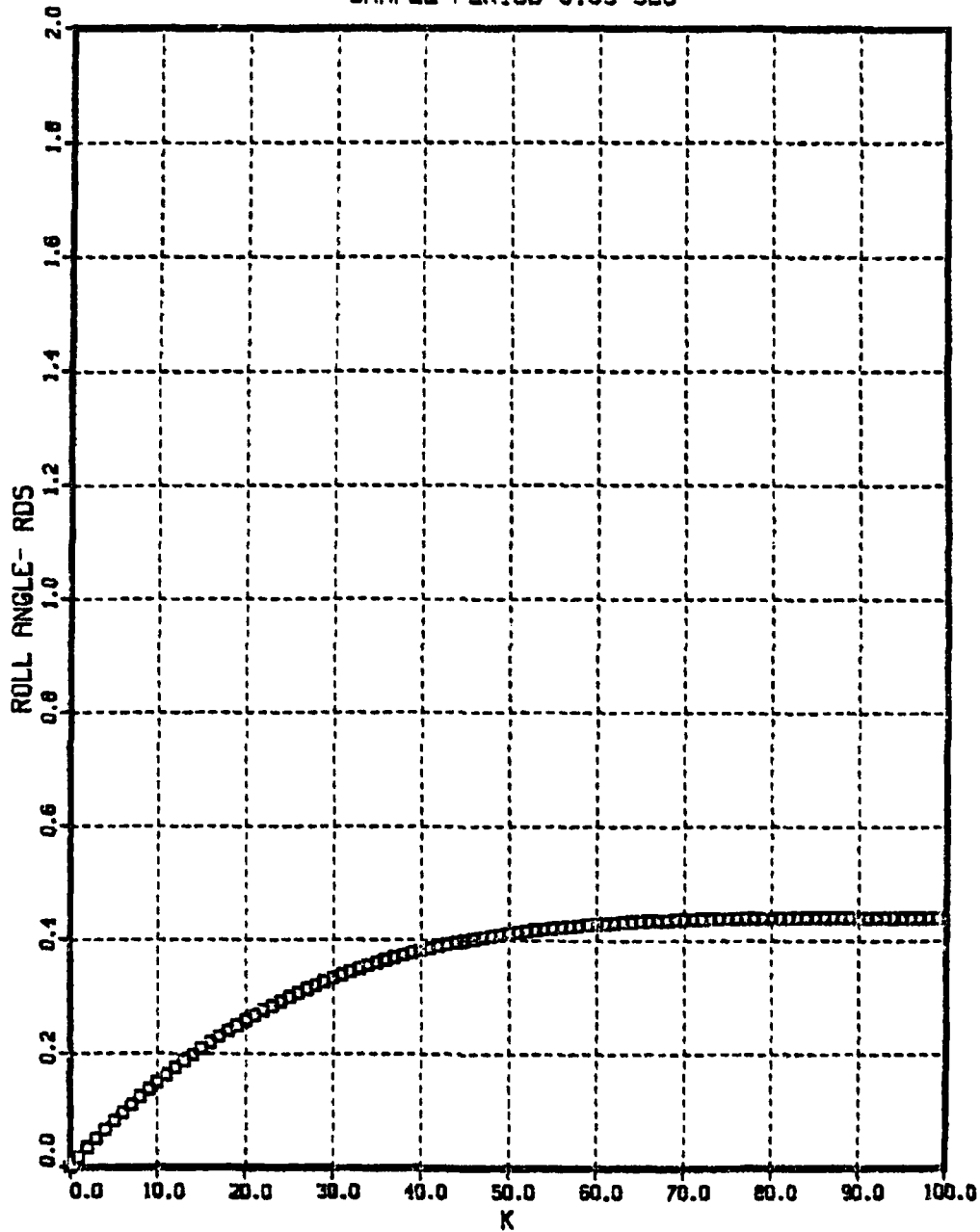


Figure 3.11 Roll Angle- Case 0.

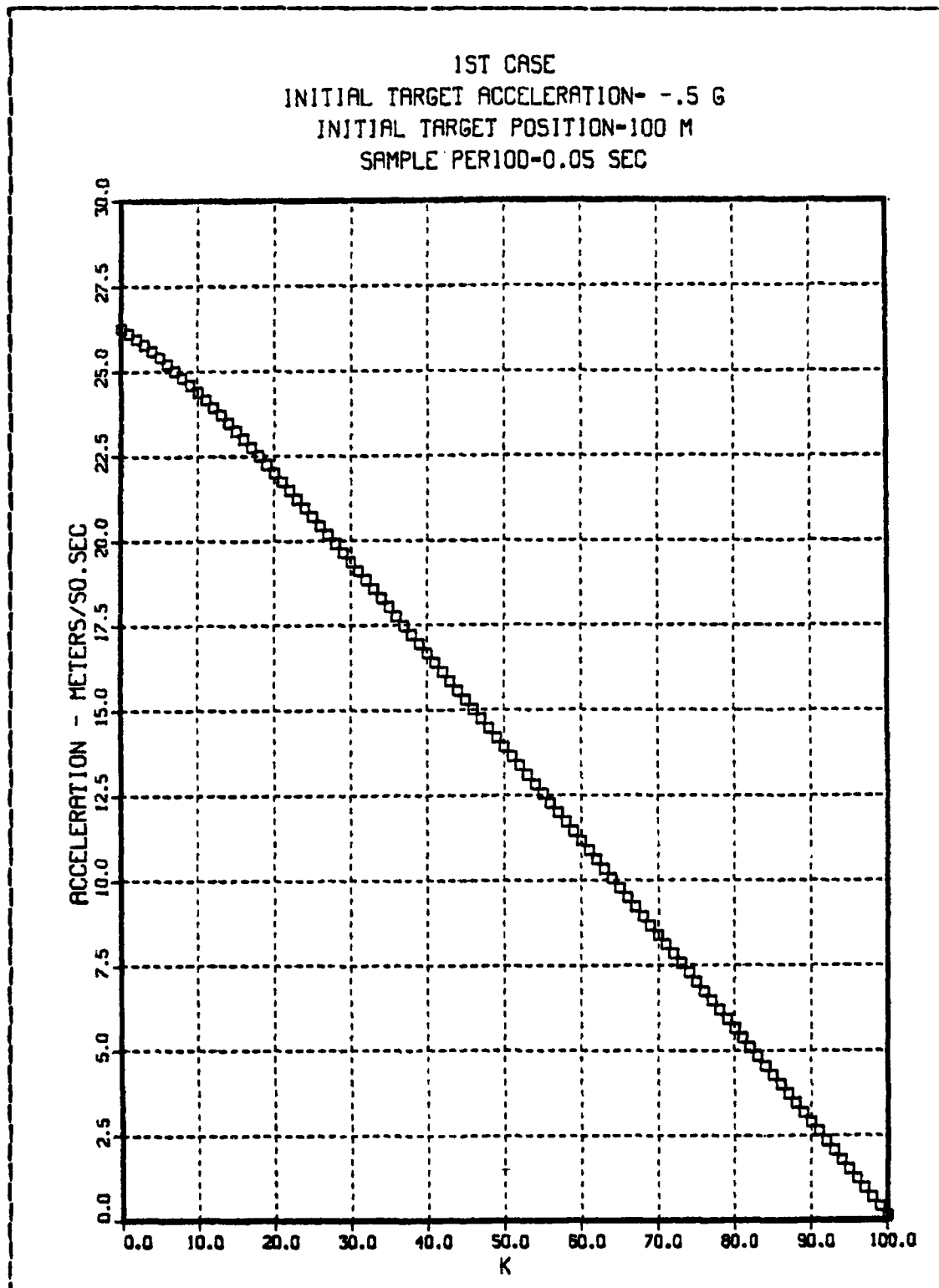


Figure 3.12 Commanded Acceleration- Case 1.

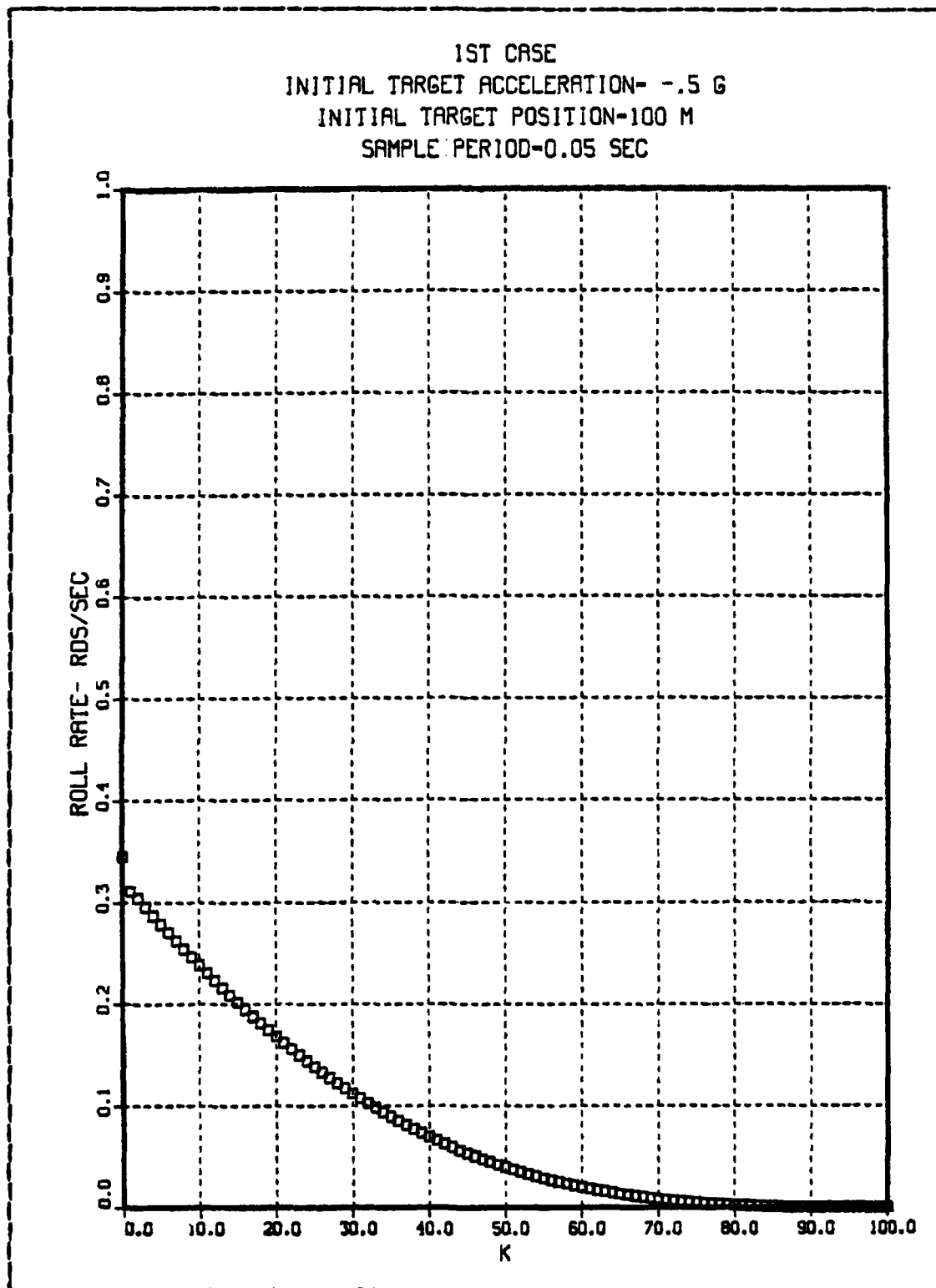


Figure 3.13 Commanded Roll Rate- Case 1.

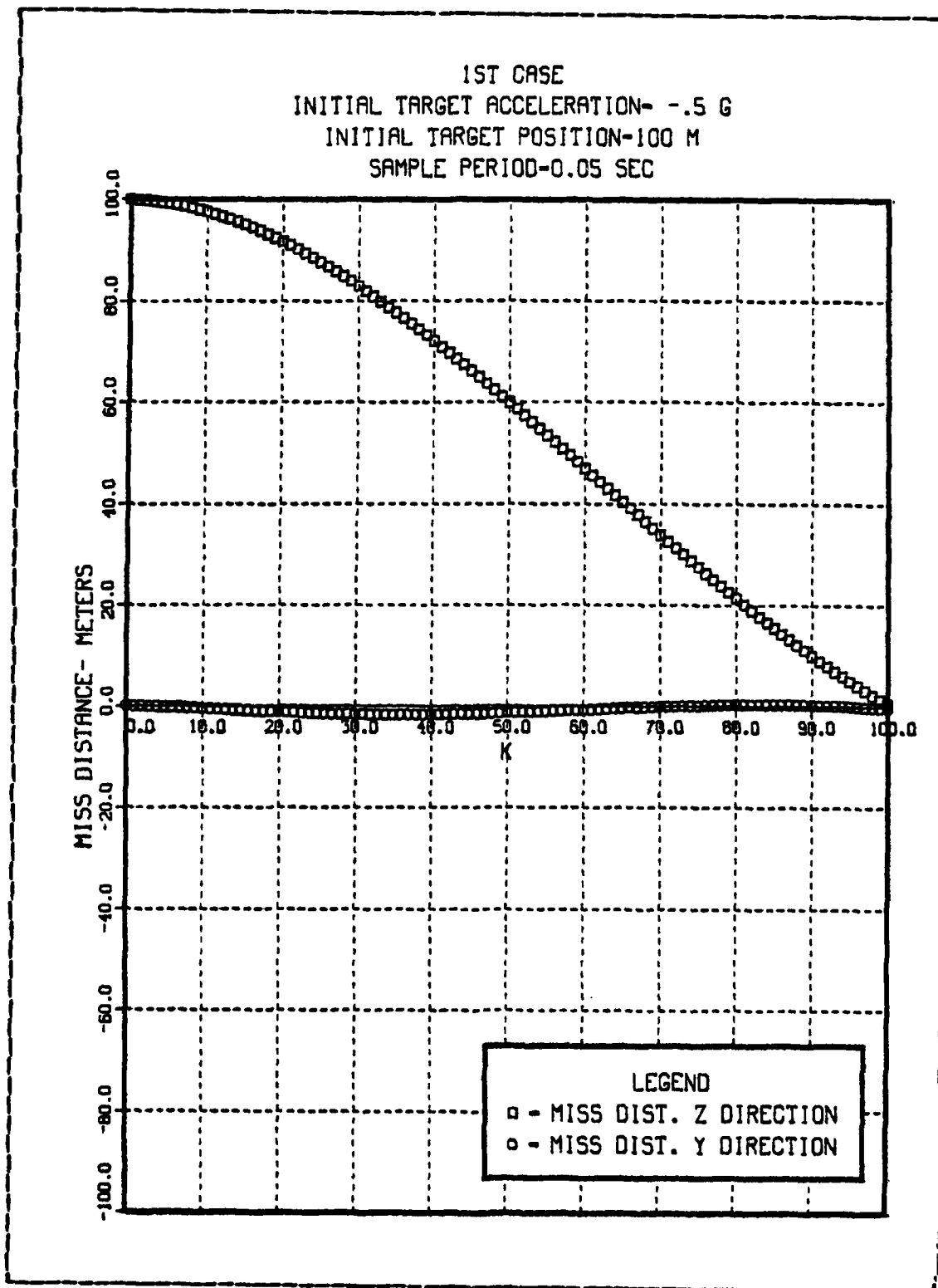


Figure 3.14 Miss Distance- Case1.

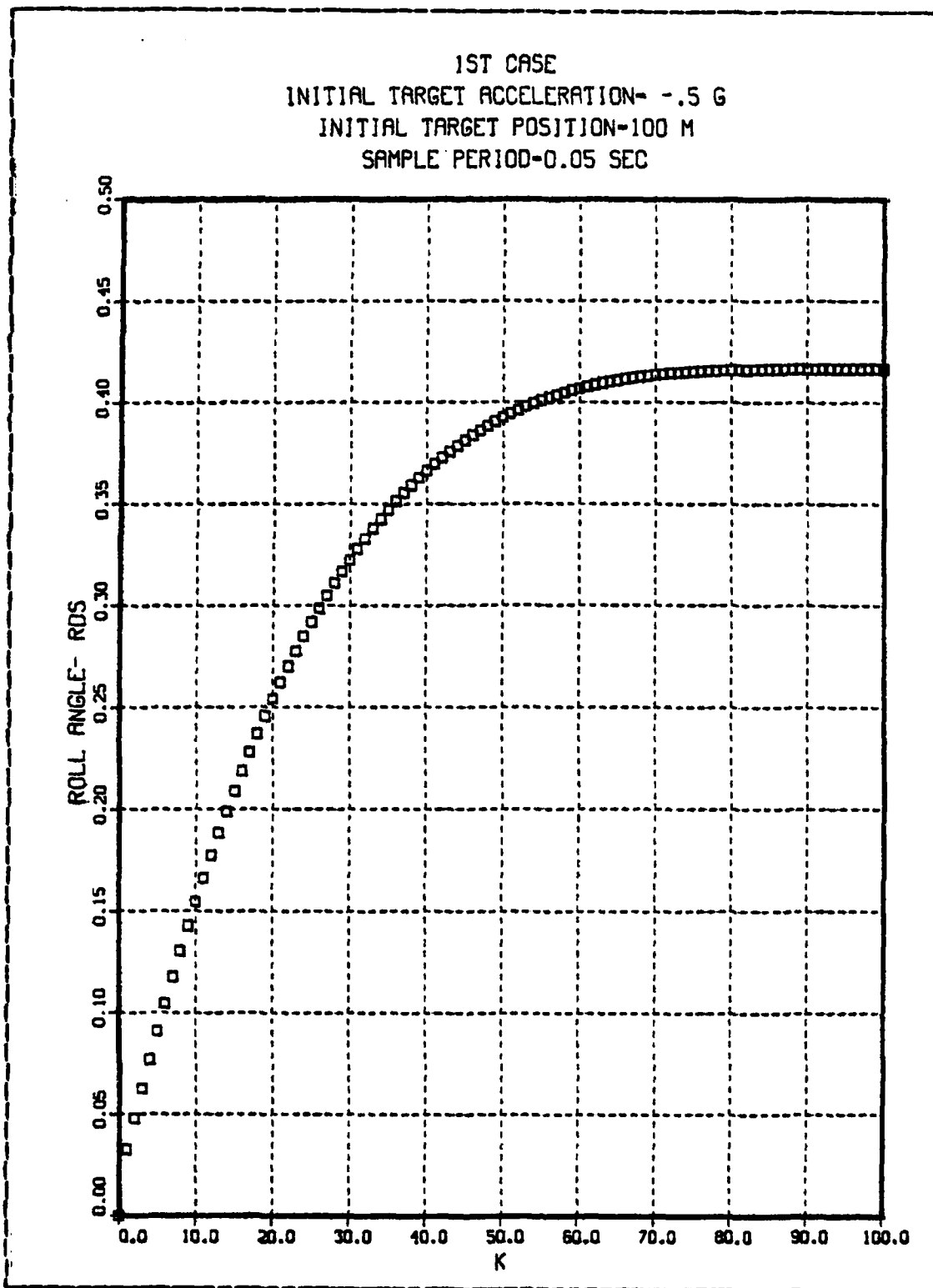


Figure 3.15 Roll Angle- Case 1.

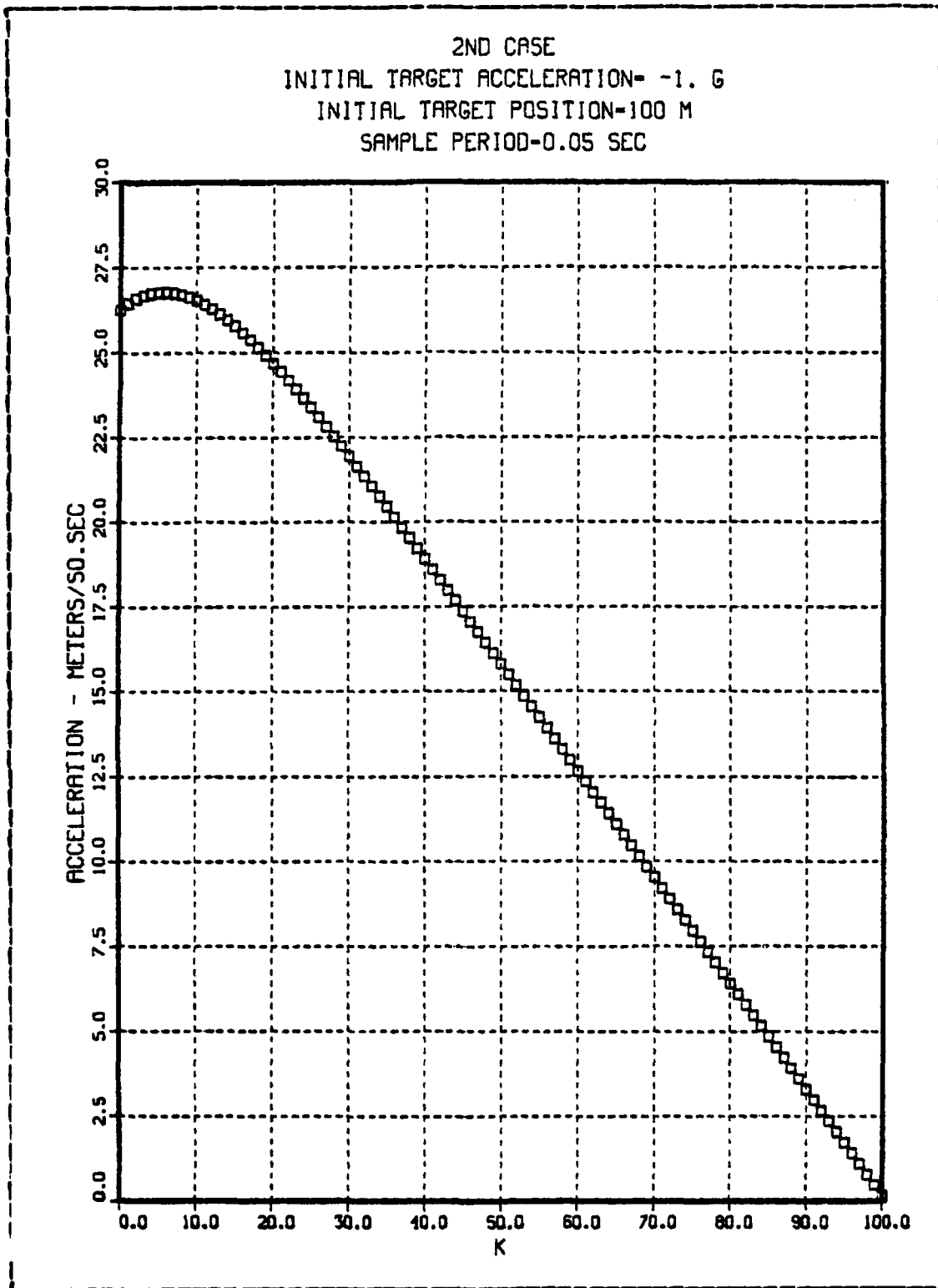


Figure 3.16 Commanded Acceleration- Case 2.

2ND CASE  
INITIAL TARGET ACCELERATION- -1. G  
INITIAL TARGET POSITION-100 M  
SAMPLE PERIOD-0.05 SEC

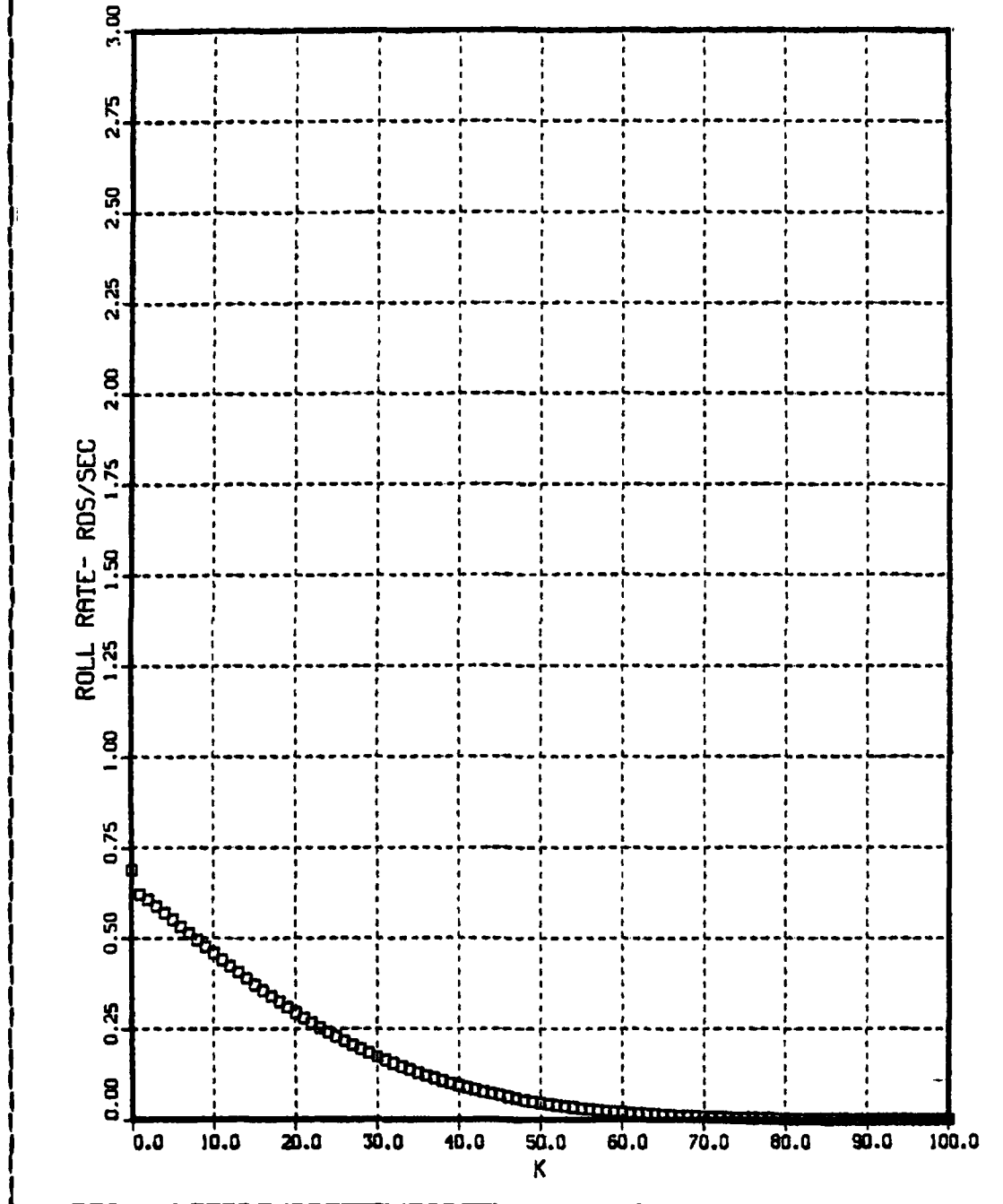


Figure 3.17 Commanded Roll Rate- Case 2.

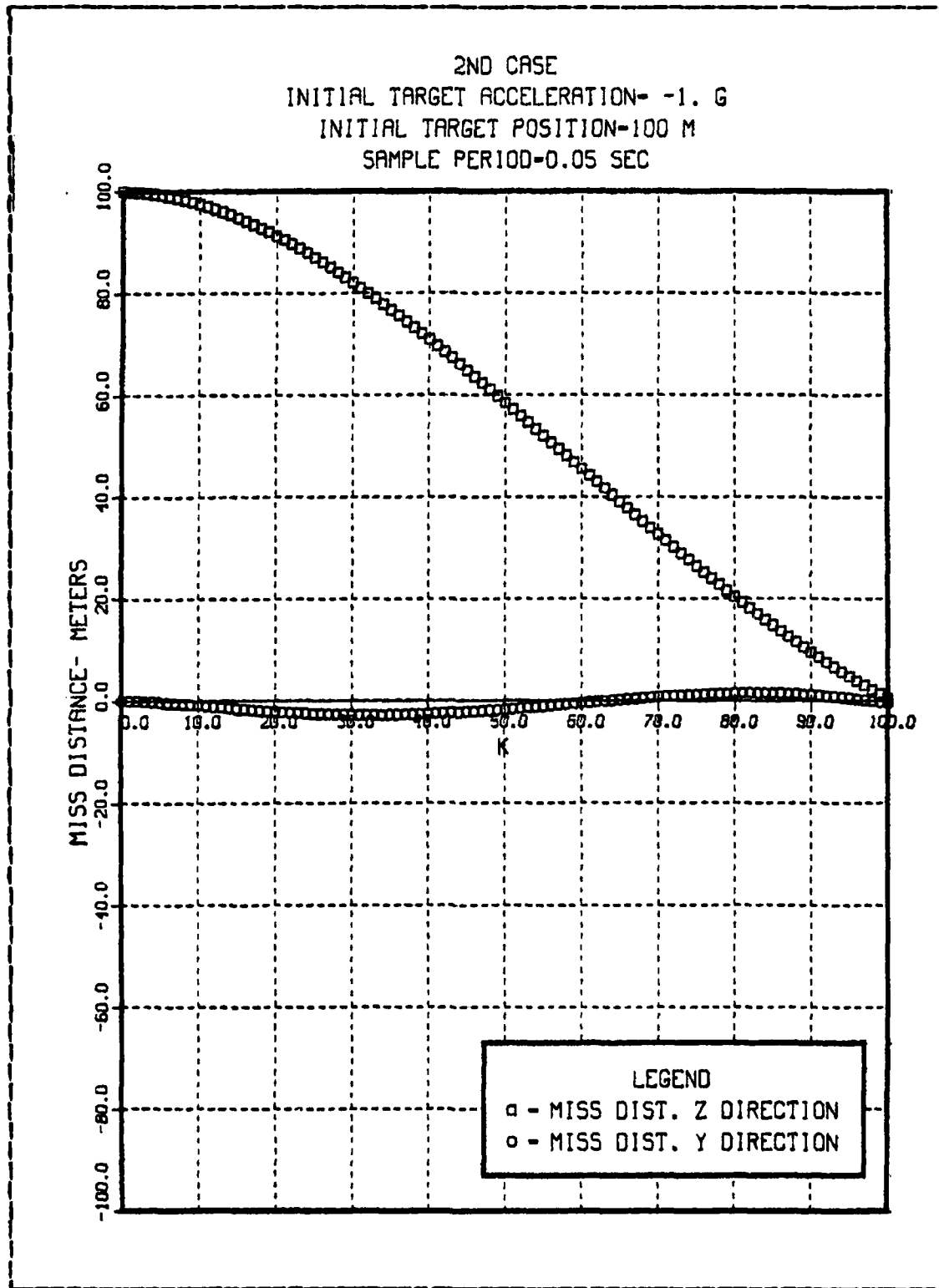


Figure 3.18 Miss Distance- Case 2.

2ND CASE  
INITIAL TARGET ACCELERATION- -1. G  
INITIAL TARGET POSITION-100 M  
SAMPLE PERIOD-0.05 SEC

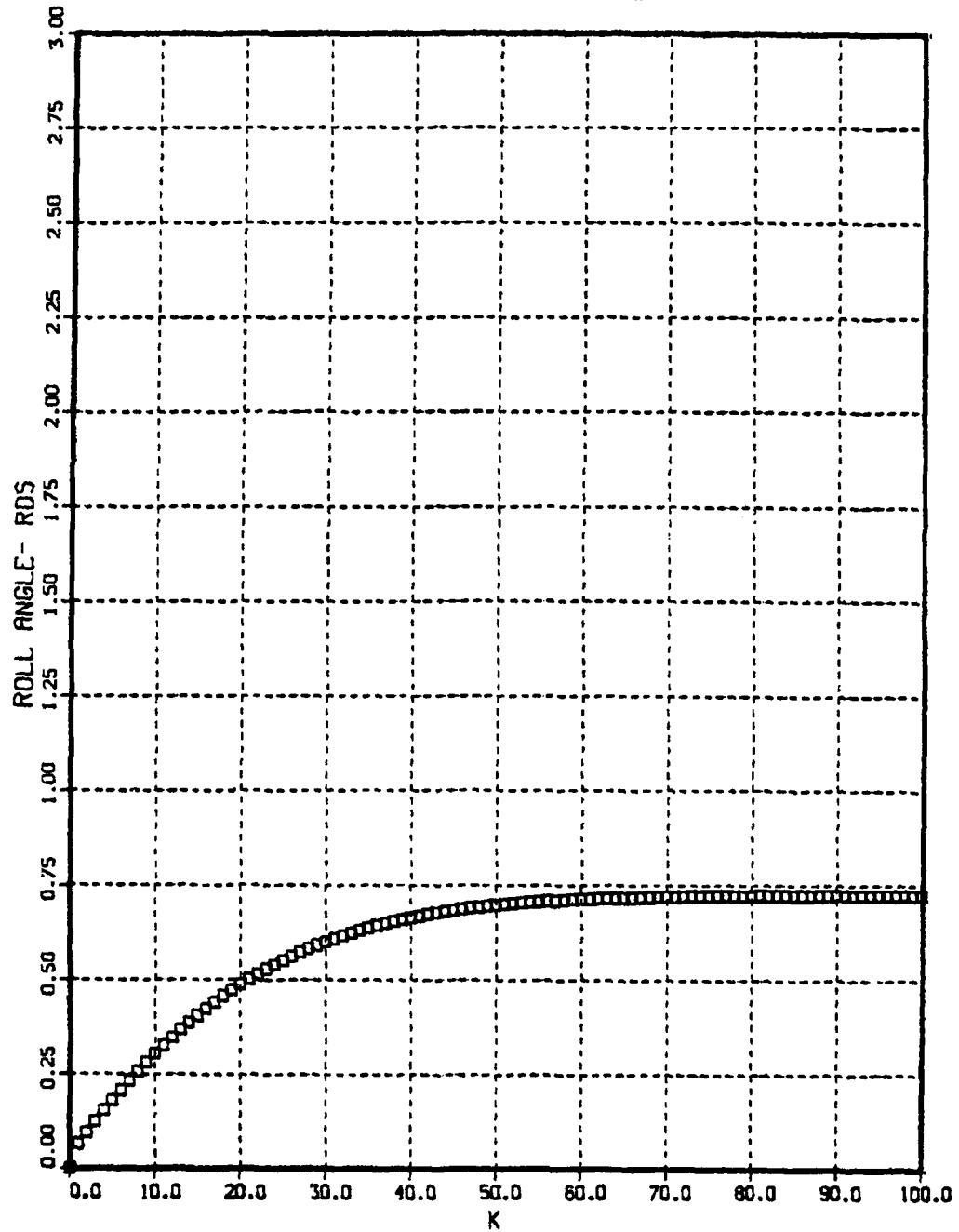


Figure 3.19 Roll Angle- Case 2.

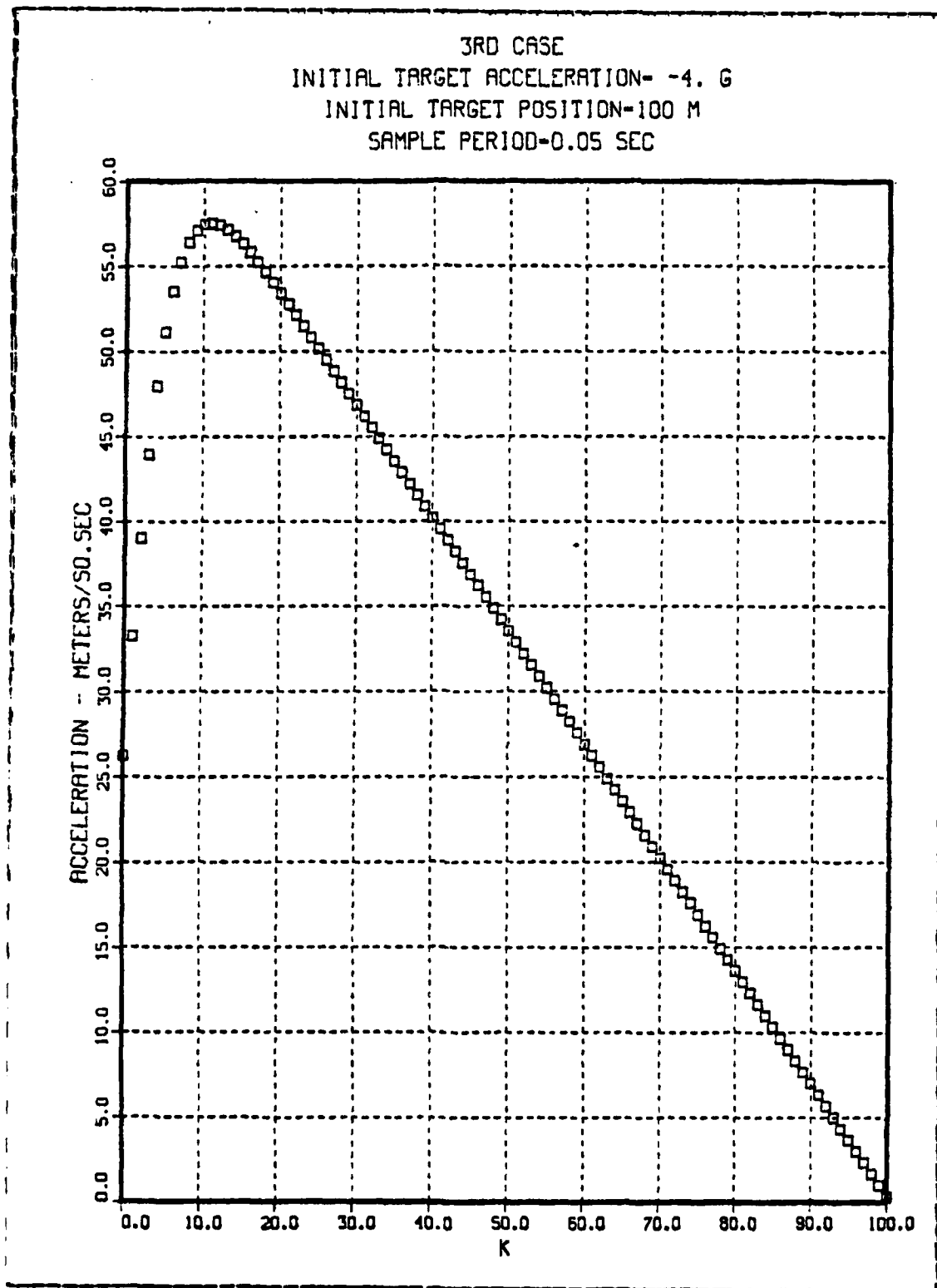


Figure 3.20 Commanded Acceleration- Case 3.

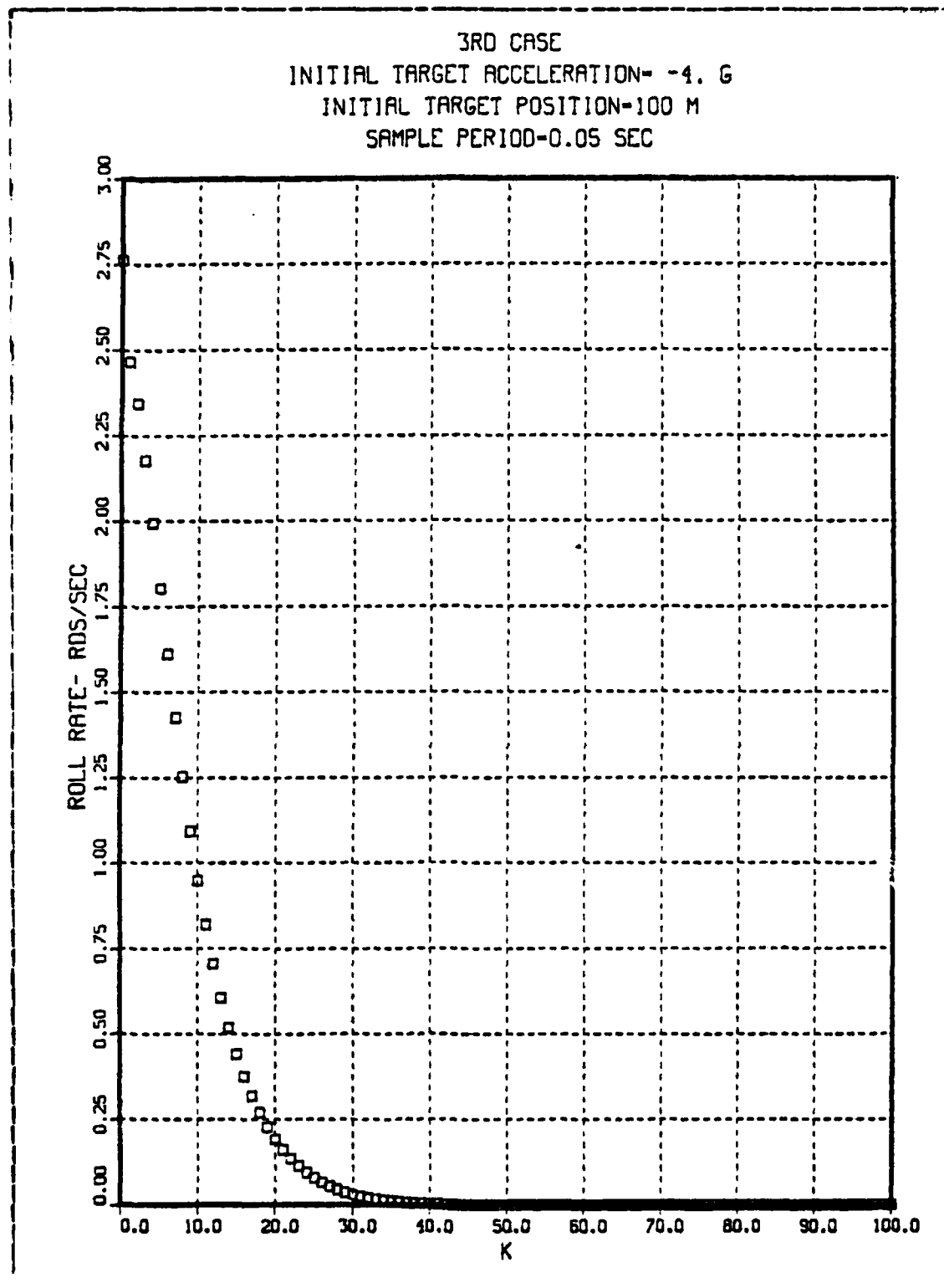


Figure 3.21 Commanded Roll Rate- Case 3.

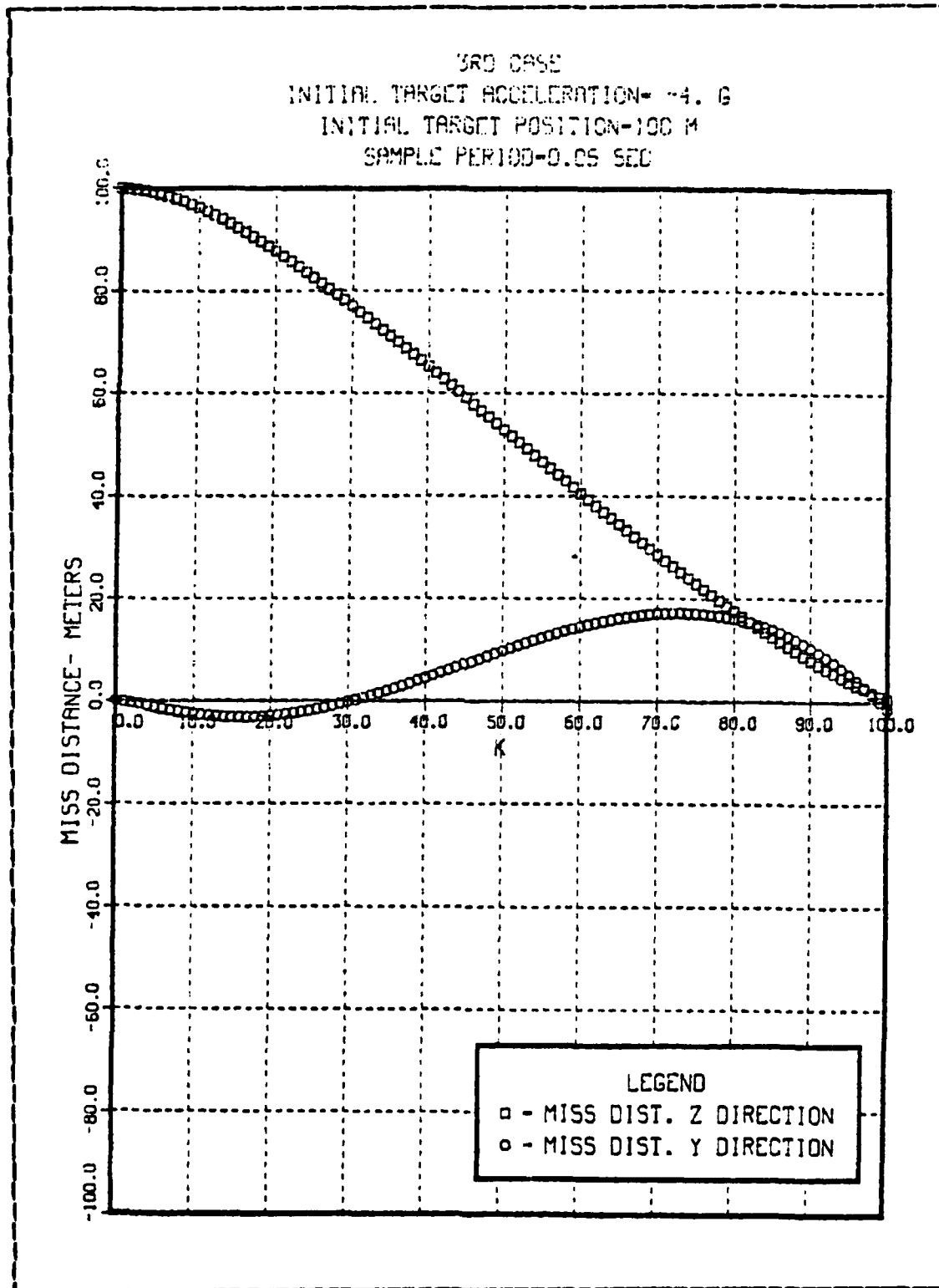


Figure 3.22 Miss Distance- Case3.

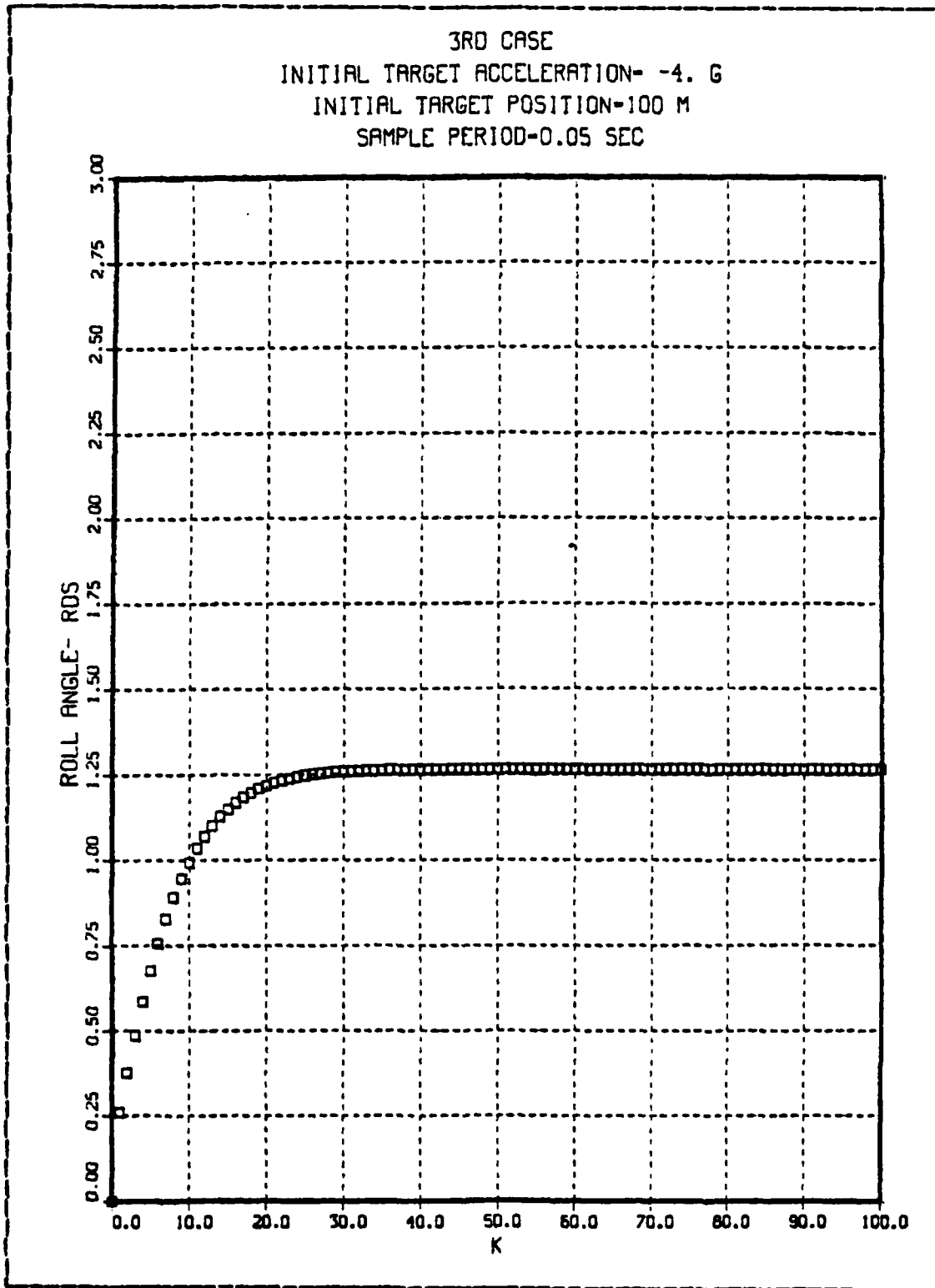


Figure 3.23 Roll Angle- Case 3.

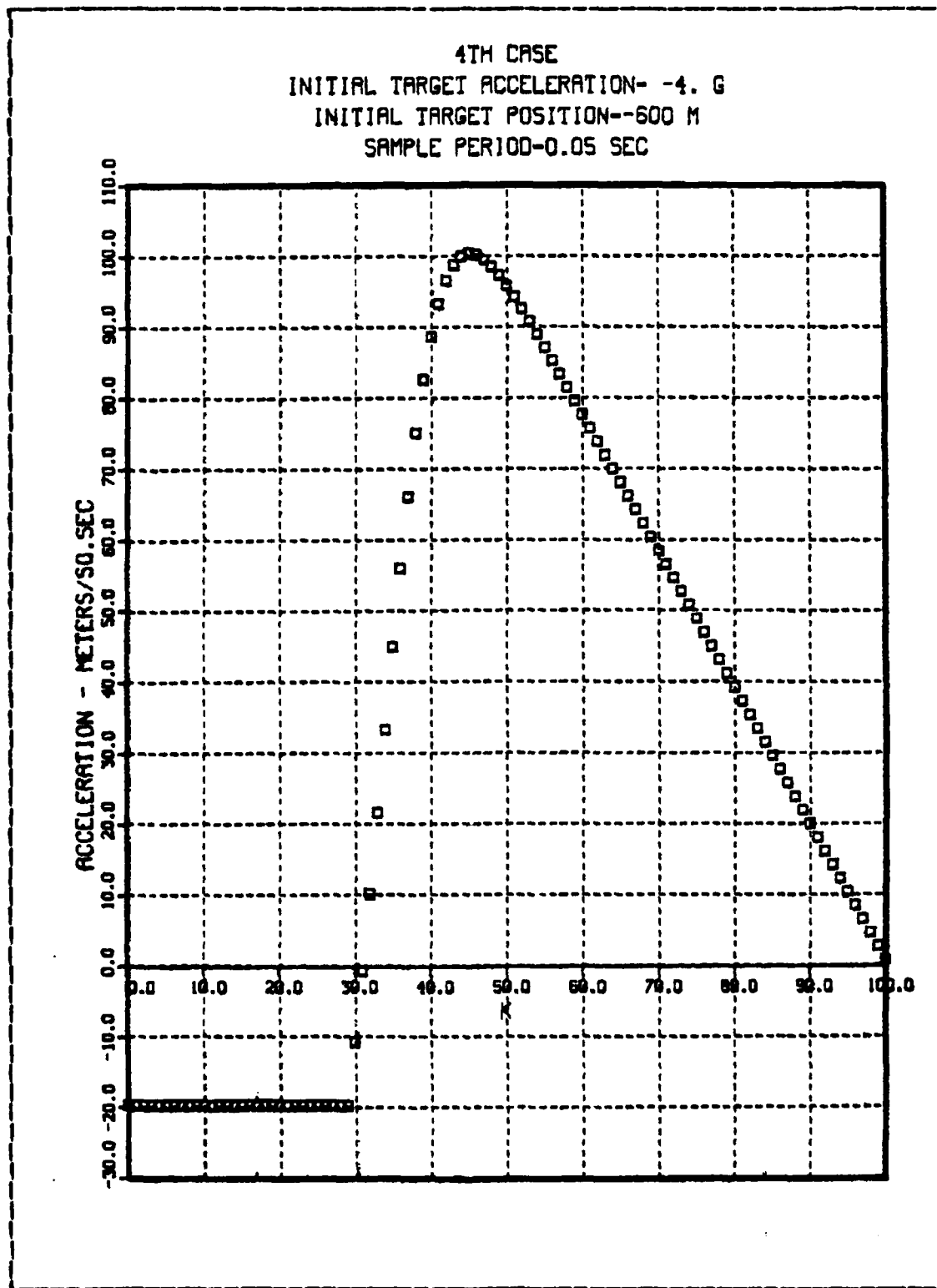


Figure 3.24 Commanded Acceleration- Case 4.

4TH CASE  
INITIAL TARGET ACCELERATION- -4. G  
INITIAL TARGET POSITION--600 M  
SAMPLE PERIOD-0.05 SEC

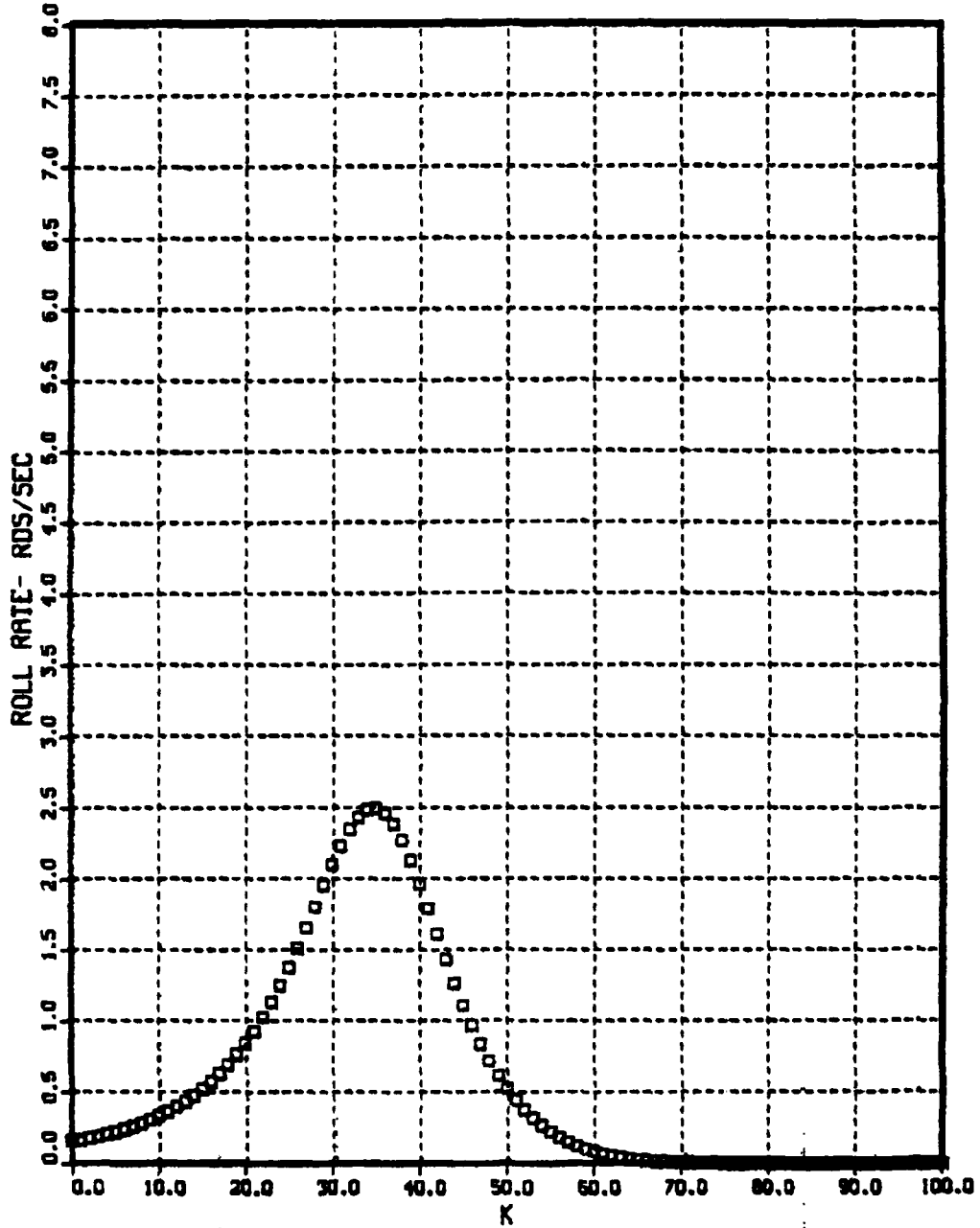


Figure 3.25 Commanded Roll Rate- Case 4.

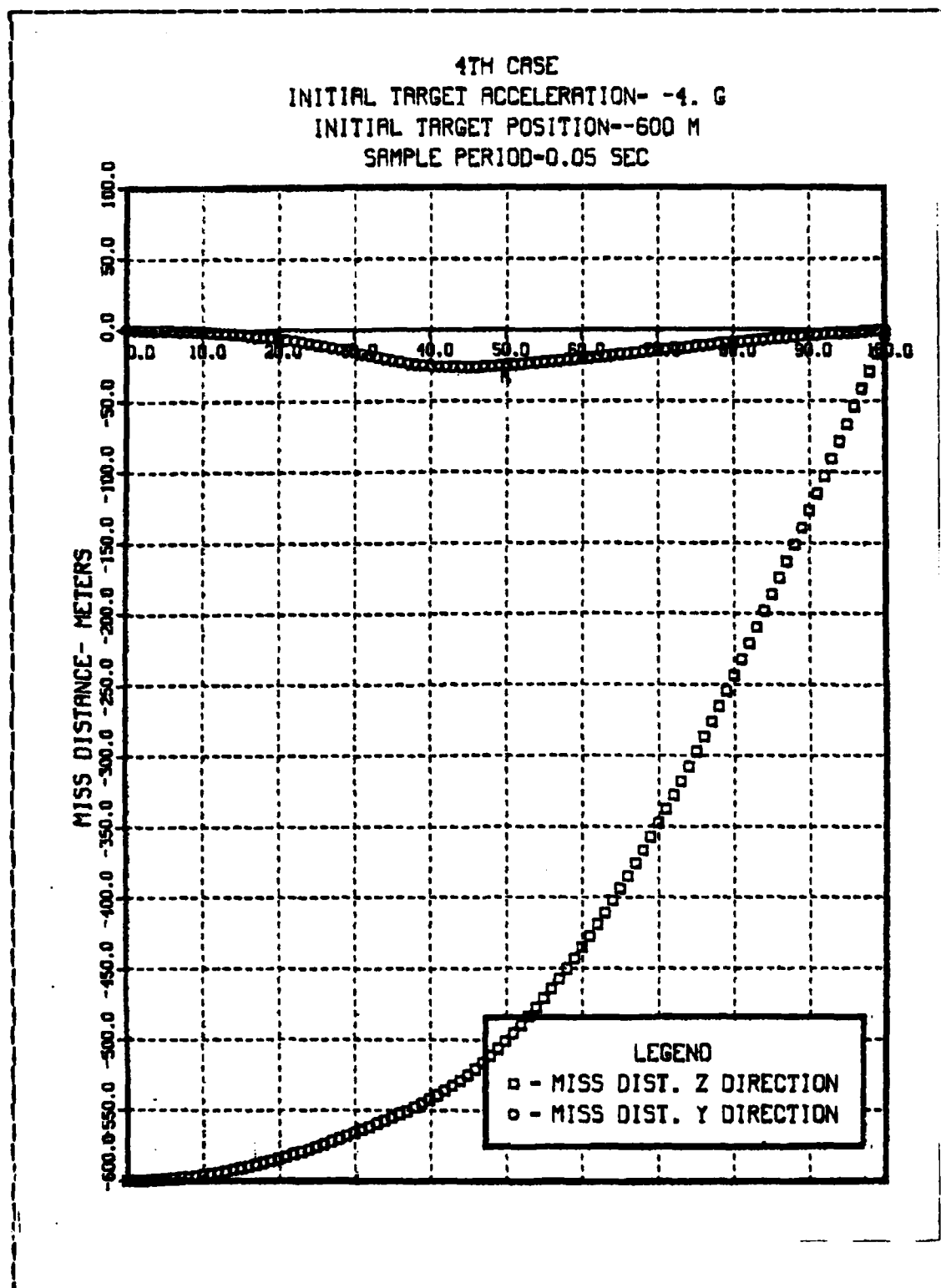


Figure 3.26 Miss Distance- Case 4.

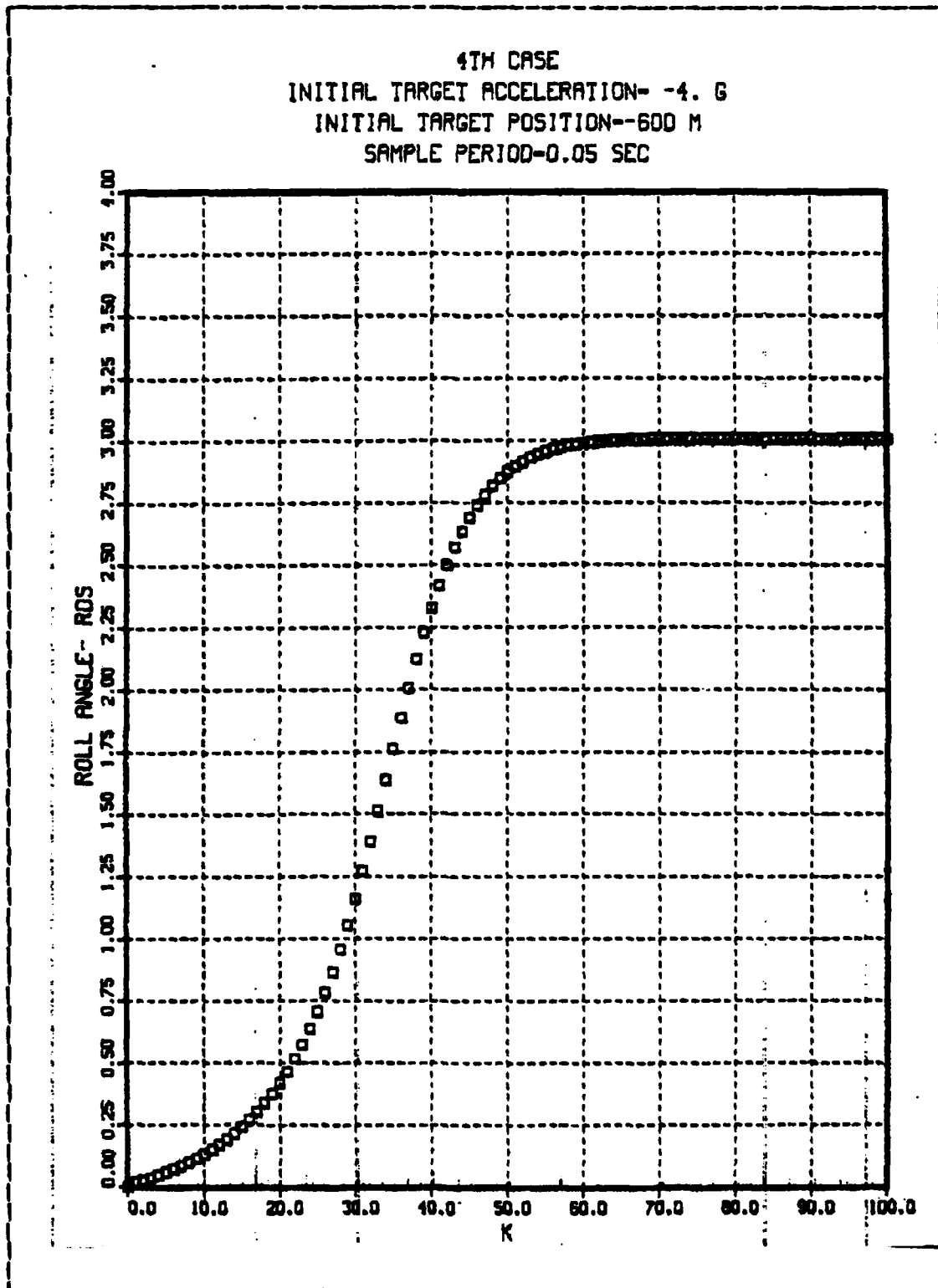


Figure 3.27 Roll Angle- Case 4.

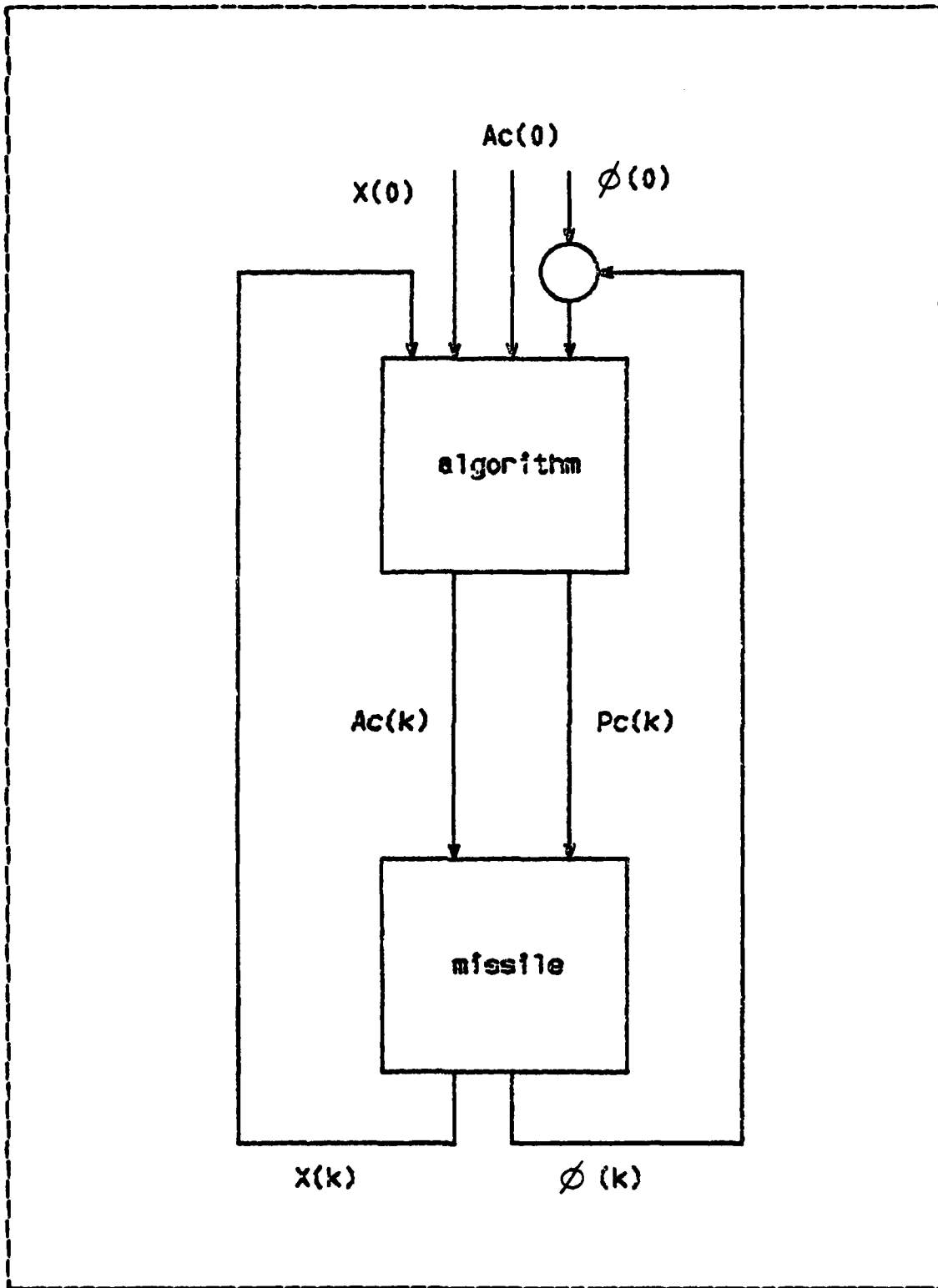


Figure 3.28 Corrected Model.

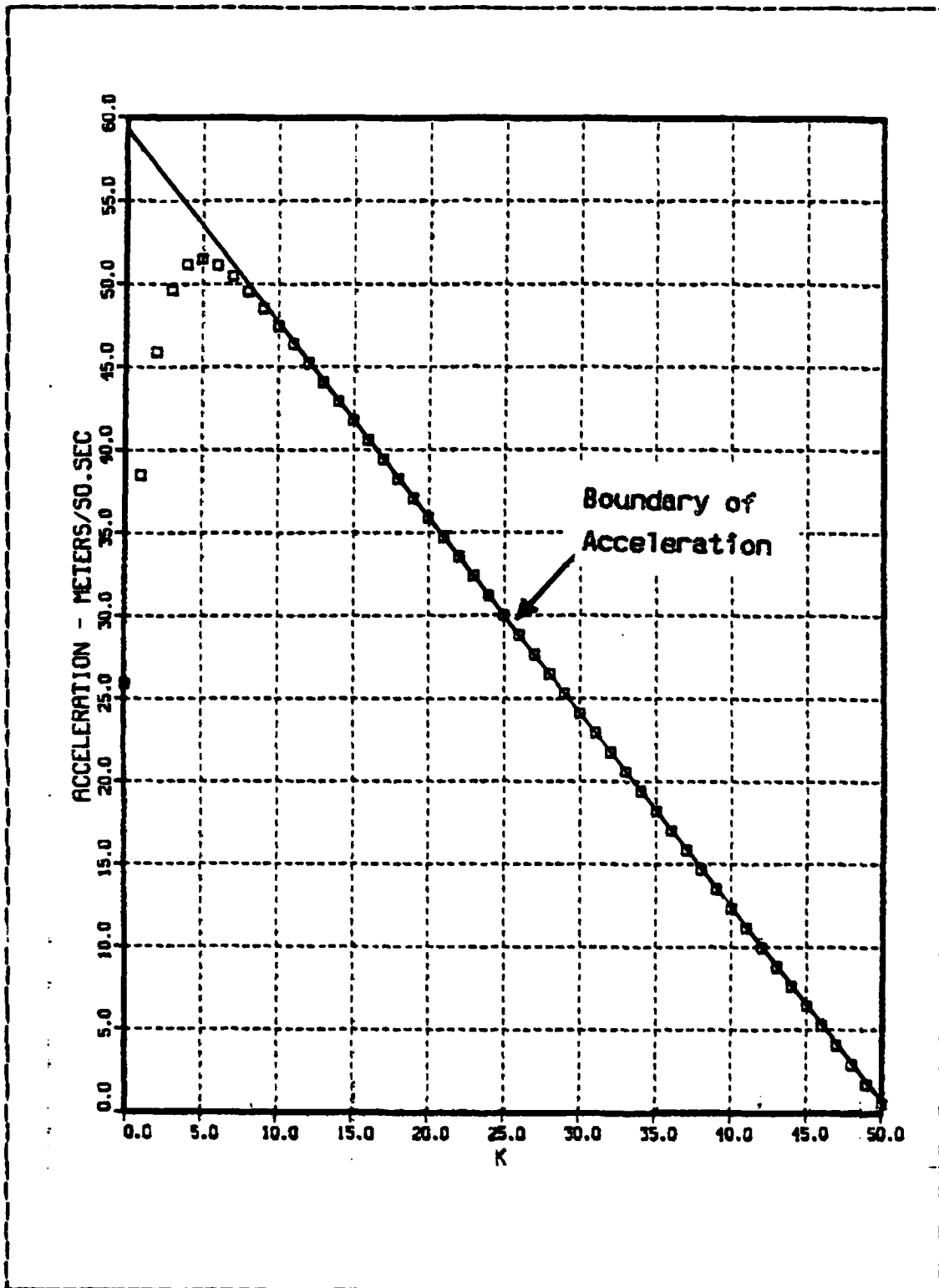


Figure 3.29 Boundary of the Commanded Acceleration.

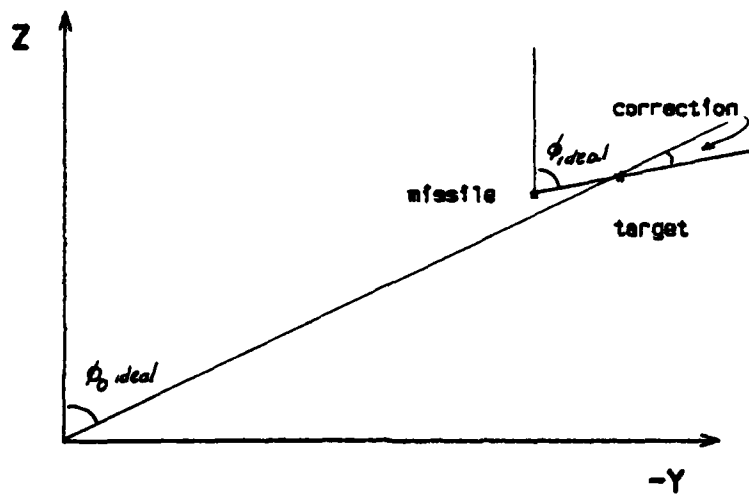


Fig. 3.30 a Large target accelerations

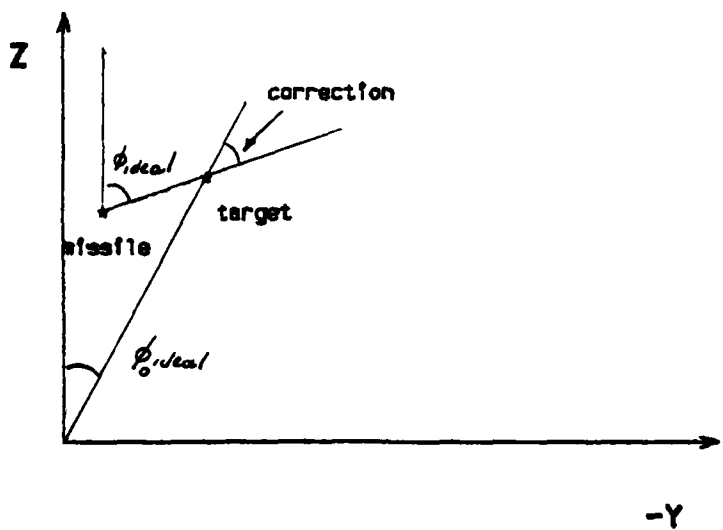


Fig. 3.30 b Small target accelerations

Figure 3.30 Corrections on the Roll Angle.

TABLE I  
Results From Tests

case	t	AC (m/sec)	PC (rad/sec)	miss distance y defraction (m)	miss distance z defraction (m)	$\phi$ (rad)	CG-to-CG miss distance (m)
0	0	26.47	.345	0.0	100.	0.0	100.
	Tf	.133	0.0	- .542	1.50	.439	1.51
1	0	26.47	.345	0.0	100.	0.0	100.
	Tf	.138	0.0	- .383	.528	.416	.652
2	0	26.47	.691	0.0	100.	0.0	100.
	Tf	.157	0.0	- .575	.458	.724	.735
3	0	26.47	2.76	0.0	100.	0.0	100.
	Tf	.332	0.0	-1.47	.046	1.27	1.54
4	0	-19.6	.167	0.0	-600.	0.0	600.
	Tf	.959	0.0	.592	-4.39	3.01	4.44

#### IV. ANALYSIS OF GAINS, SAMPLE RATE AND PITCH ANGLE

##### A. ANALYSIS OF THE GAINS

In chapter 3 has been developed a solution for the optimal control of a system as:

$$x(k+1) = A(k) x(k) + B(k) u(k) + E g$$

It would be interesting to check if the optimal gains reach steady state, but at the moment that the extension for large roll excursions has been introduced, and the system is being feed with optimal commands which are varying each step of time, such idea can not be applied. However one can do such check in the model for small roll excursions, which is actually used to compute the optimal commands.

Doing this, one has the time history of those gains as in 4.1 and 4.2

One can notice in fig. 4.1 that the gain  $FG(2,1)$  associated with the effect of gravity has no effect on the commanded roll rate, and that  $FG(1,1)$ , as shown in fig. 4.2, has a large effect on the commanded acceleration. Furthermore, this gain reaches steady state very fast, thus it can be assumed that the gain  $FG$  will be equal to the steady state value during all time.

From eqn. 3.19, and assuming steady state:

$$u(k) = -F(k) x(k) - FG(k) g \quad (4.1)$$

and substituting  $g$ :

$$u(k) = -F(k) x(k) - C \quad (4.2)$$

where the second term in the right hand side is a constant, and its value is exactly equal to the value of the commanded acceleration necessary at  $t=0$  to correct the gravity fall of the missile (or to correct the initial ZEM due to gravity).

It might be supposed that one could solve the optimal control problem for the system represented by eqn. 4.1, just considering one reduced system represented by:

$$x(k+1) = A(k) x(k) + B(k) u(k) \quad (4.3)$$

with a bias in the control as:

$$u(k) = -F(k) x(k) + C \quad (4.4)$$

But as showed in the following analysis, this is not possible.

The constant term in the right hand side of eqn. 4.4 is calculated as follows:

from eqn.:

$$\text{initial ZEM due to gravity} = ZEM = \frac{1}{2} g t^2$$

$$C = \frac{ZEM_g}{\left[ \frac{t^2}{2} - \frac{t^3}{6T_1} \right] \cos \phi_0}$$

and the gains  $F(k)$  are calculated using a Ricatti equation as usual.

Case 5 was tested using the above considerations, and using the same scenario of case 3.

Figures 4.3 and 4.4, show the time history of the controls. One can see that the commanded acceleration has begun at same values as in case 3, but the commanded acceleration reaches a peak considerable higher, then decreases does not following a linear law, with a final at 14.7 meters per second square, being this terminal value due to the constant term representing the effect of the gravity.

Referring to fig. 4.4, the commanded roll rate begins at a same value as in case 3, but as the control  $A_c$  is too high, it reaches negative values, going to zero almost at the end of the running time. This behaviour of the control leads to a large miss distance as seen in figure 4.5, and table II.

Figure 4.6 shows the time history of the roll angle, which rises to values close to 1.5 radians. As the acceleration at this point is larger than the correct value, the corrections are excessive and the roll angle decreases at the end of the running time to the value of .12 radians.

Thus, one can see that the gain due to the gravity's acceleration can not be replaced by its steady state value. This kind of simplification can thus not be done in the system being studied.

#### B. EFFECT OF THE SAMPLE RATE

Throughout all the simulations a sample period of .05 seconds has been used. In this section a brief study of the effect of the change of this sample rate is given.

Two best cases have been selected to illustrate the effect of the sample period.

The first case, case 6, has been run with a sample period of .1 seconds and consists of the same scenario as case 3.

As one can see in figure 4.7 and table III, there is no noticeable change in the commanded acceleration, but the commanded roll rate begins at smaller value than in case 3, as is seen in fig. 4.8. This initial decrease in roll rate, leads to a large miss distance in Y direction as shown in fig. 4.9, and to a small value of roll angle (see fig. 4.10).

The second case, case 7, has a sample period of 0.025 seconds. There is no noticeable change in the time history of the control  $A_c$  as shown in fig. 4.11. The commanded roll rate begins at a higher value than in case 3 as shows fig. 4.12, which leads to a final miss distance in Y direction of -2.22 meters and in Z direction smaller than case 6 (see fig. 4.13). Figure 4.14 shows that the final roll angle is increased and the missile cross the target with 1.28 radians and with a CG-to-CG distance of 2.5 meters.

In both cases, the miss distance was increased over the nominal value obtained with a sampling rate of 0.05 seconds. Thus, it would appear that there is an optimal value for the sampling rate, which may be connected with the geometry of the scenario and with time to go.

### C. EFFECT OF THE INITIAL PITCH ANGLE

It is important at this step to remember that throughout this work as we have been discussing a dimensional model, where there is no information on the X coordinate, so it is impossible to verify the behavior of the pitch angle.

In this work, since in all the previous scenarios the initial angle  $\theta$  was equal to zero, this value has been kept as a constant during all time, and considering that without any information of a third dimension it was not possible to correct the time to intercept, this time was also kept constant and equal to the nominal value of 5 seconds.

Notice that this assumption is likely to be correct if one has the horizontal initial distance from target to missile compared with the initial vertical distance between target and missile large enough in order to have small angles.

The question that rises is, how could this pitch angle affect the system if it was not small?

As seen in fig.4.15, the missile velocity in the X direction would be:

$$V_{mx} = V_m \cos\theta + g \cos\theta \sin\theta t \quad (4.5)$$

which has an effect not only from the pitch angle, represented by the  $\cos\theta$ , but also from the gravity's acceleration, which will leads to a different time to intercept.

Considering the same physical scenario as in case 4, but changing the initial pitch angle, in order to have the missile pointing to the target (see fig.4.16), and keeping the missiles velocity of 1000 m/sec in the X direction, one has a completely different geometry of the problem as seen from the flight path reference frame.

With this new situation (see fig. 4.16), case 8 has been run. Figures 4.17 and 4.18 show that now the missile is comanding large positive accelerations, and the roll rate at the begining of the flight is too high, going to zero in a very small period of time. The miss distance as seen in fig.4.19 are increased in the initial part of the flighth and as the missile corrects its trejectory it is decreased to reach a final CG-to-CG miss distance of 2.17 m. The roll angle, due to the large control Pc is oscilatory in the begining and becomes constant with a value of .57 radians (see fig.4.20 and table IV).

Notice that the high values of acceleration needed are in some part due to a vertical component of target's velocity, which is seen from the flight path frame as the target was manouvering in the Z direction with constant velocity. These large accelerations leads to roll rates too large for the physical integrity of the missile. This means that although although the good results obtained, if compared with case 4, they are not practical.

In order to get rid of the vertical manouever of the target, case 9 has been run. In this case, the scenario is the same as before with the target also pointing down, with the same pitch angle as the missile, and has a X velocity equal to the previous case (see fig.4.16).

From fig.4.21, one can see that the decrease in the control  $A_c$  is substantial if compared with case 8, but the commanded roll rate is still too large as shows fig.4.22 The time history of the miss distance is better, resulting in a final CG-to-CG distance of about 50% of case 8 (see fig.4.23). The roll angle is not oscillatory as seen in fig.4.24 and the missile cross the target with 1.3 radians in roll. (see tableIV).

The results obtained in the two previous cases, suggests that the algorithm developed in this work could be readily applied to air-to-surface missiles. In the latter, the scenario would be favorable to the missile than in either previous cases, since one can consider that the target could be essentially stationary in comparison with the missile speed.

Case 10 has been run with this assumption, and the scenario as in fig. 4.16. The target is with zero velocity and acceleration, and the missile begins its flight 600 meters above it, with the same initial pitch angle as before.

Fig.4.25 shows the time history of the commanded acceleration, where one can see that as there is no roll rate to

be commanded, the acceleration is following a straight line with very reasonable values. The miss distance is shown in figure 4.27, which shows the final CG-to-CG distance of .31 meters.

Based on the results of these tests, one can see that there will be some effect of the pitch angle on the miss distance, not only due to its effect on the time to intercept, but also because at the moment that there is a pitch angle different from zero, even if the target is keeping its flight level, in the flight path frame a component of the target's velocity will show up leading the missile to command large accelerations and roll rates. Although this results harm the performance in an air-to-air missile, in the case of air-to-surface missiles, when the target has been considered with no motion, good results have been obtained.

#### D. EFFECT OF TIME TO INTERCEPT

In the simulation of case 1 and 2 in chapter 3, it has been observed that when the target was at small accelerations, the missile did larger corrections on its roll angle, with respect to the ideal initial roll angle, than when the target was with large accelerations. One can think that must be some kind of compromise between the velocity rate of target and missile (which will be reflected on the time to intercept), and the relative position between them, which will affect the miss distance.

In order to do a brief analysis on this, case 11 and 12 has been run.

In case 11, the scenario of case 2 has been kept, with the exception that the missile's velocity was changed to 2000 m/sec., which means that  $T_i$  was changed to 2.5 seconds.

Figure 4.29 shows that the acceleration is largely increased due to the small time required to correct the ZEM, and the commanded roll rate is almost twice of case 2 (see fig. 4.30). The final miss distance is more than four times the value obtained in case 2, as seen in fig. 4.31 and table V. The final roll angle is about half as in case 2, since the projected final position of the target in the Y direction is less than in case 2 (see fig. 4.32).

Case 12 was run with a scenario less favorable to the missile, where all the conditions of the previous case was kept, except the target position that has been increased to 200 meters above the missile.

Now, the commanded acceleration are much larger, with a initial  $A_{co}$  of  $103 \text{ m/sec}^2$ , being almost impossible to see the difference of the time history of the acceleration from one straight line, as shown in fig. 4.33. The commanded roll rate is small, about the same as in case 2 (see fig. 4.34). The change in the miss distance is noticeable, with a final CG-to-CG distance of 4.8 meters as in table V, and figure 4.35. The final roll angle explain the shape of the acceleration curve, since with the small roll angle as shown in fig. 4.36, the system is behaving as for small roll excursions.

Notice that from this analysis, one has to realize that there is some kind of envelope where the 2-D system is valid. And in order to determine this envelope, one has to take in account not only the geometry of the scenario, but also the time to intercept, which is determined not only by the relation of velocities of missile and target, but the pitch angle too.

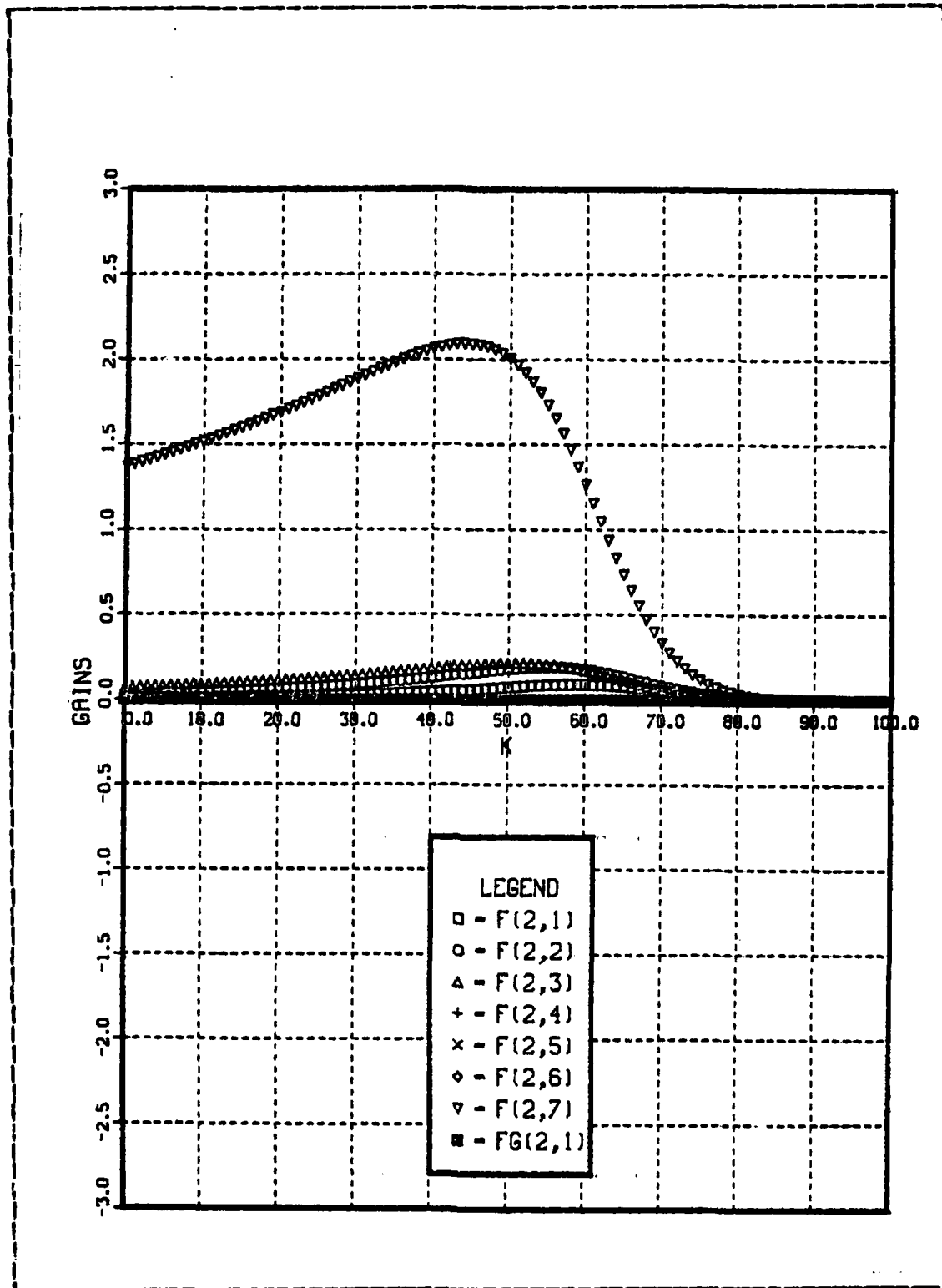


Figure 4.1 Gains affecting the commanded acceleration.

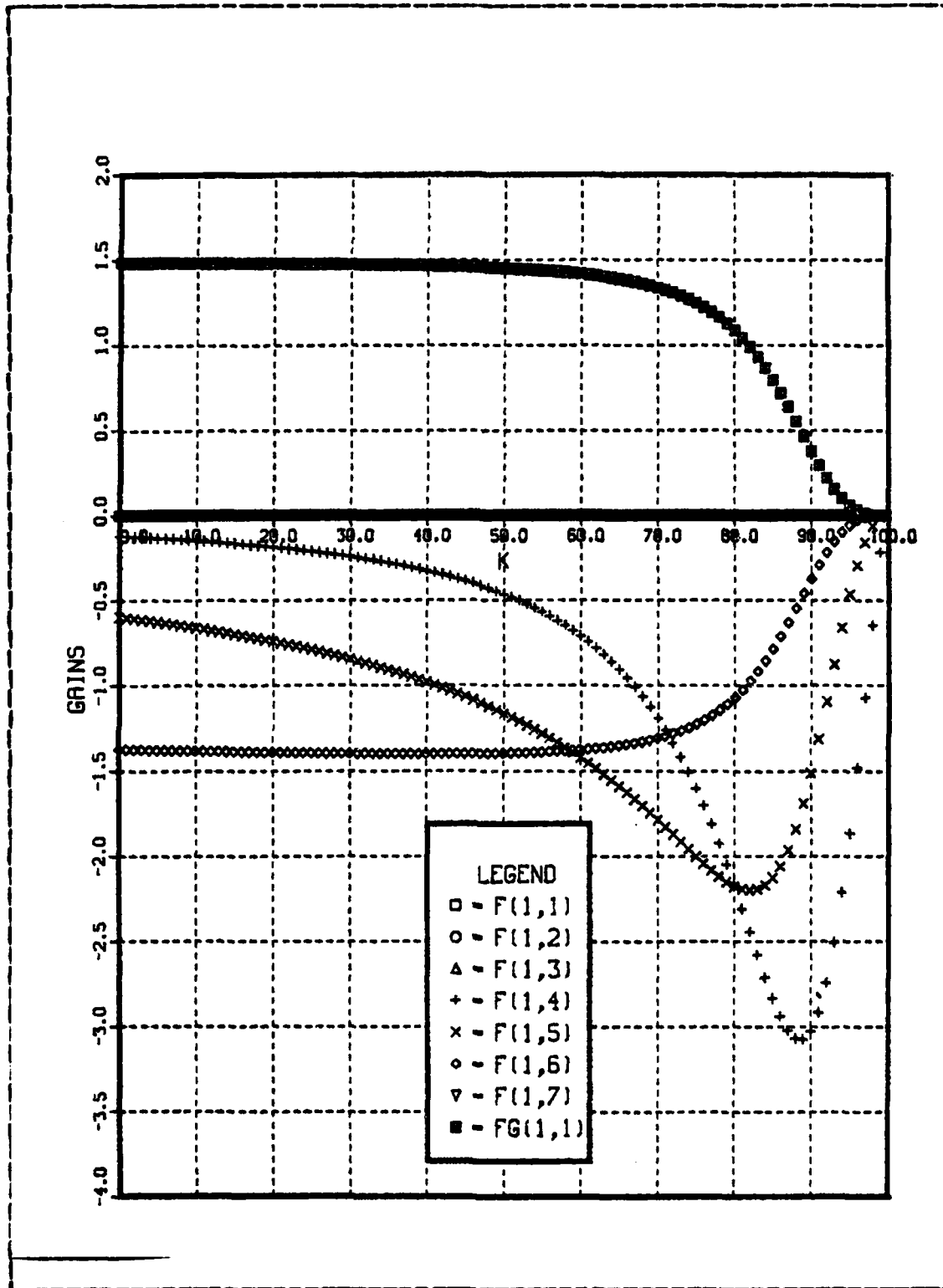


Figure 4.2 Gains Affecting the Commanded Roll Rate.

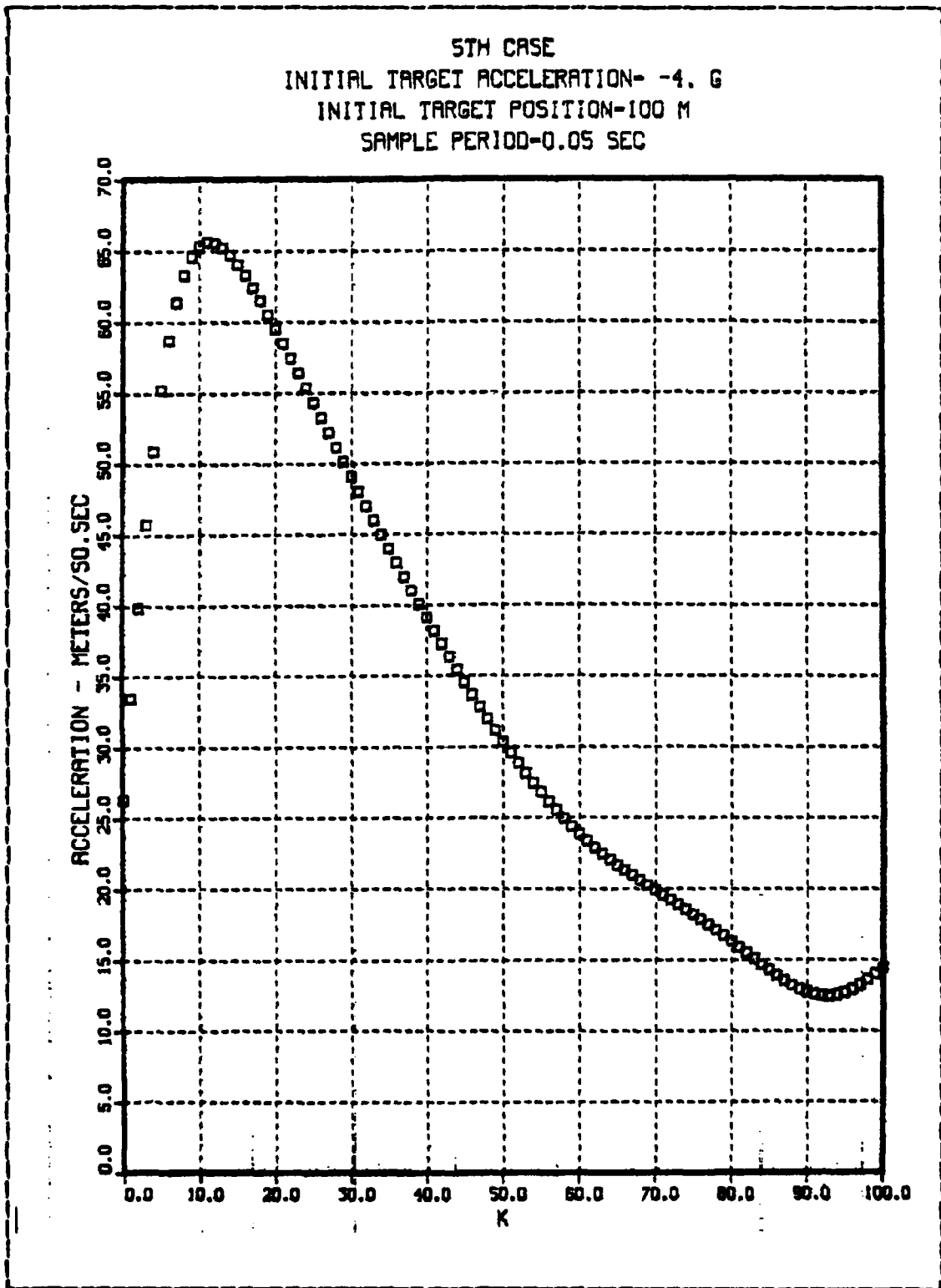


Figure 4.3 Commanded Acceleration-Case 5.

5TH CASE  
INITIAL TARGET ACCELERATION- -4. G  
INITIAL TARGET POSITION-100 M  
SAMPLE PERIOD-0.05 SEC

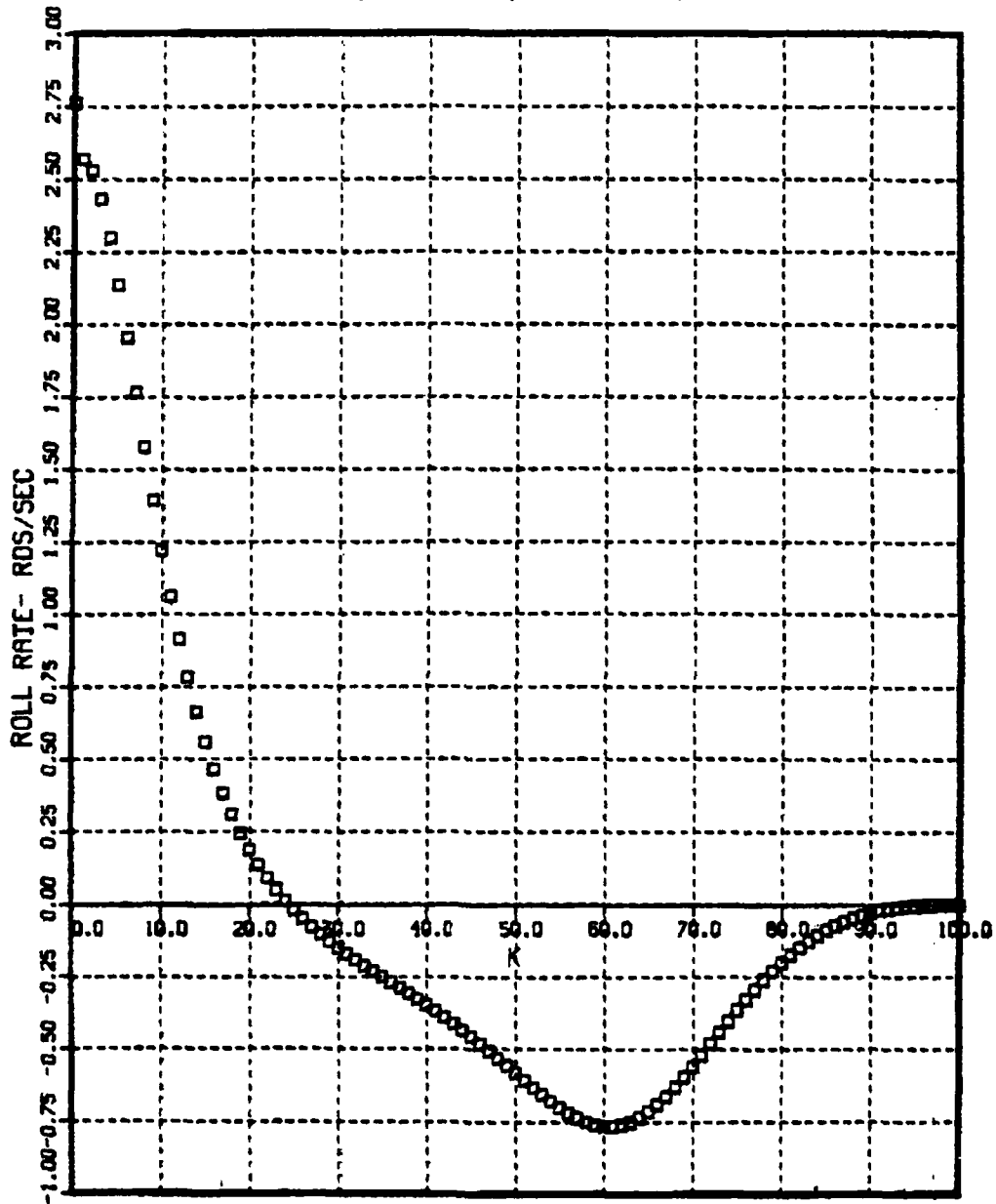


Figure 4.4 Commanded Roll Rate-Case 5.

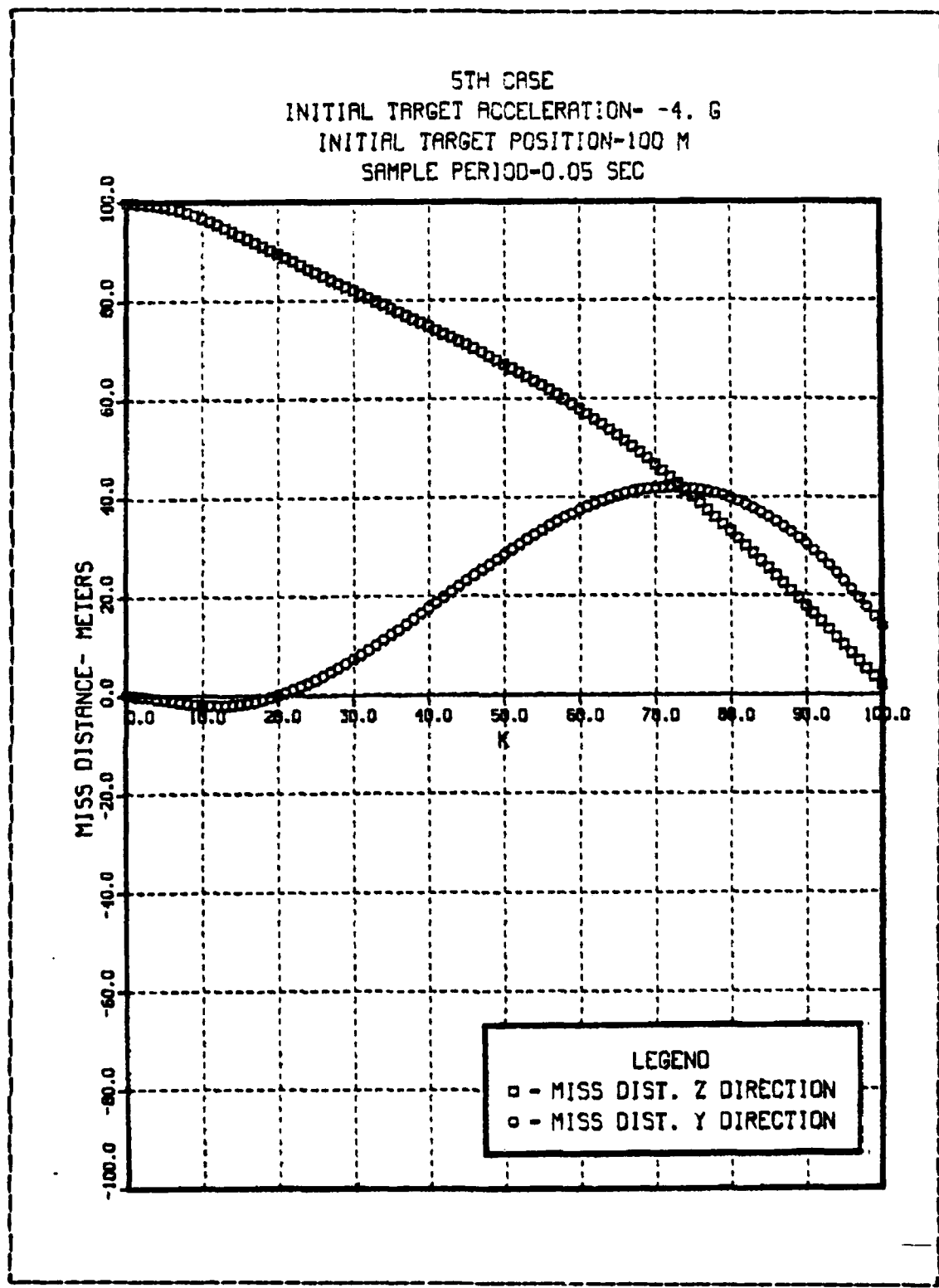


Figure 4.5 Miss Distance-Case 5.

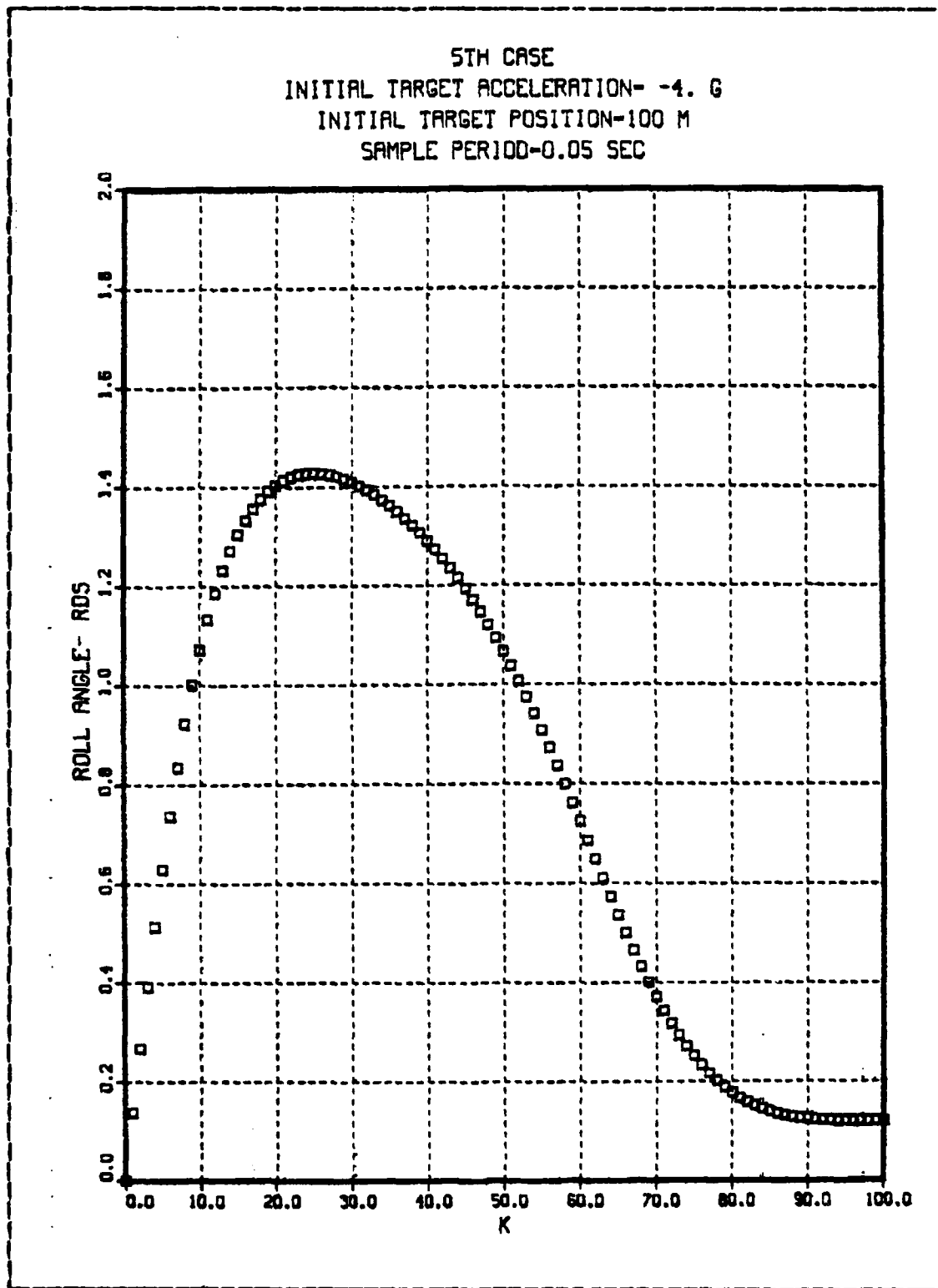


Figure 4.6 Roll Angle-Case 5.

AD-A144 043

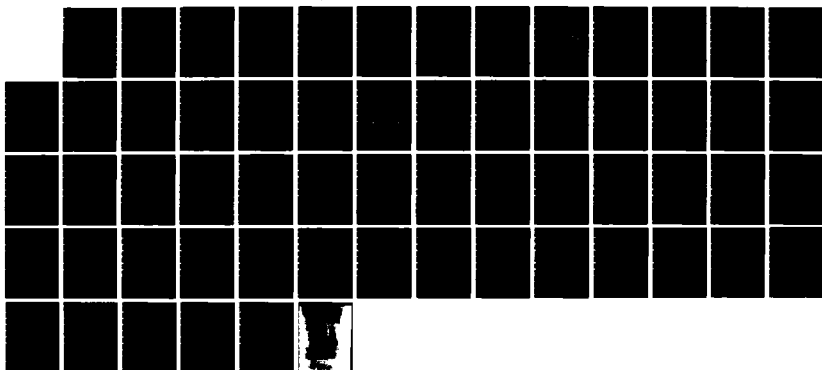
OPTIMAL DIGITAL CONTROL OF A BANK-TO-TURN MISSILE(U)  
NAVAL POSTGRADUATE SCHOOL MONTEREY CA C A VELLOSO  
MAR 84

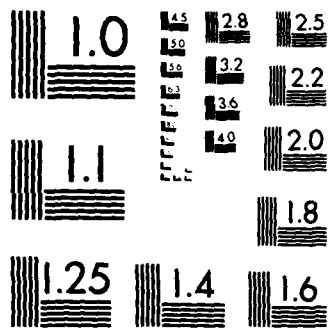
2/2

UNCLASSIFIED

F/G 1/3

NL





MICROCOPY RESOLUTION TEST CHART  
NATIONAL BUREAU OF STANDARDS-1963-A

**TABLE II**  
**Results from Biased Control**

t	Ac (m/sec)	Pc (rad/sec)	miss distance Y direction (m)	miss distance Z direction (m)	$\phi$ (rad)	CG-to-CG miss distance (m)
0	26.37	2.76	0.0	100.	0.0	100.
Tf	14.47	0.0	13.78	2.00	.119	13.93

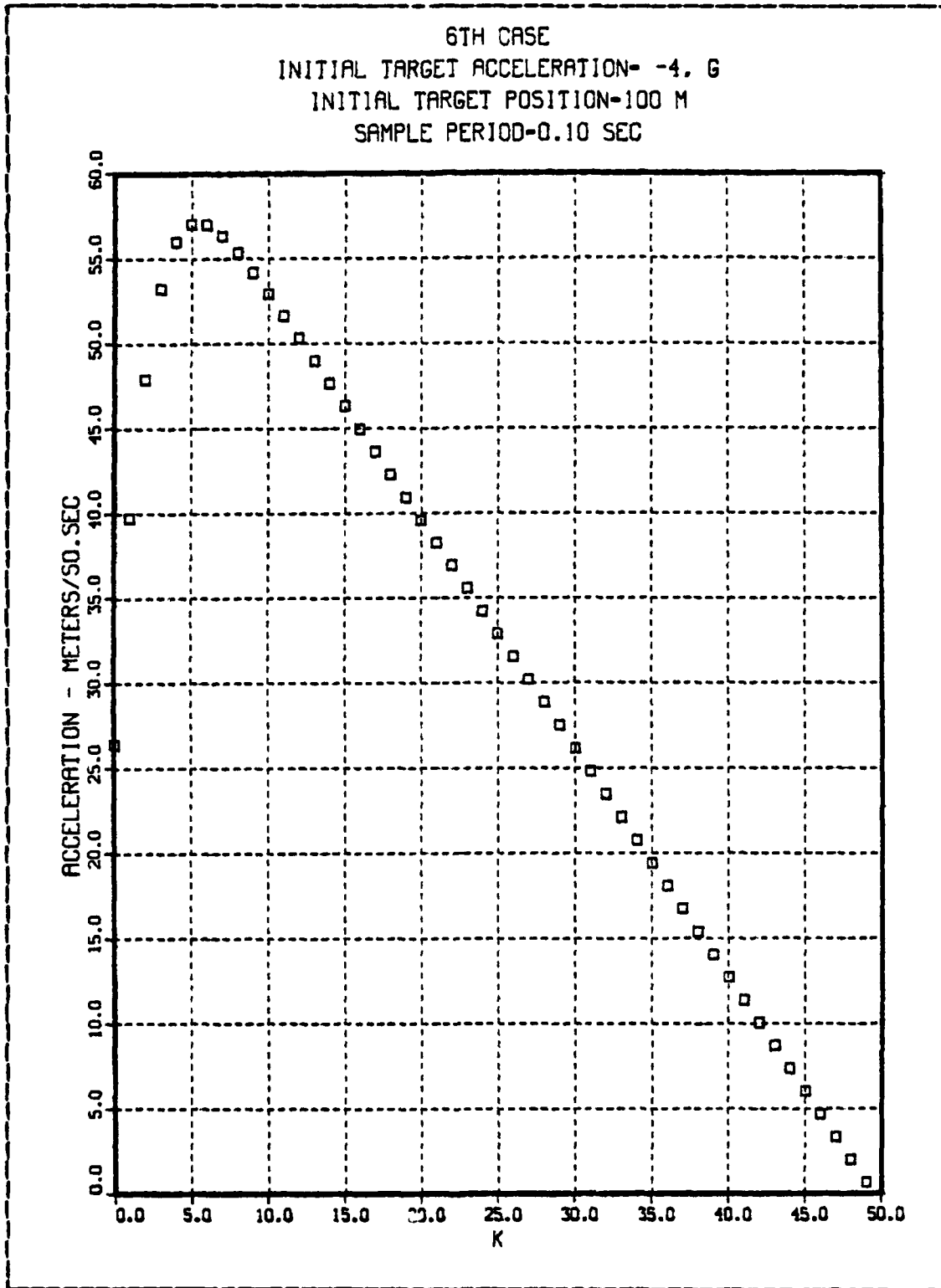


Figure 4.7 Commanded Acceleration-Case 6.

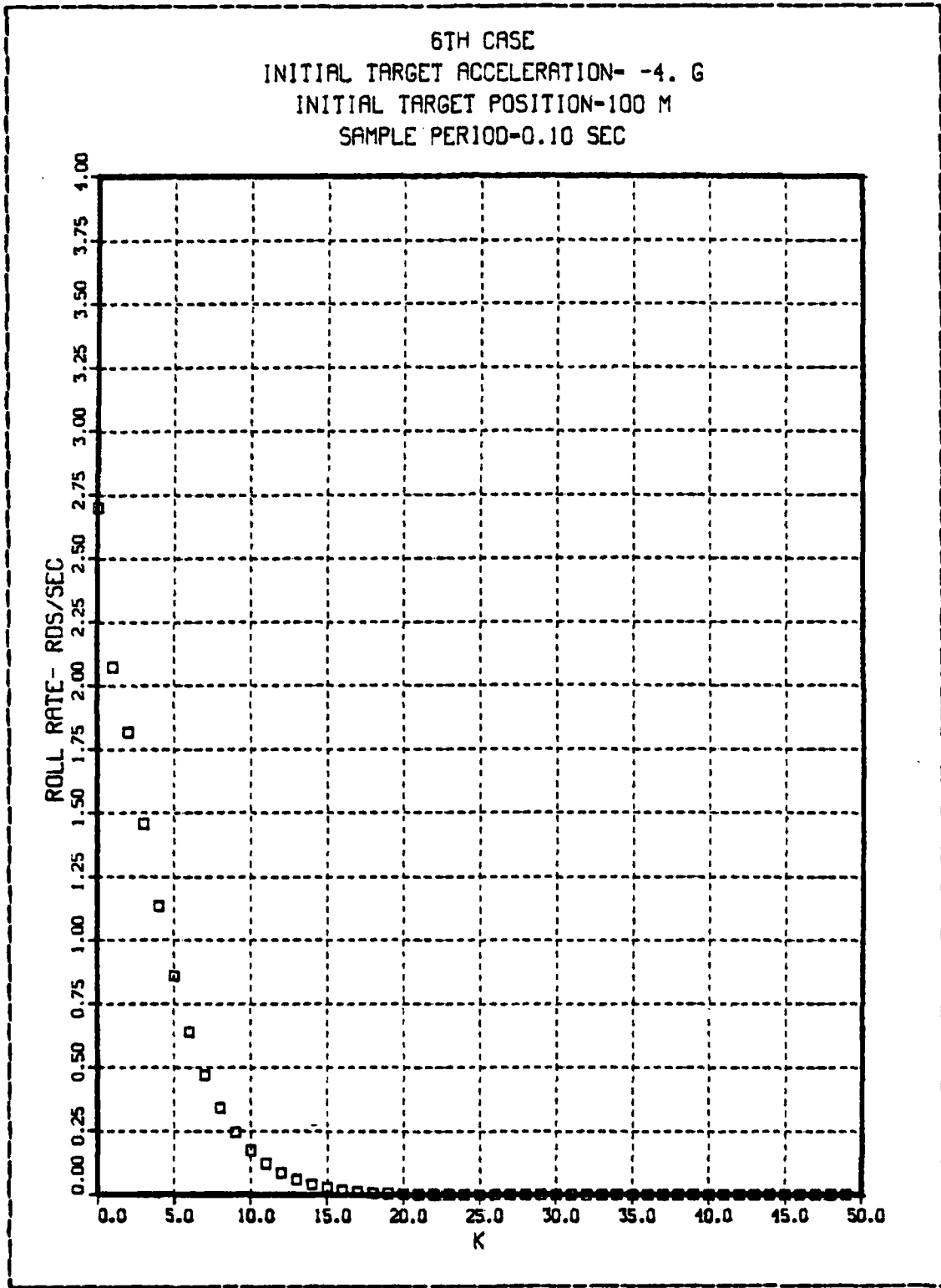


Figure 4.8 Commanded Roll Rate-Case 6.

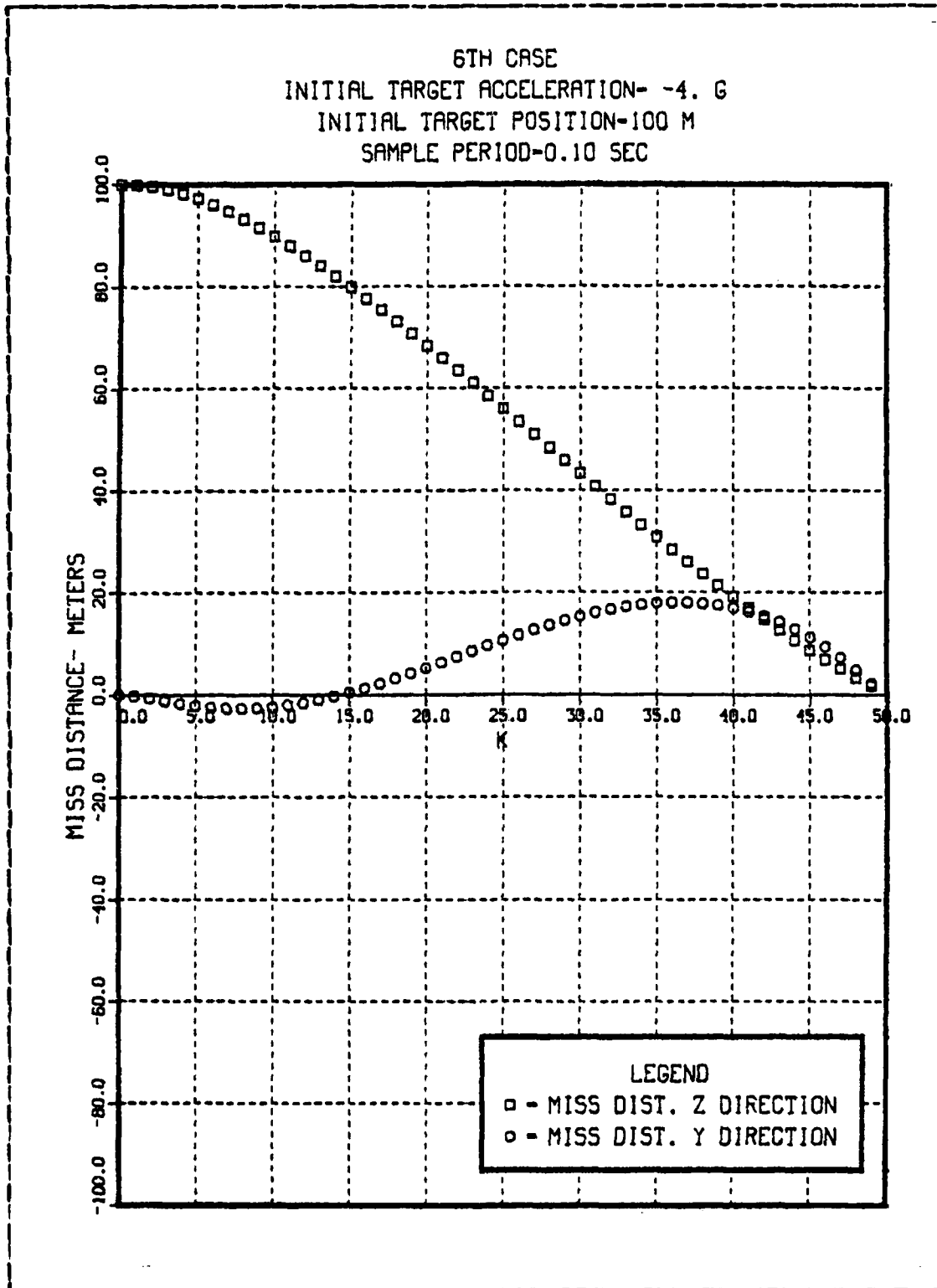


Figure 4.9 Miss Distance-Case 6.

6TH CASE  
INITIAL TARGET ACCELERATION- -4. G  
INITIAL TARGET POSITION-100 M  
SAMPLE PERIOD-0.05 SEC

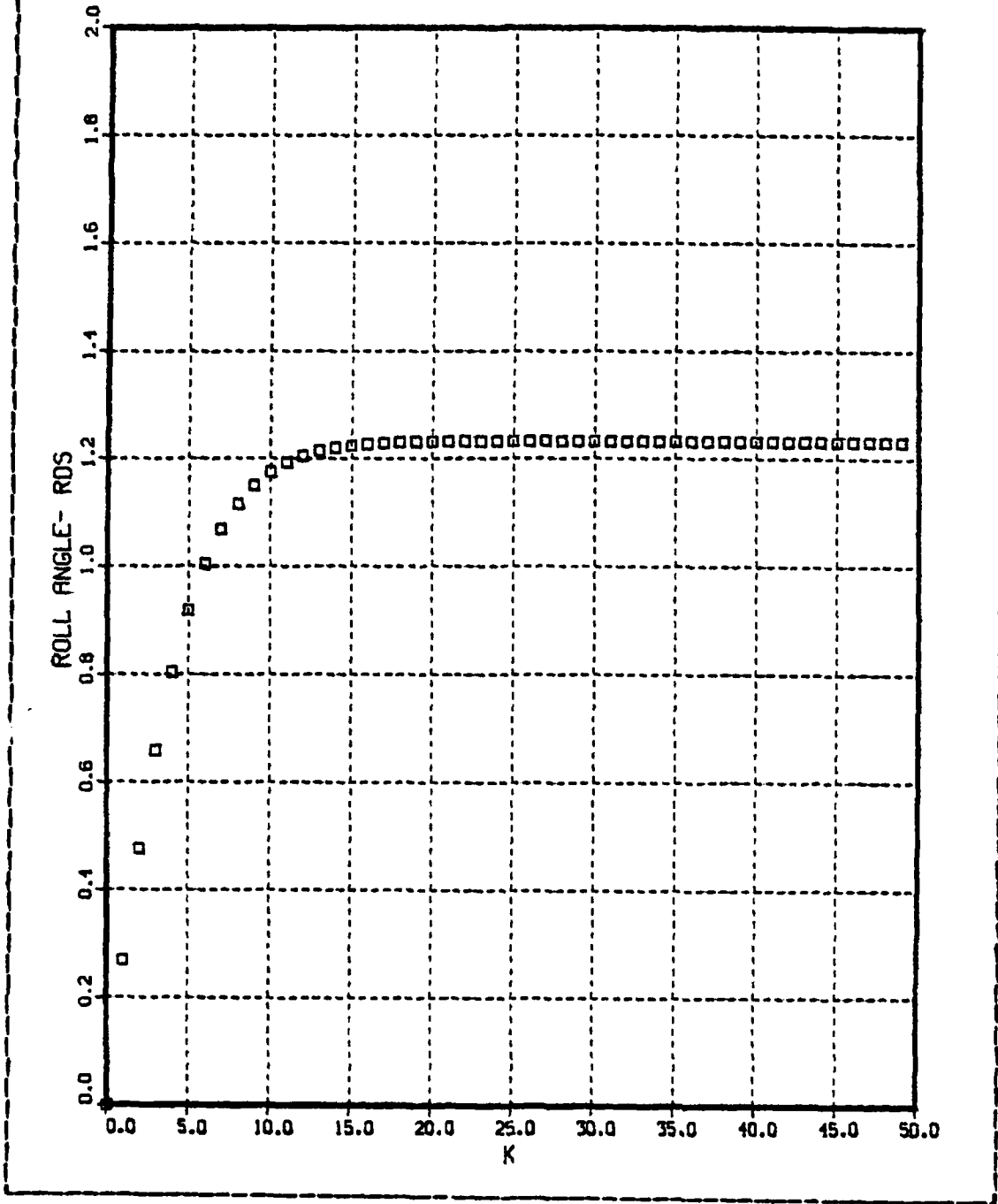


Figure 4.10 Roll Angle-Case 6.

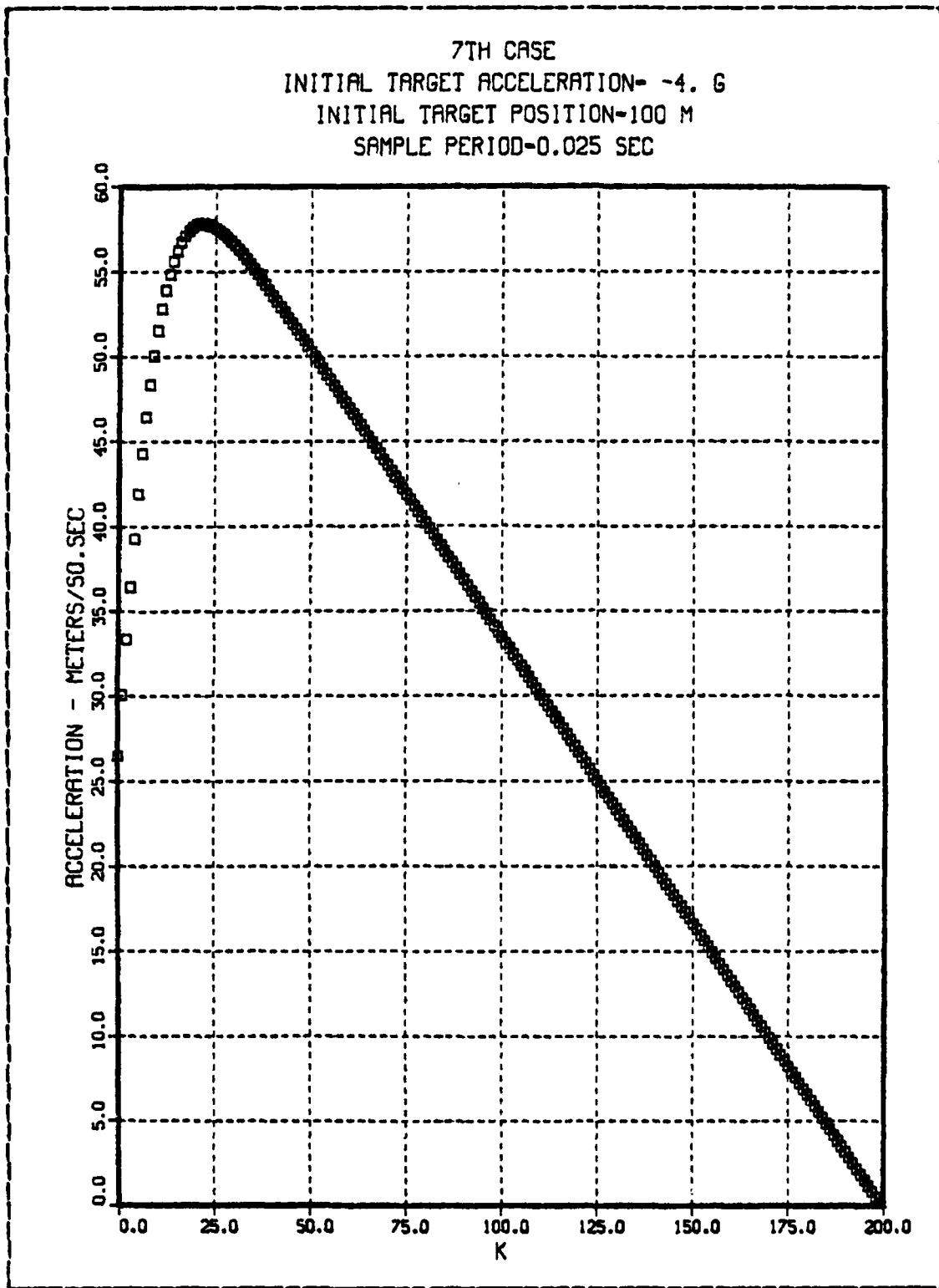


Figure 4.11 Commanded Acceleration-Case 7.

7TH CASE  
INITIAL TARGET ACCELERATION- -4. G  
INITIAL TARGET POSITION-100 M  
SAMPLE PERIOD-0.025 SEC

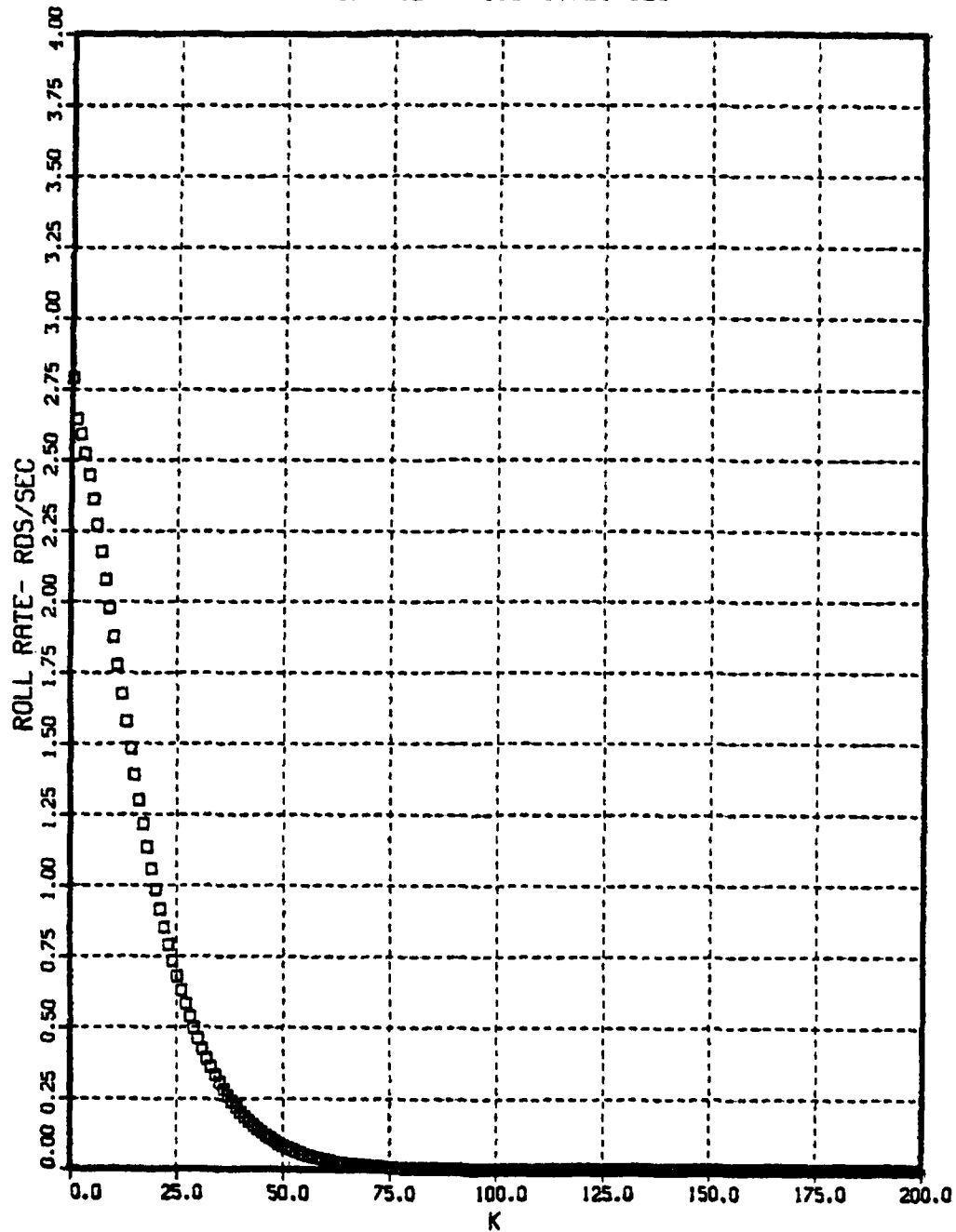


Figure 4.12 Commanded Roll Rate-Case 7.

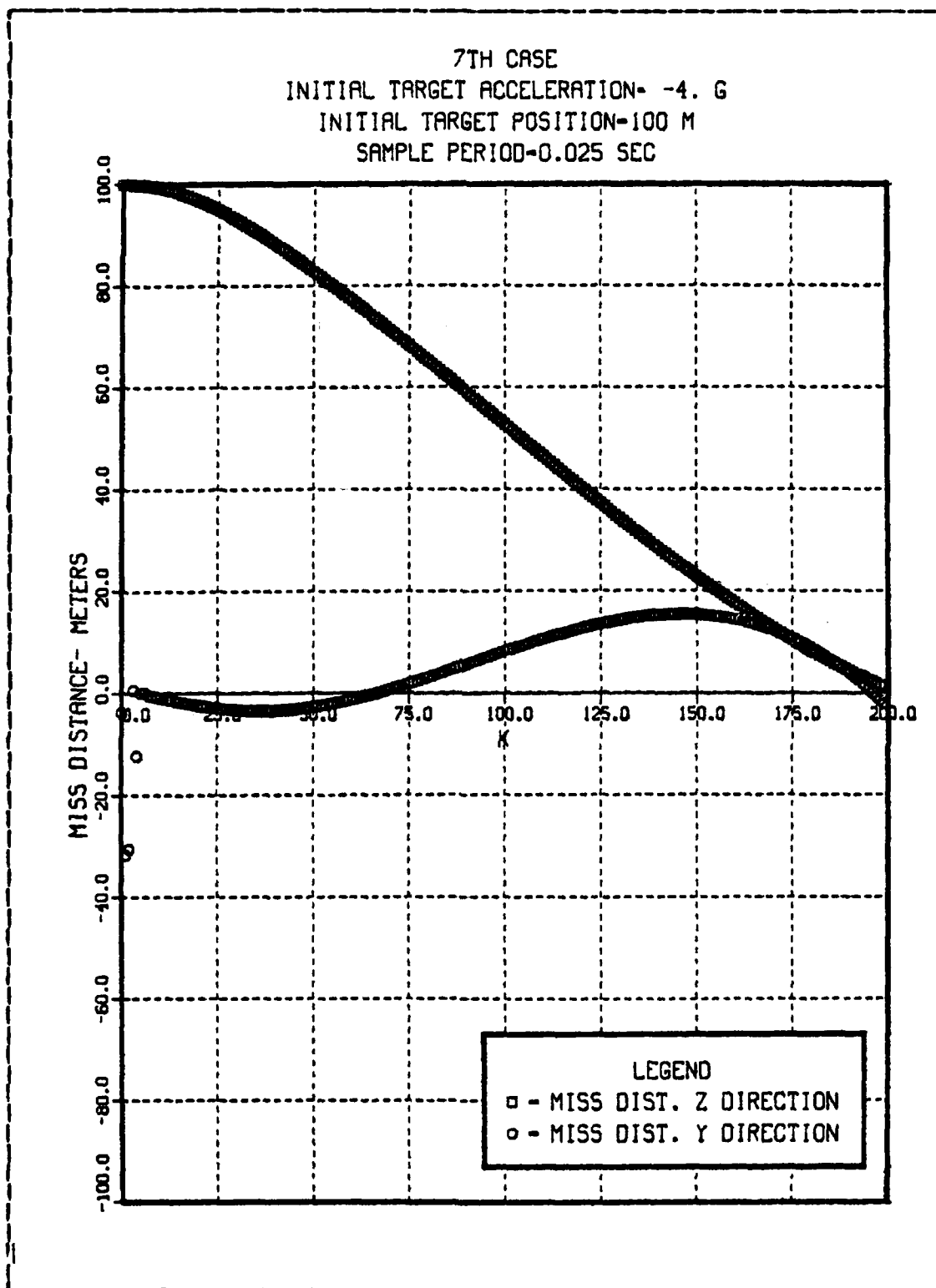


Figure 4.13 Miss distance-Case 7.

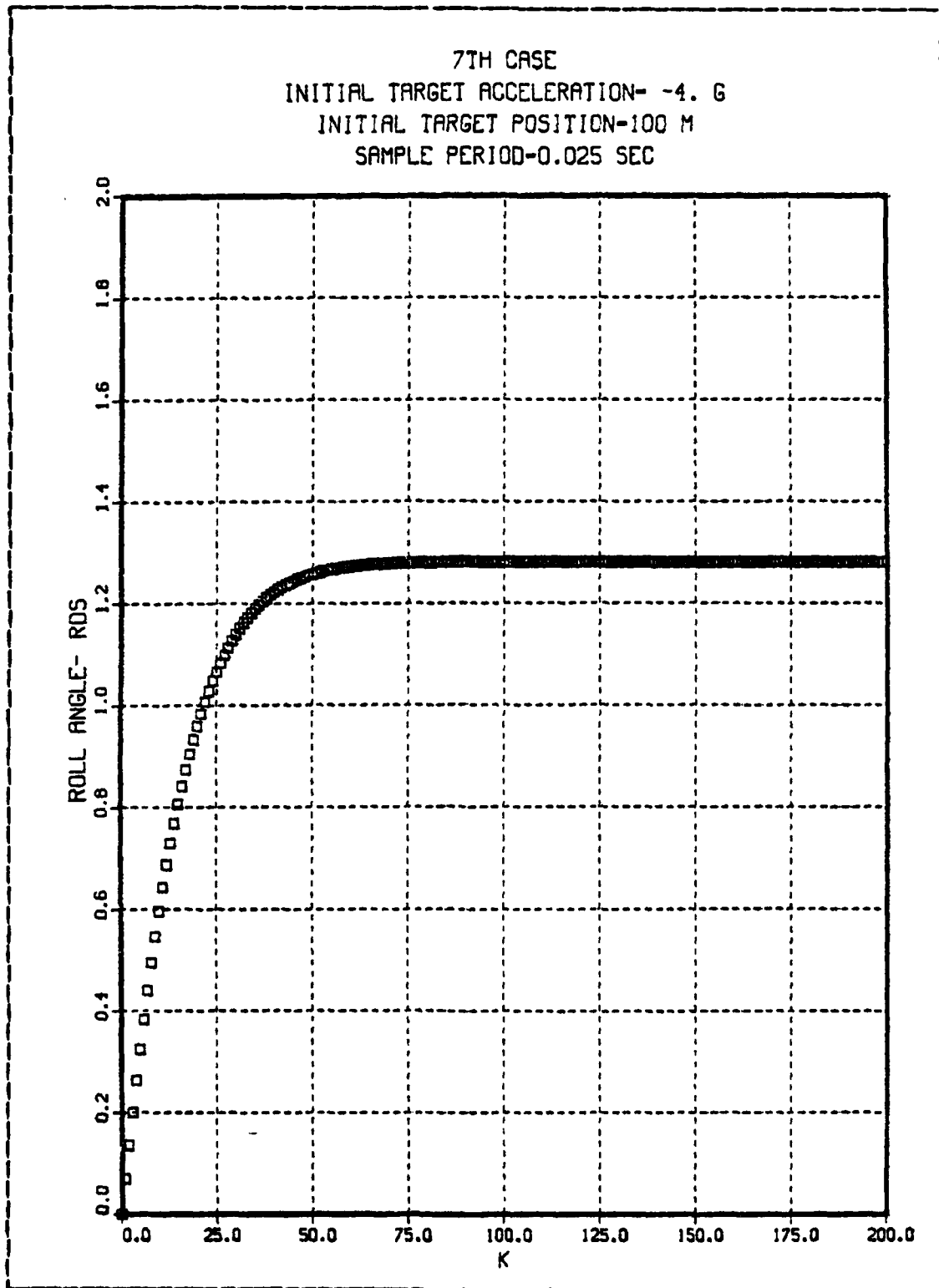


Figure 4.14 Roll Angle-Case 7.

TABLE III  
Results for Differents Sample Periods

T (sec)	CASE	t	AC (m/sec)	PC (rad/sec)	$\frac{m}{ss}$ distance y direction (m)	$\frac{m}{ss}$ distance z direction (m)	$\phi$ (rad)	CG-to-CG miss distance (m)
.1	6	0	26.40	2.70	0.0	100.	0.0	100.
		Tf	.67	0.0	2.23	1.77	1.23	2.85
.025	7	0	26.48	2.79	0.0	100.	0.0	100.
		Tf	.68	0.0	2.22	1.20	1.28	2.53
.05	3	0	26.47	2.76	0.0	100.	0.0	100.
		Tf	.33	0.0	-1.47	.046	1.27	1.54

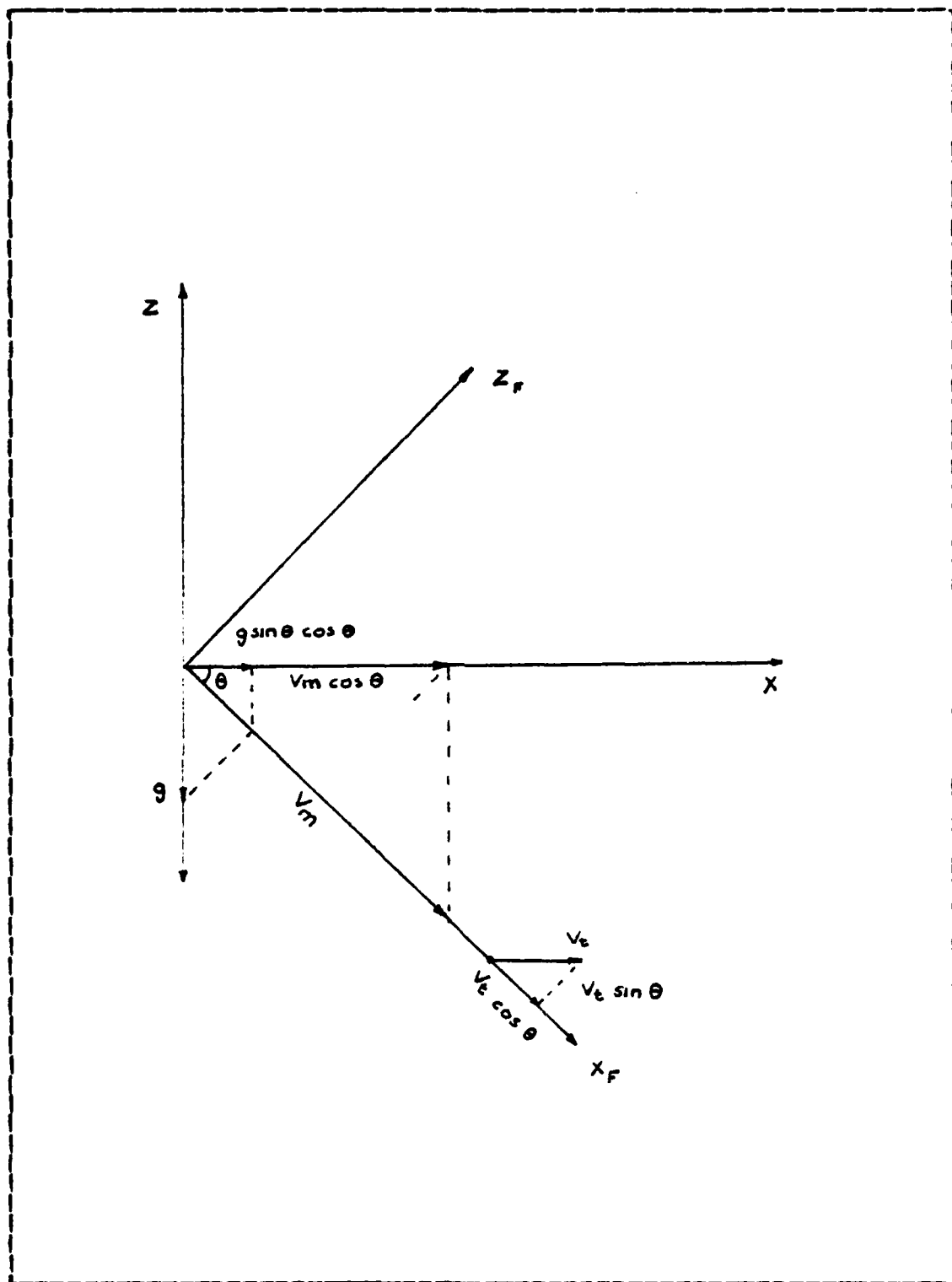


Figure 4.15 Effect of Initial Pitch Angle.

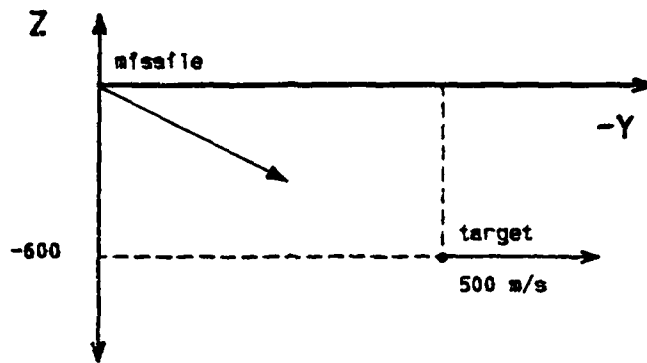


Figure 4.16a Case 8

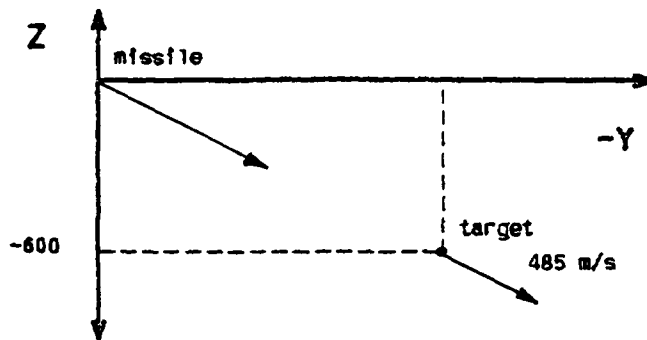


Figure 4.16b Case 9

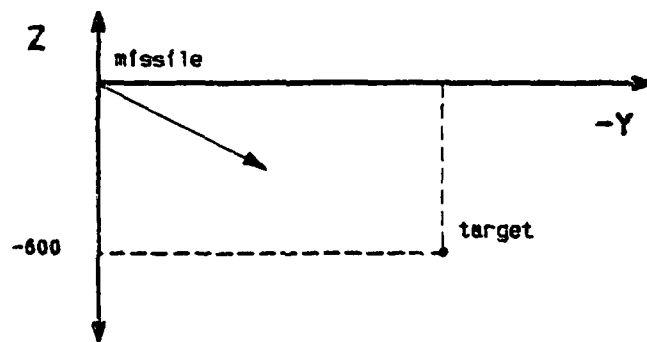


Figure 4.16c Case 10

Figure 4.16 Scenarios With Pitch Angle.

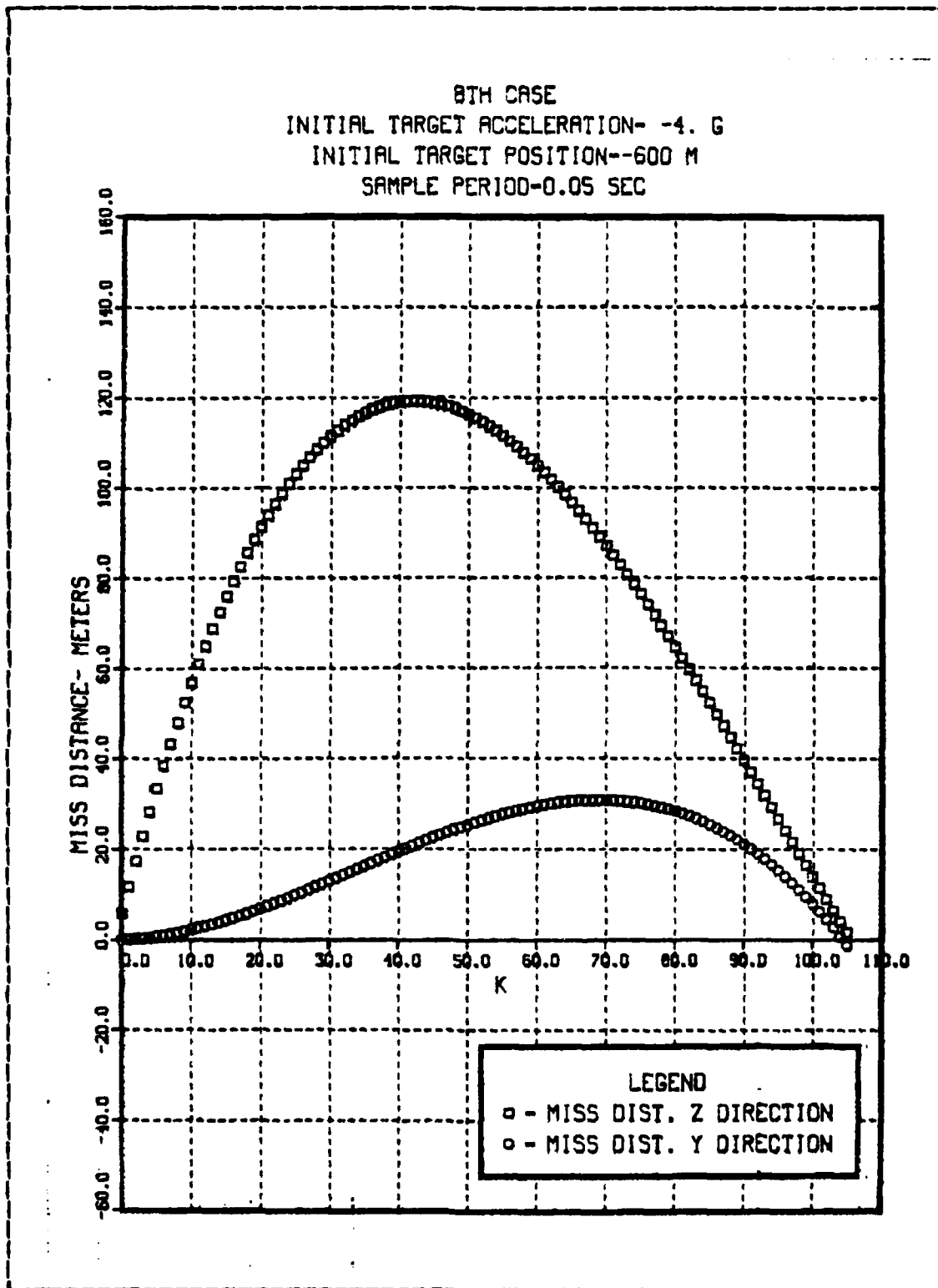


Figure 4.17 Commanded Acceleration-Case 8.

8TH CASE  
INITIAL TARGET ACCELERATION- -4. G  
INITIAL TARGET POSITION--600 M  
SAMPLE PERIOD-0.05 SEC

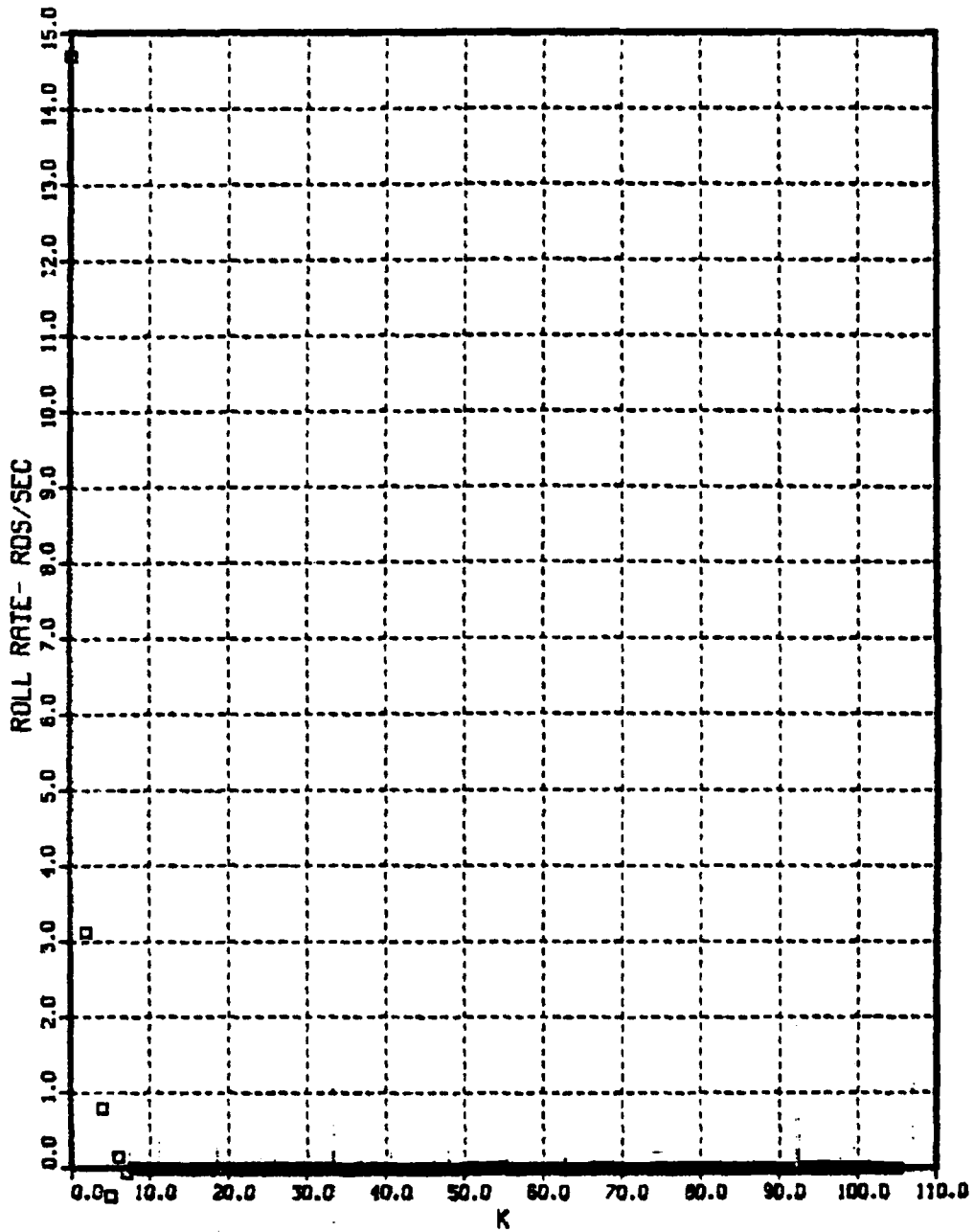


Figure 4.18 Commanded Roll Rate-Case 8.

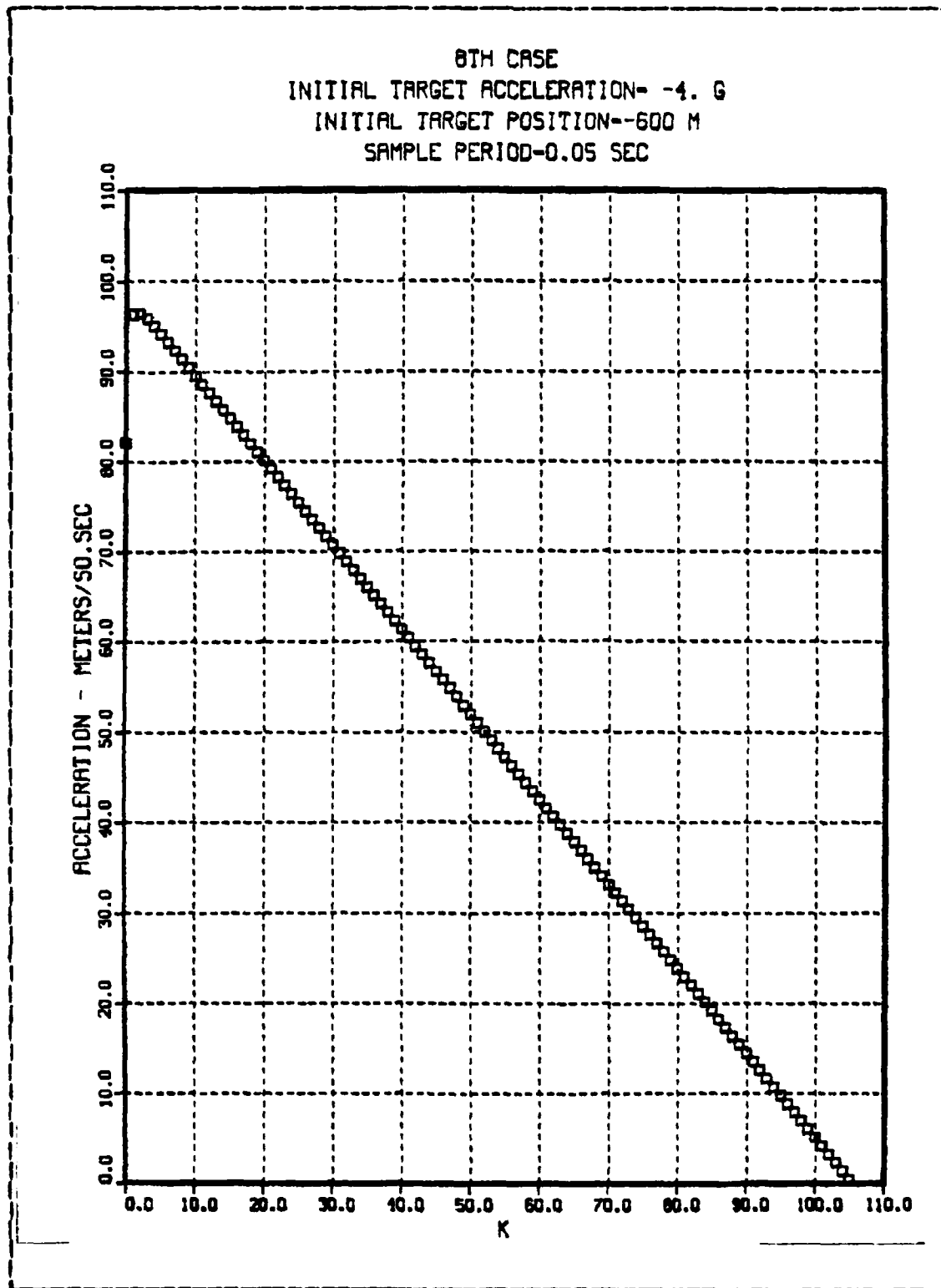


Figure 4.19 Miss Distance-Case 8.

8TH CASE  
INITIAL TARGET ACCELERATION- -4. G  
INITIAL TARGET POSITION--600 M  
SAMPLE PERIOD-0.05 SEC

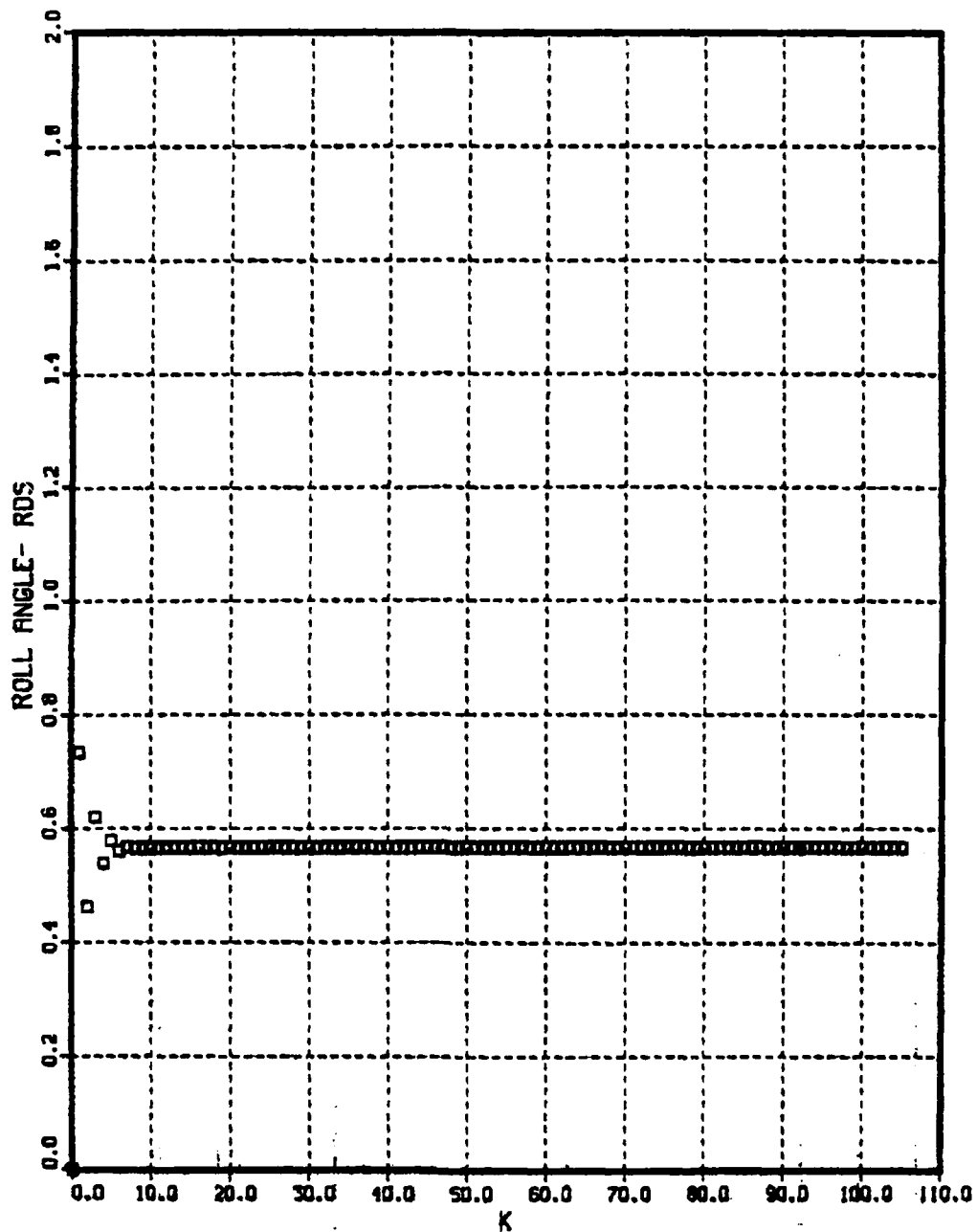


Figure 4.20 Roll Angle-Case 8.

9TH CASE  
INITIAL TARGET ACCELERATION- -4. G  
INITIAL TARGET POSITION--600 M  
SAMPLE PERIOD-0.05 SEC

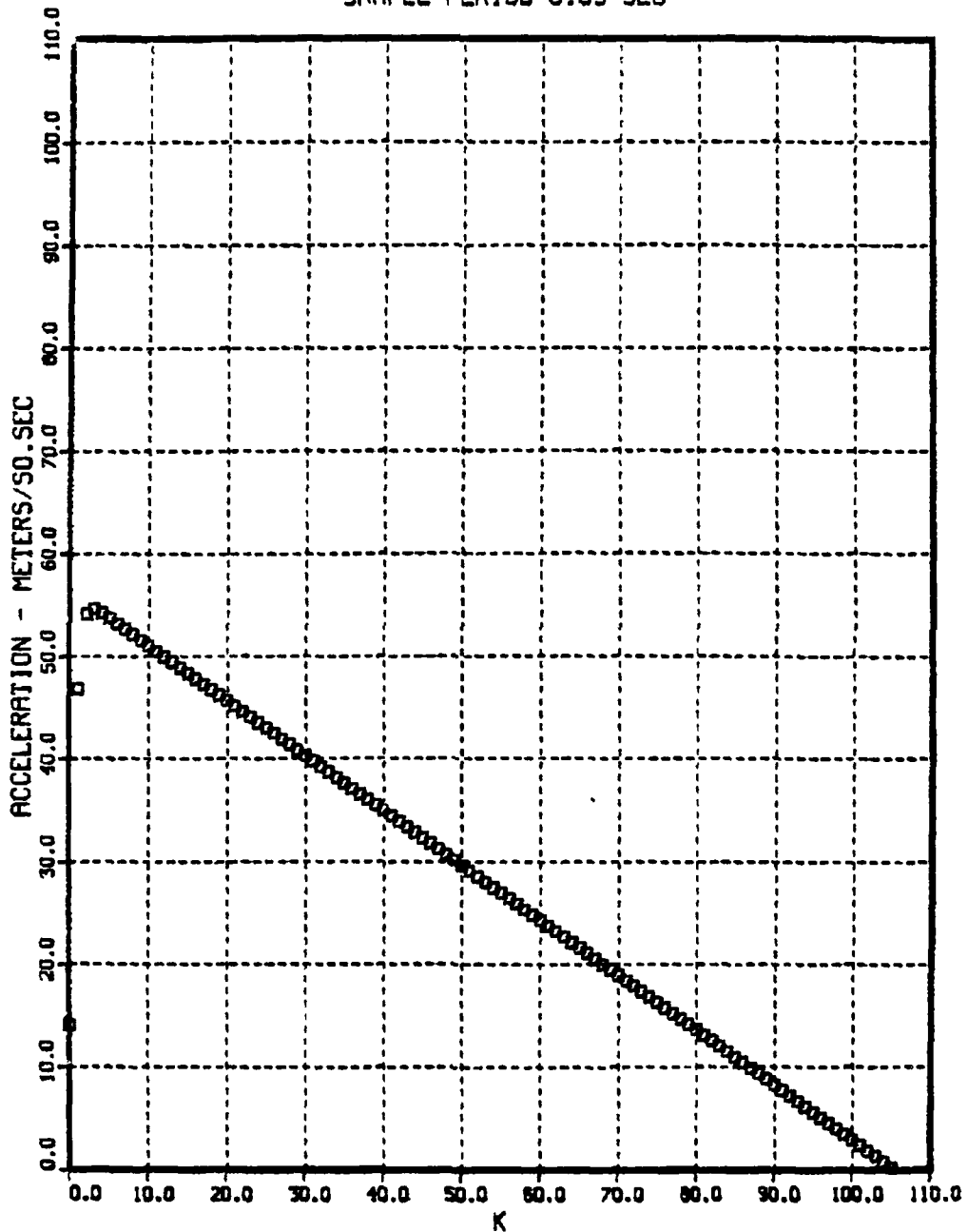


Figure 4.21 Commanded Acceleration-Case 9.

9TH CASE  
INITIAL TARGET ACCELERATION- -4. G  
INITIAL TARGET POSITION--600 M  
SAMPLE PERIOD-0.05 SEC

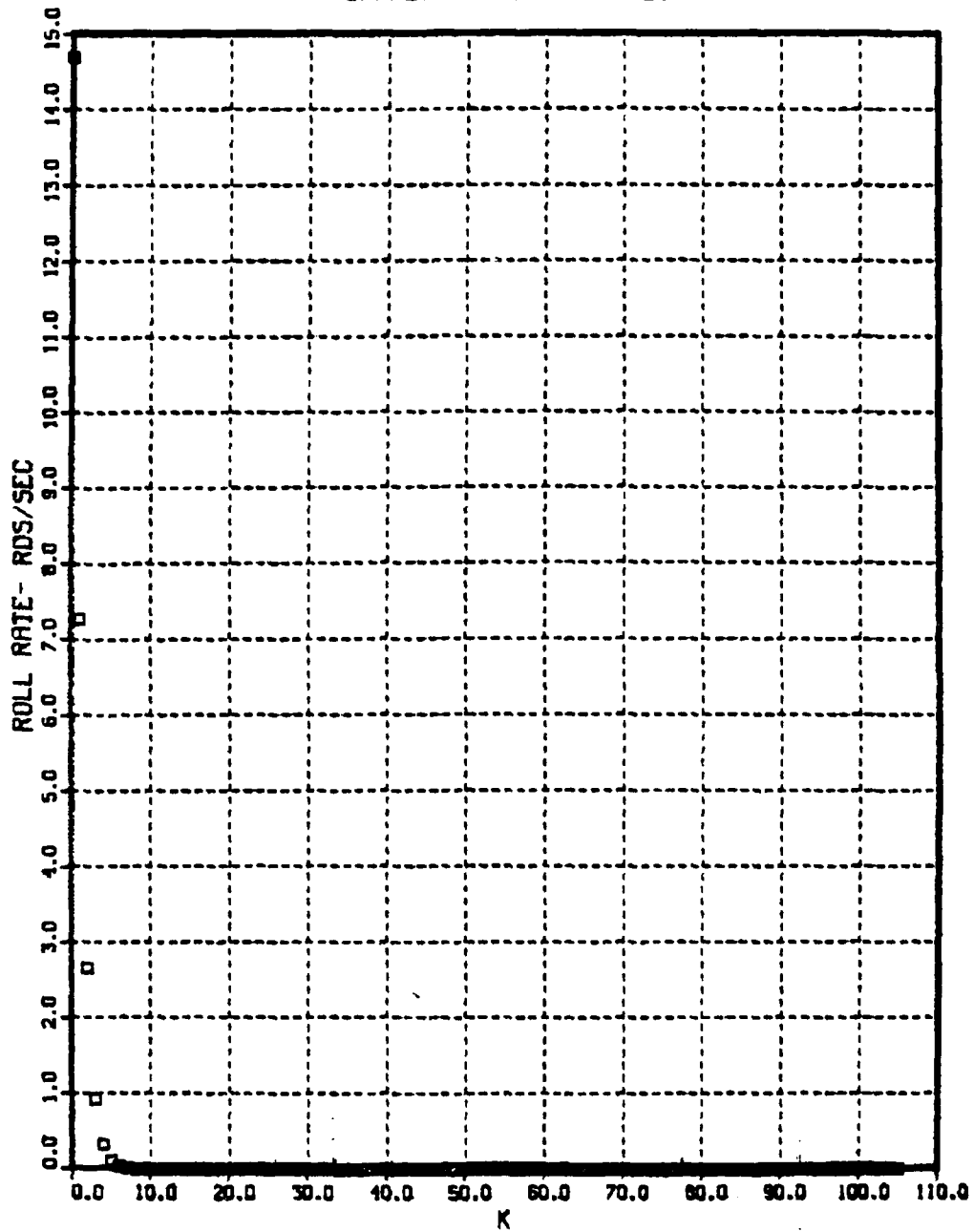


Figure 4.22 Commanded Roll Rate-Case 9.

9TH CASE  
INITIAL TARGET ACCELERATION- -4. G  
INITIAL TARGET POSITION--600 M  
SAMPLE PERIOD-0.05 SEC

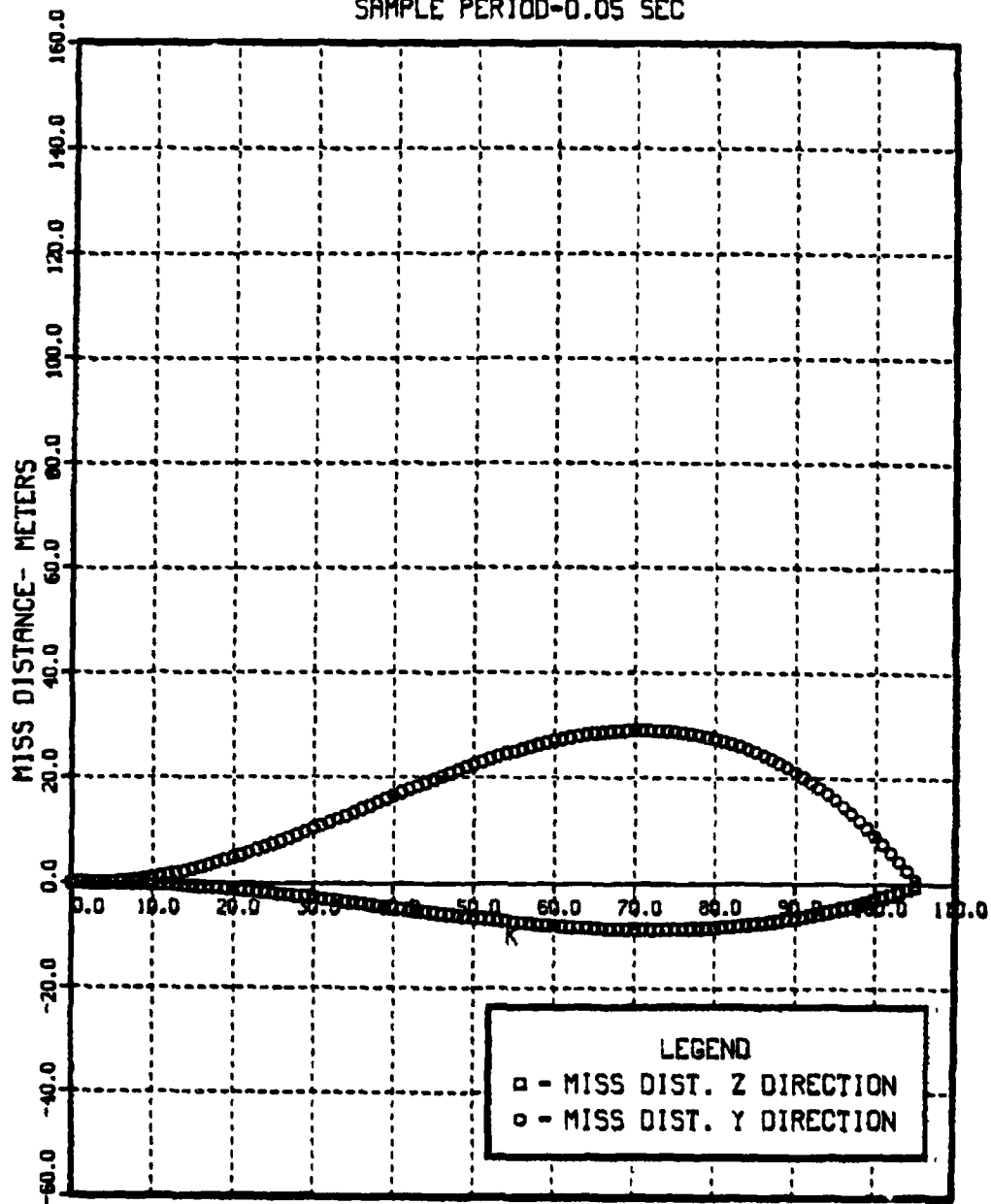


Figure 4.23 Miss Distance-Case 9.

9TH CASE  
INITIAL TARGET ACCELERATION- -4. G  
INITIAL TARGET POSITION--600 M  
SAMPLE PERIOD-0.05 SEC

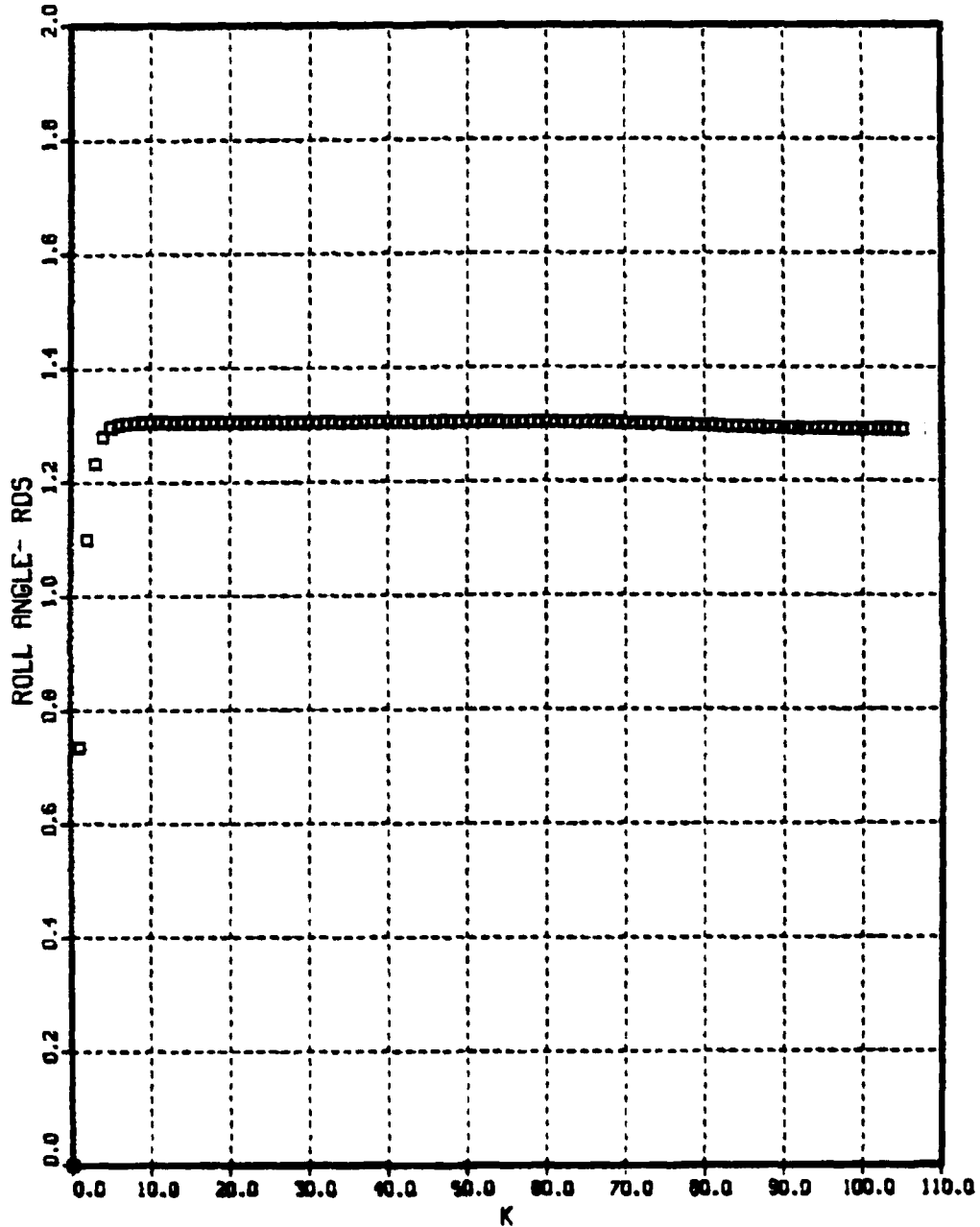


Figure 4.25 Roll Angle-Case 9.

10TH CASE  
INITIAL TARGET ACCELERATION--4. G  
INITIAL TARGET POSITION--600 M  
SAMPLE PERIOD--0.05 SEC

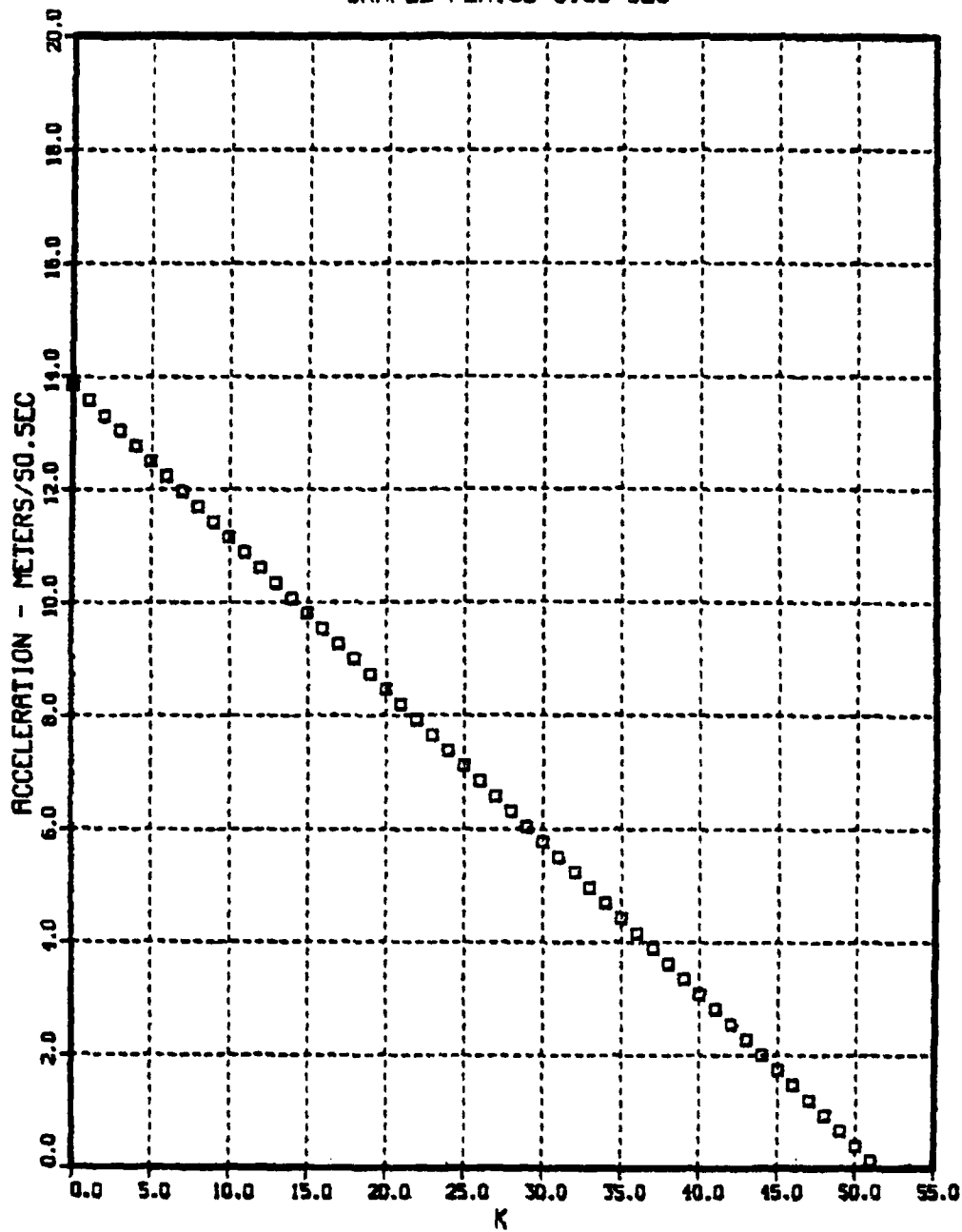


Figure 4.25 Commanded Acceleration-Case 10.

10TH CASE  
INITIAL TARGET ACCELERATION--4. G  
INITIAL TARGET POSITION--600 M  
SAMPLE PERIOD-0.05 SEC

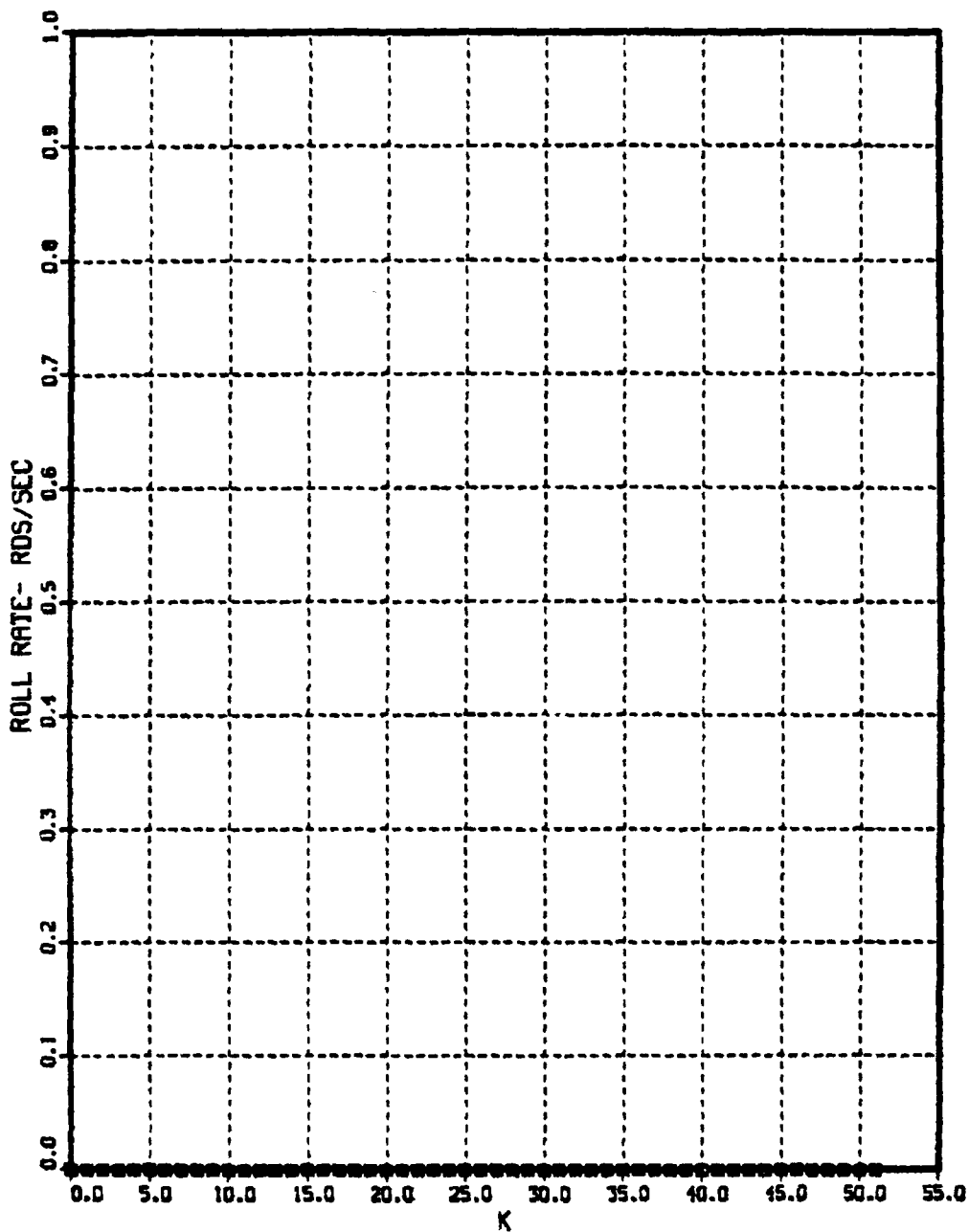


Figure 4.26 Commanded Roll Rate-Case 10.

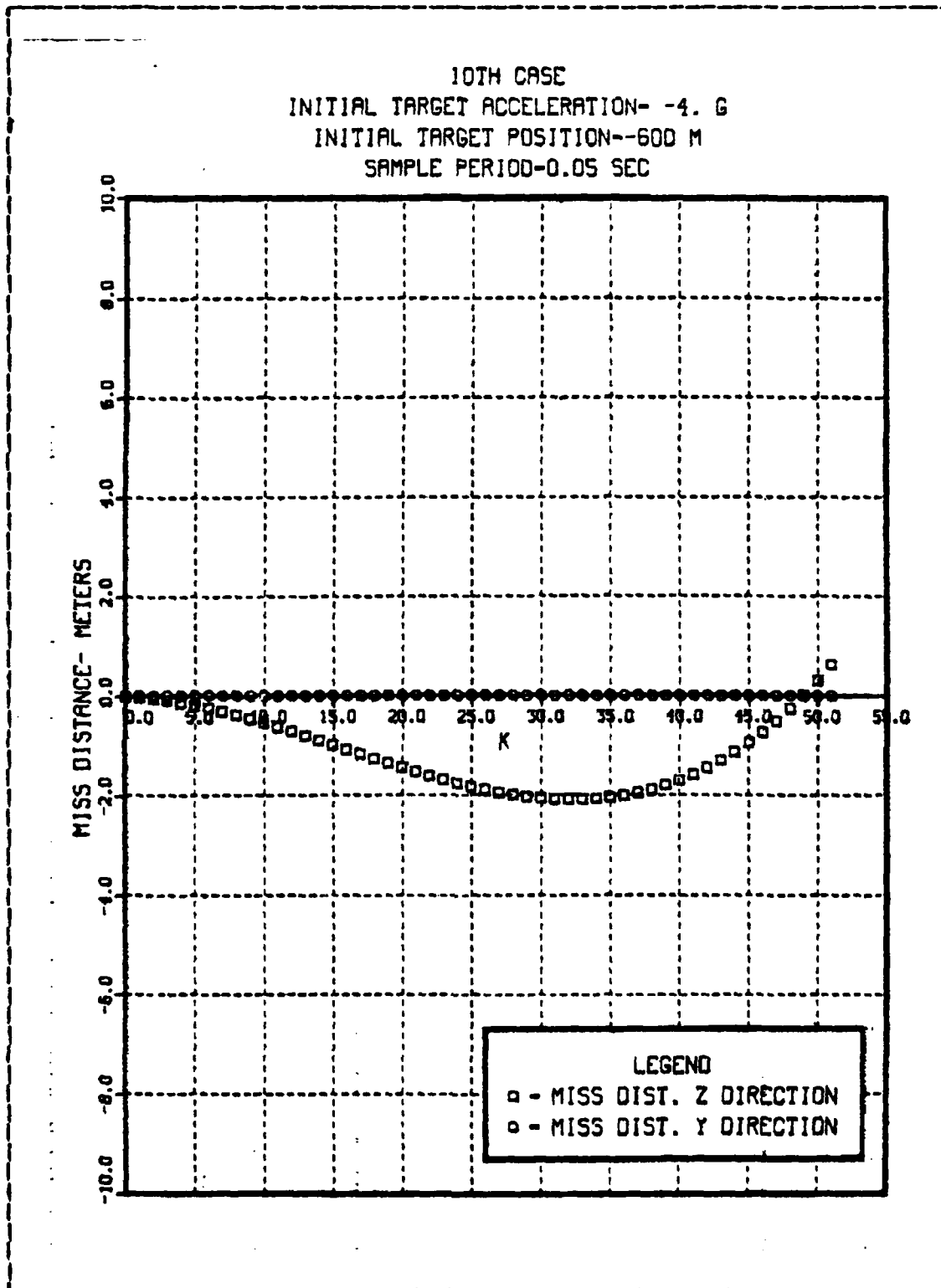


Figure 4.27 Miss Distance-Case 10.

10TH CASE  
INITIAL TARGET ACCELERATION- -4. G  
INITIAL TARGET POSITION--600 M  
SAMPLE PERIOD-0.05 SEC

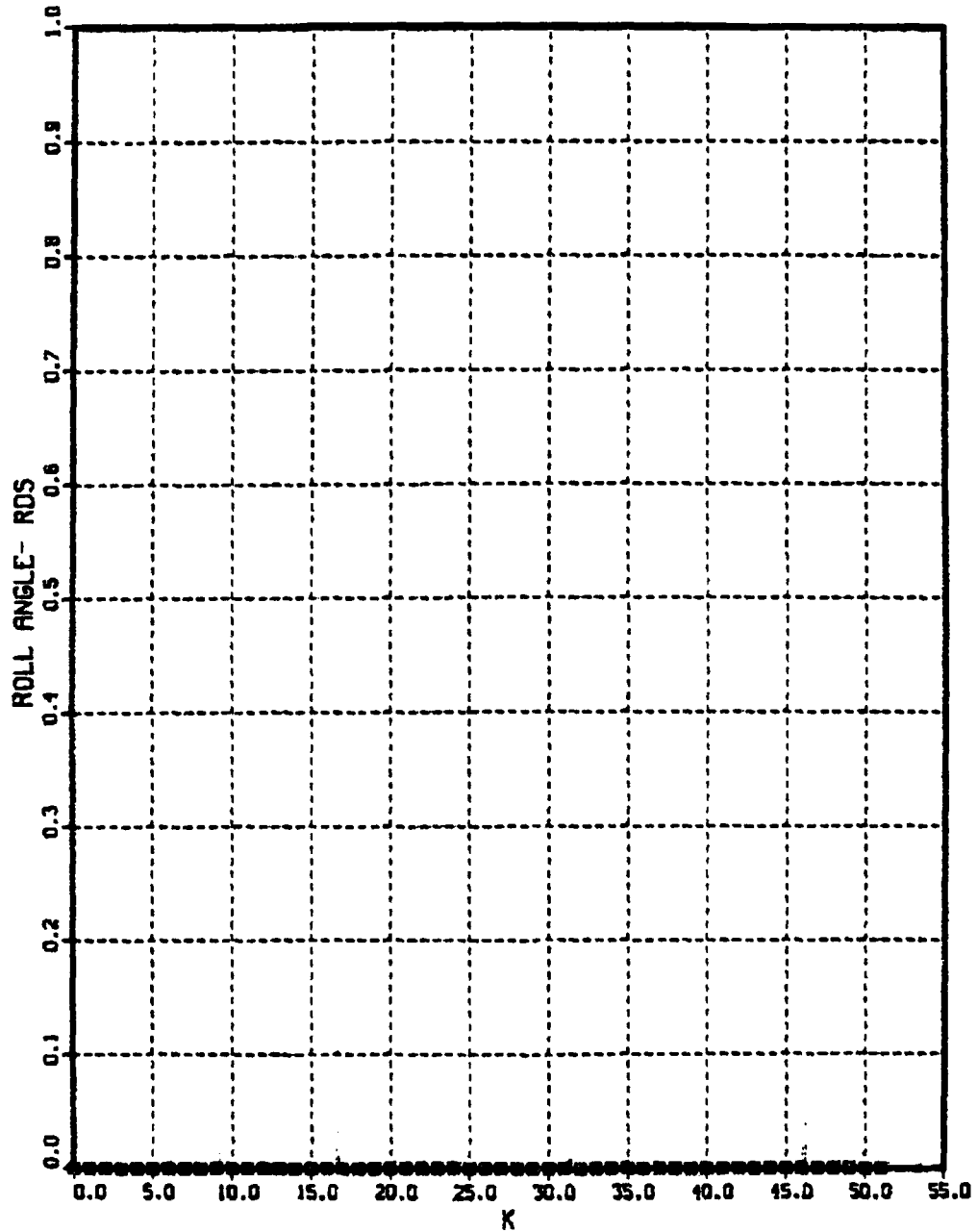


Figure 4.28 Roll Angle-Case 10.

**TABLE IV**  
**Results Using Pitch Angle**

case	t	AC (m/sec)	PC (rad/sec)	miss distance y direction (m)	miss distance z direction (m)	(rad)	CG-to-CG miss distance (m)
8	0	82.13	14.71	0.0	-600	0.0	600
	Tf	.466	0.0	-1.17	.188	.562	2.17
9	0	14.16	14.71	0.0	-600	0.0	600
	Tf	.268	0.0	-1.12	.176	1.29	1.249
10	0	13.83	0.0	0.0	-600	0.0	600
	Tf	.135	0.0	0.0	.307	0.0	.307

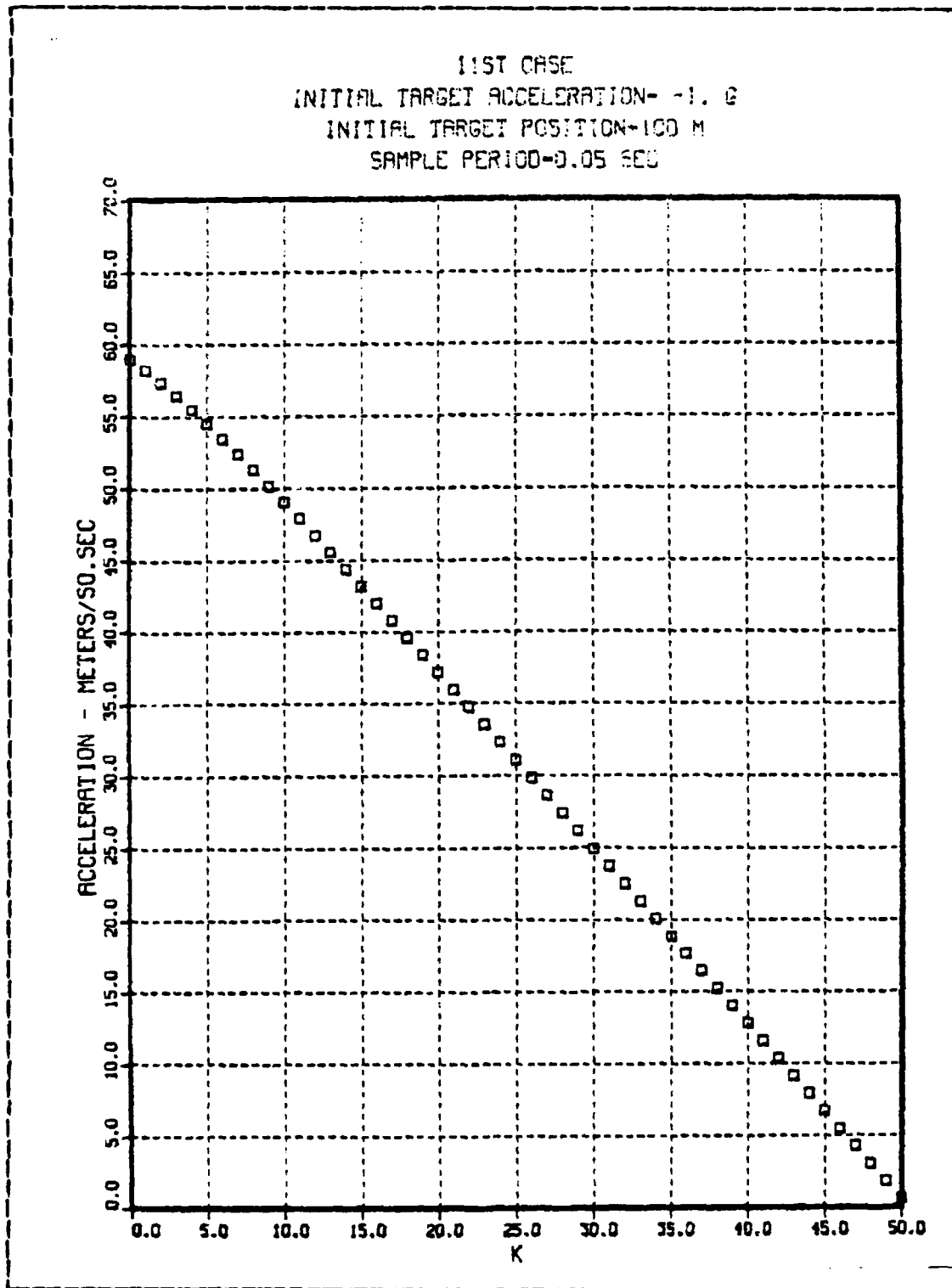


Figure 4.29 Commanded Acceleration-Case 11.

11ST CASE  
INITIAL TARGET ACCELERATION- -1. G  
INITIAL TARGET POSITION-100 M  
SAMPLE PERIOD-0.05 SEC

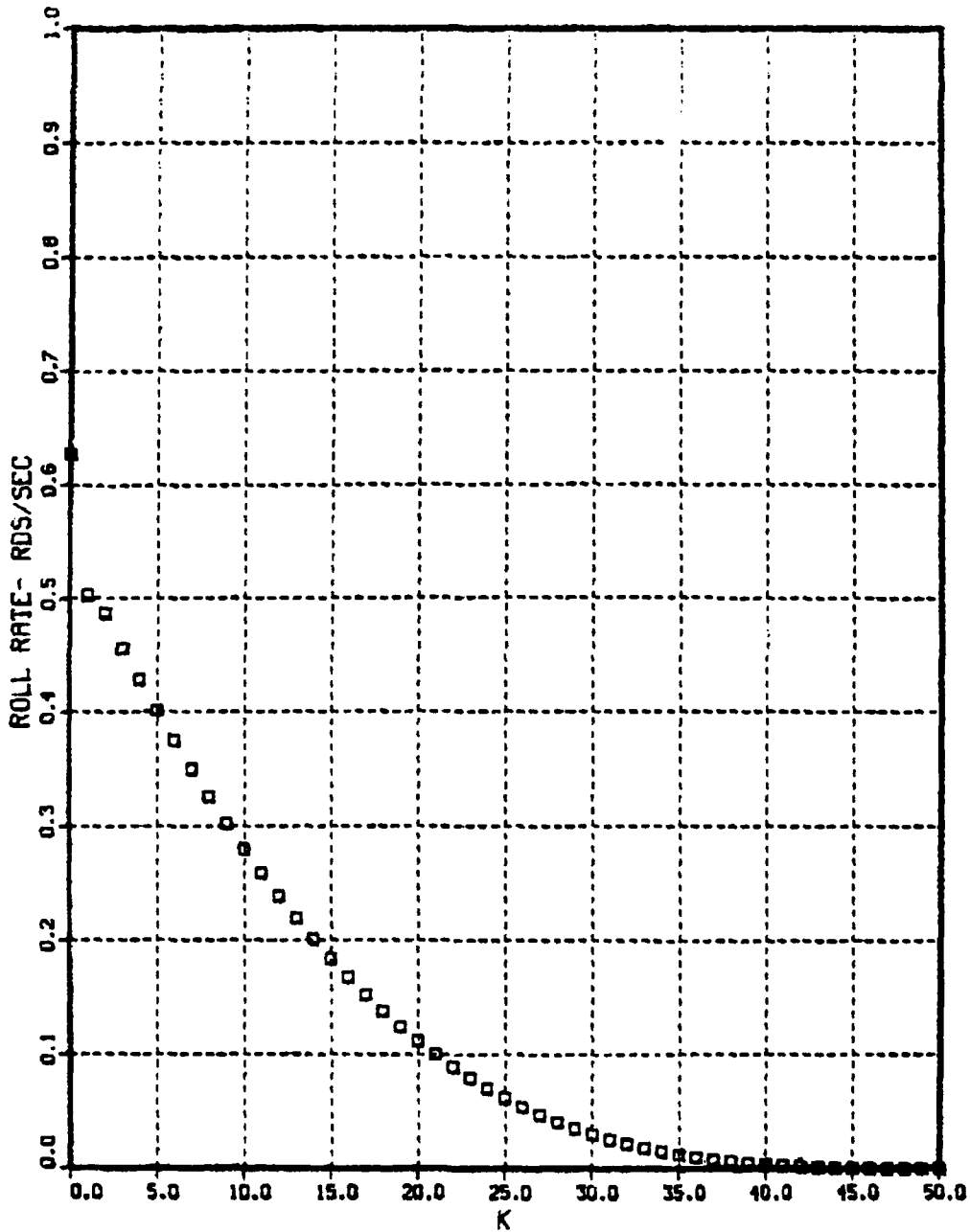


Figure 4.30 Commanded Roll Rate-Case 11.

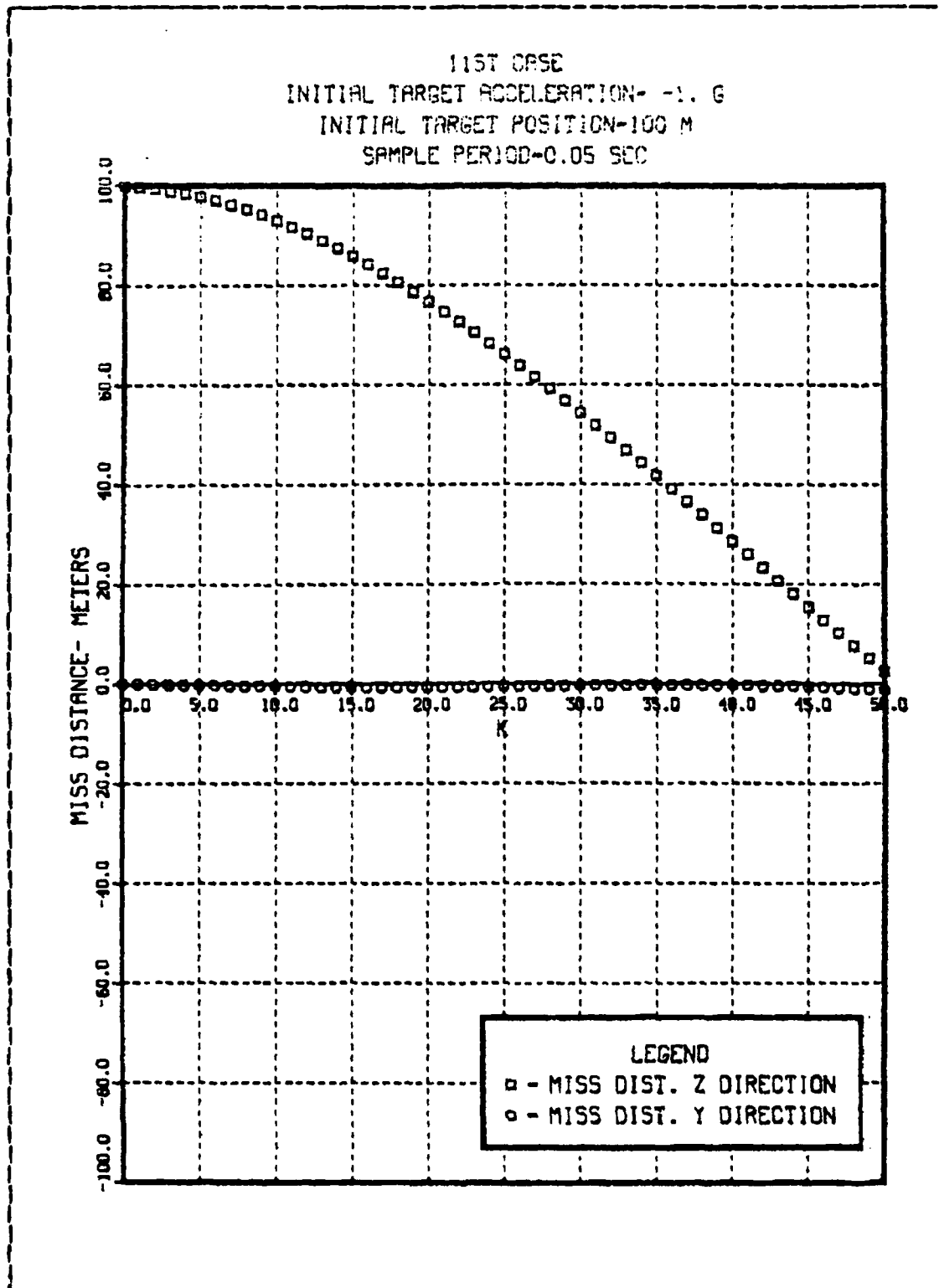


Figure 4.31 Miss Distance-Case 11.

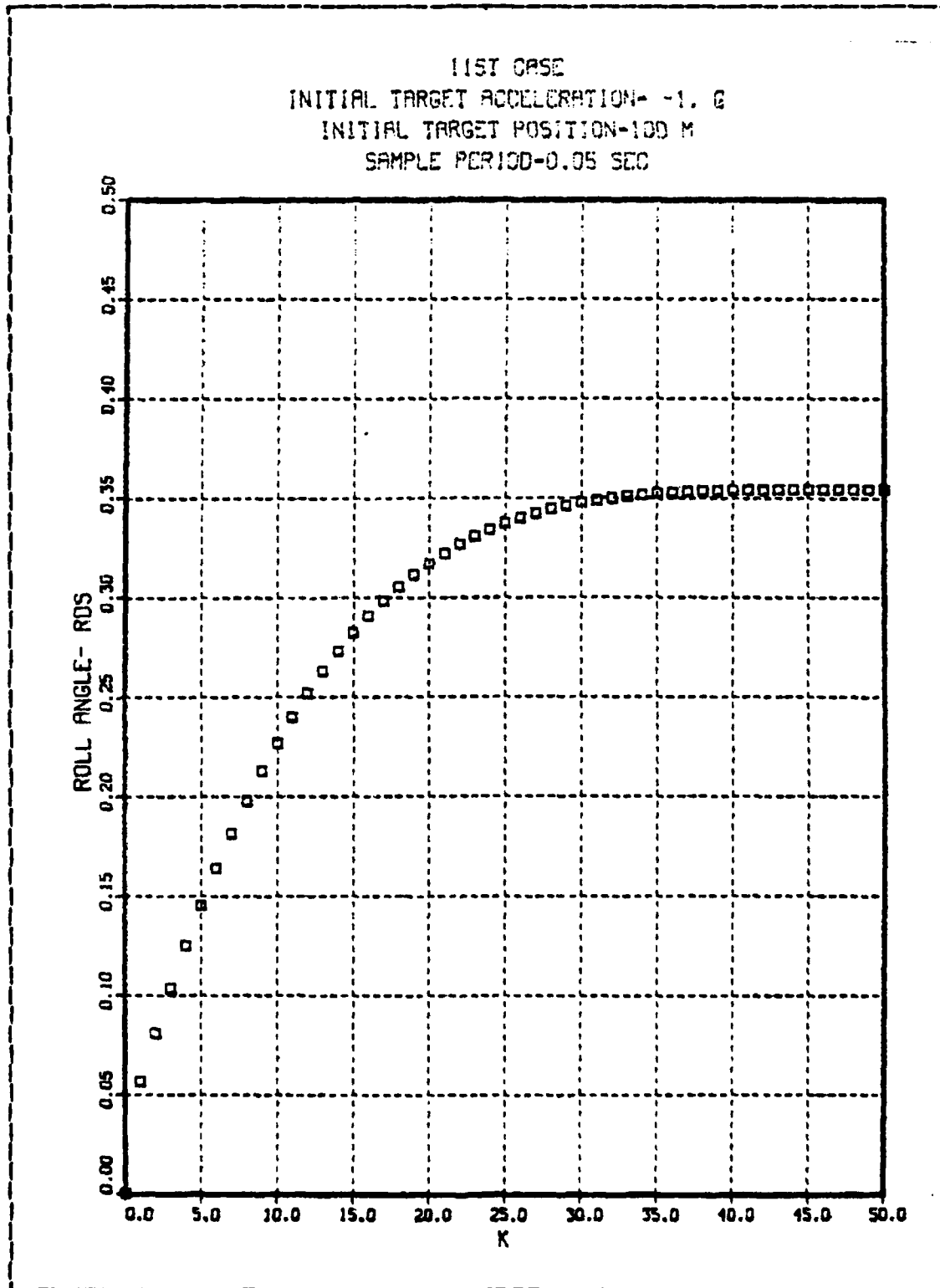


Figure 4.32 Roll Angle-Case 11.

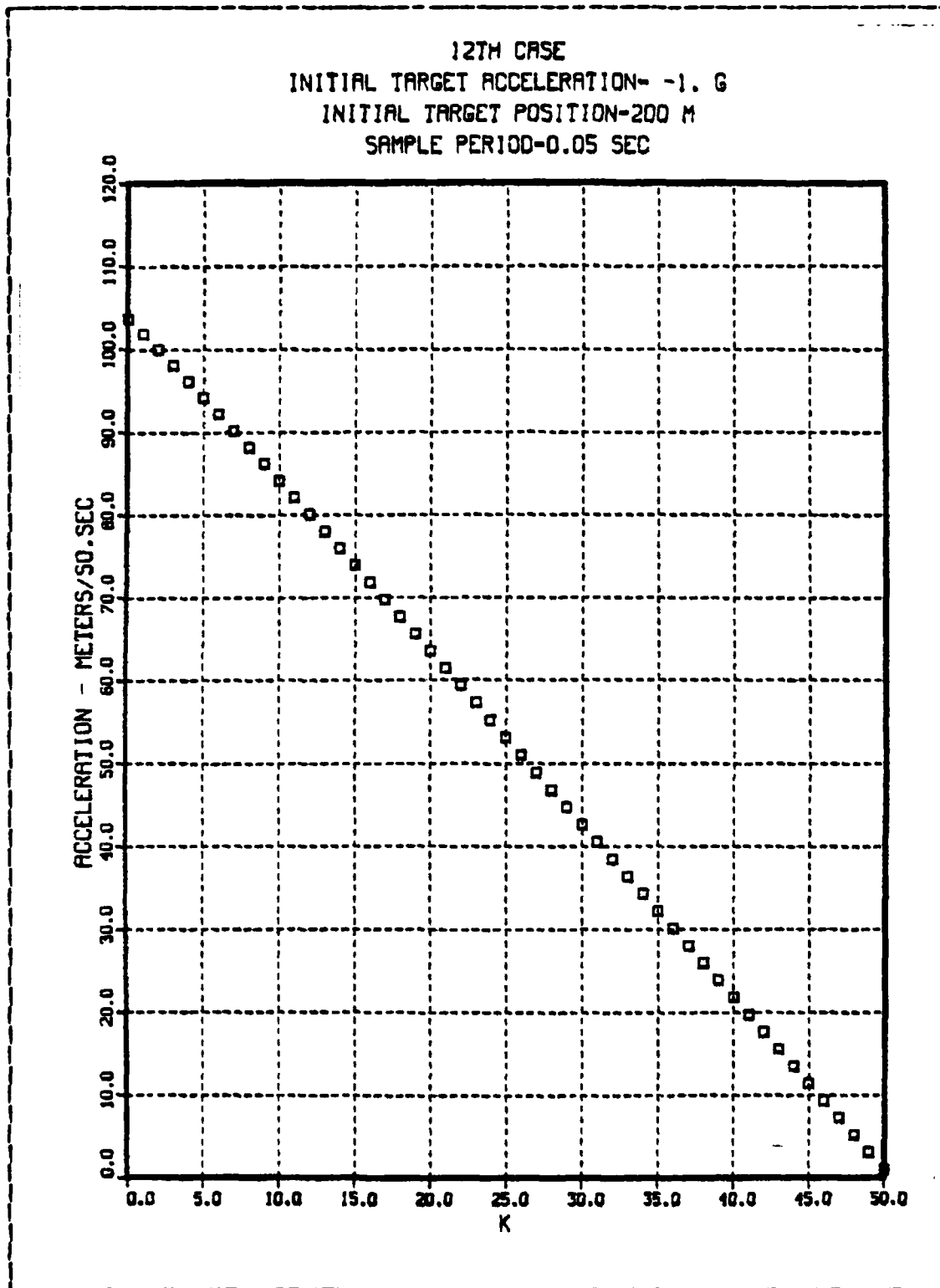


Figure 4.33 Commanded Acceleration-Case 12.

12TH CASE  
INITIAL TARGET ACCELERATION- -1. G  
INITIAL TARGET POSITION-200 M  
SAMPLE PERIOD-0.05 SEC

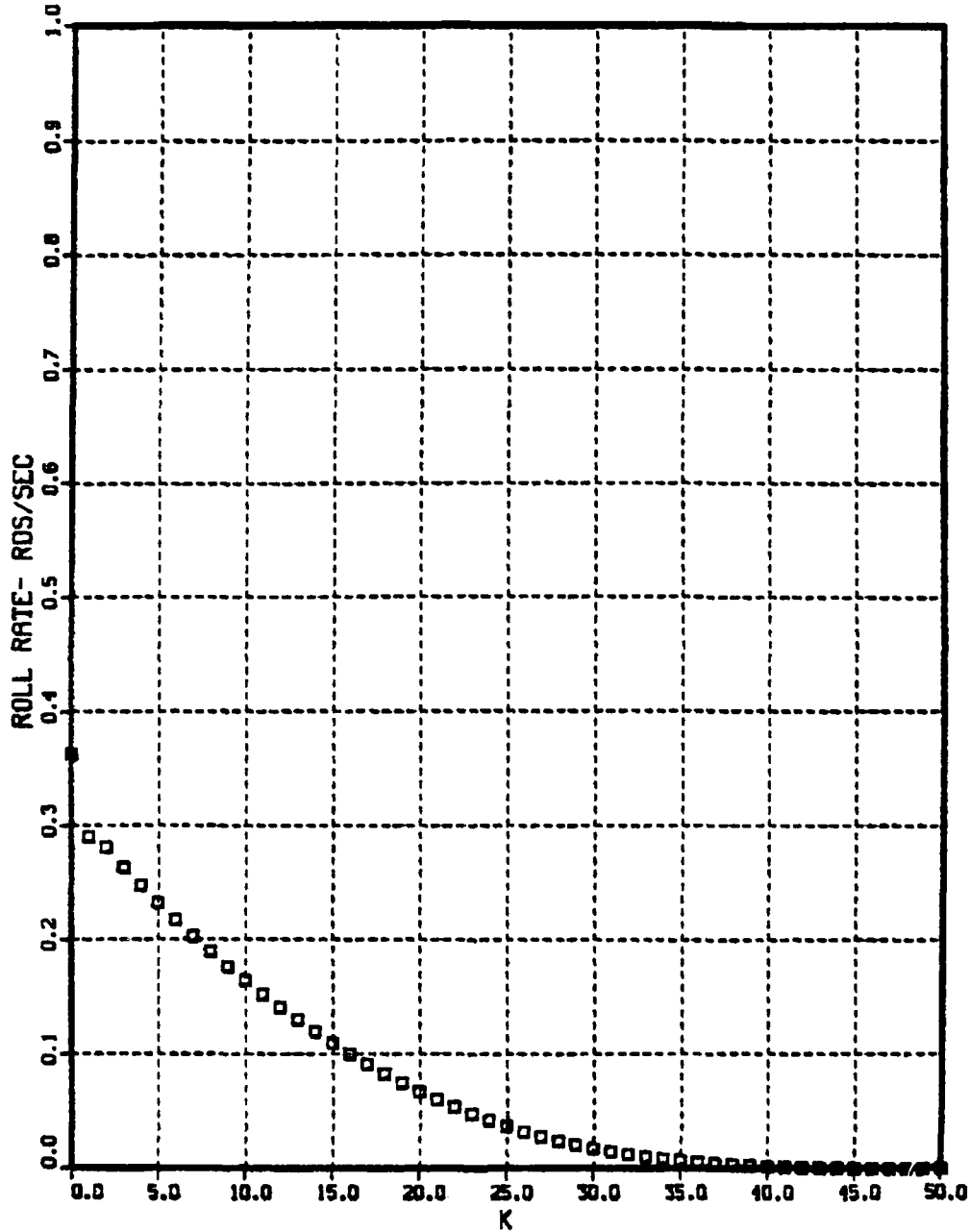


Figure 4.34 Commanded Roll Rate-Case 12.

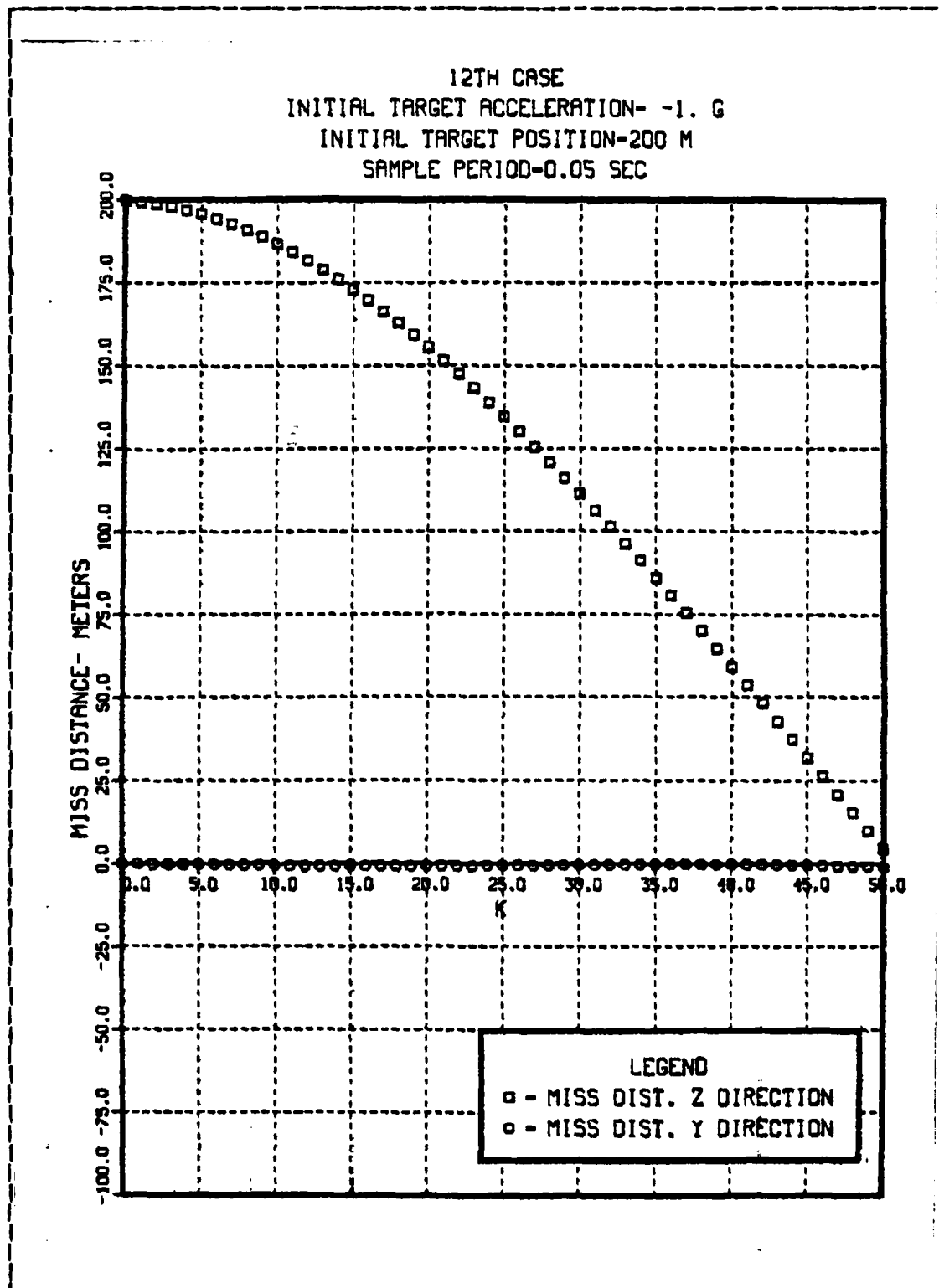


Figure 4.35 Miss Distance-Case 12.

12TH CASE  
INITIAL TARGET ACCELERATION- -1. G  
INITIAL TARGET POSITION-200 M  
SAMPLE PERIOD-0.05 SEC

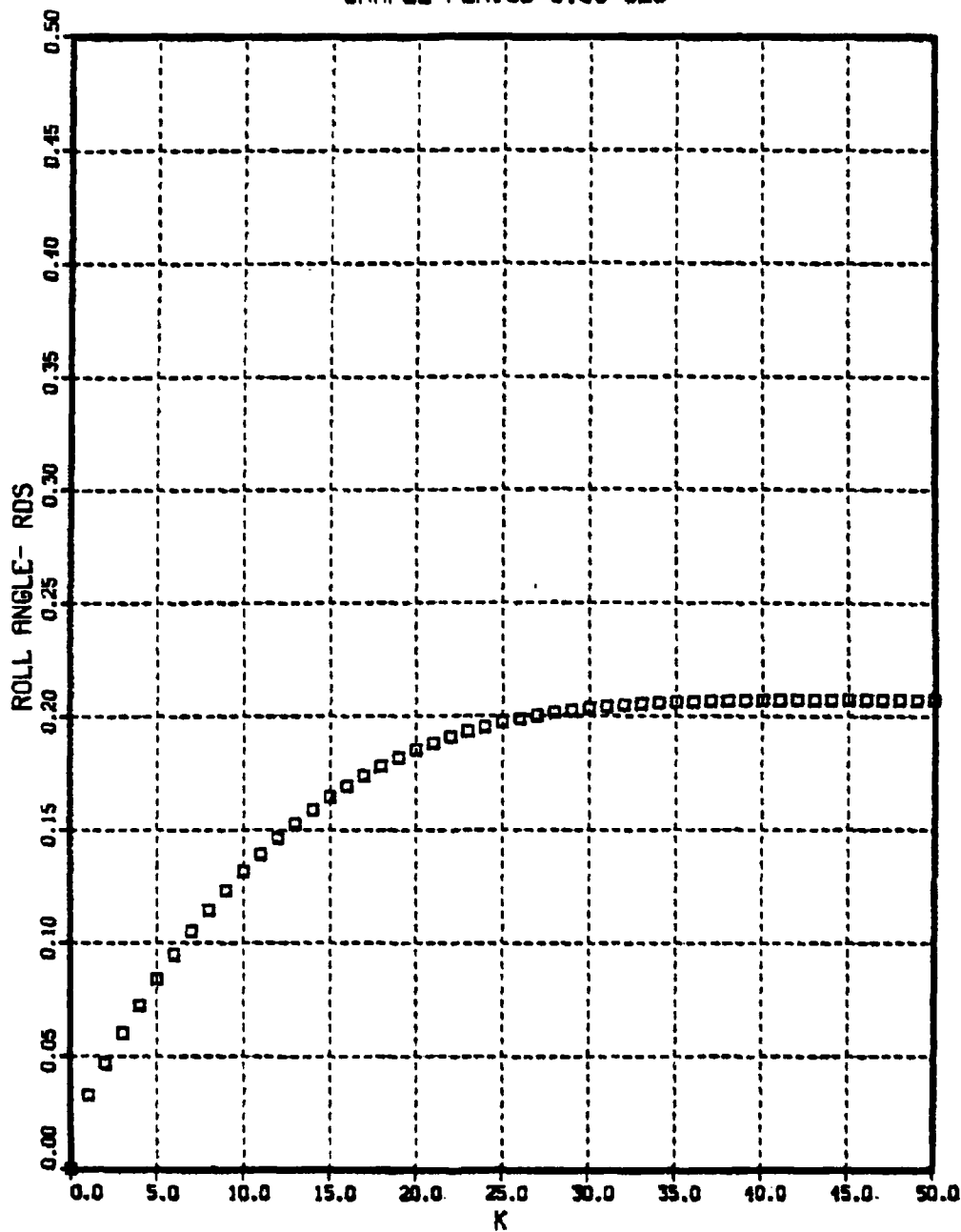


Figure 4.36 Roll Angle-Case 12.

**TABLE V**  
**Effect of Time to Intercept**

case	t	AC (m/sec)	PC (rad/sec)	miss distance y direction (m)	miss distance z direction (m)	(rad)	CG-to-CG miss distance (m)
11	0	59.01	.627	0.0	100.	0.0	100.
	11	.608	0.0	-1.31	2.53	.354	2.85
12	0	103.78	.363	0.0	200.	0.0	200.
	11	1.04	0.0	-1.01	4.69	.207	4.82

## V. FINAL CONCLUSIONS AND COMMENTS

The scope of the present work was the development of an optimal digital control to be applied on a bank-to turn missile.

A two dimensional model, as suggested in reference 1, was adopted. After the digitalization of the continuous model it was necessary to solve a modified Ricatti equation since in the state equation there was a third term representing the gravity's effect. The approach that has been adopted is new, and although good results were obtained for the scenarios considered in this work, it is necessary that the algorithm be further tested and evaluated in similar problems due to its novelty.

The optimal was solved with an initial restriction to small angles. This condition was later relaxed so that large roll angles could be analyzed.

It is difficult to compare the present work with previous results since Stallard has indicated a mistake in his original paper, and further works in this area was not found.

However some comparison with Stallard work is possible. The commanded acceleration of the missile are such as to correct the ZEM at each point, this agrees with that reference. There is a proportional relationship between the commanded roll rate and the commanded acceleration, and the commanded roll rate is proportional to the defined  $\phi_{ideal}$  at each point, which again agrees with reference 1.

The algorithm developed in this work requires extensive computation at each step, and it is clear that some software optimization will be needed. The motivation for considering the constant steady-state gain due to gravity was to decrease this computational burden. This approach however resulted in unacceptable miss distance.

Another point of investigation that could reflect on the period available to the computer to perform its calculations was a change in the sample rate. Two different sample rates were investigated, both lead to larger errors than the nominal period of .05 seconds. A detailed study on this issue is left as suggestion for future works, since some optimal value of the sampling rate is clearly indicated.

It is important to keep in mind that the model adopted is two dimensional, while the actual problem is three dimensional, thus some brief studies were conducted in order to check the region of validity of the 2-D.

In the analysis of the pitch angle, one can see that is necessary to have small variations in pitch in order to approximate it as a constant. However, at the moment that this angle is different from zero, as explained in chapter 4, it is possible to have in the flight path reference frame a target maneuver in the Z direction that will lead to large acceleration commands, leading the missile to large miss distances, when considering a movable target. When the present system was tested against fixed targets, the results were quite good, this suggests the application of the model in air-to-surface missiles.

Further investigation were made on the effect of time-to-go. As expected, decreased time to go, results in increased miss distance. A detailed analysis of more complex scenarios is needed in order to properly define the effect of time to go.

Also, it would be interesting to extend the model to three dimensions and include the effects of lags on the system in future works. Finally, in appendix A, the computer model used in this work is enclosed. Some improvements in this program can be done, mainly in the data introduction, and in some optimization of the running time.

APPENDIX A  
FORTRAN PROGRAM

These appendix provides a listing of the computer program used in the present study.

Since the routines used are non-IMSL, and a small change to double-precision was necessary, they are also being provided.

```

CJOB
C
C
C
C
TESE      1      VELLUSC,CAL
VARIABLES  DECLARATIONS
REAL*8  A(7,7),B(7,2),BT(2,7),BT(2,7),TAU,DELTA,E,DET,II
REAL*8  W(1,7),BTSEG(2,1),SG(7,1),BTSEG(2,1),BTSEG(2,1)
REAL*8  S(7,7),SB(7,7),AINV(7,7),BT(2,7),BT(2,7),BT(2,7),BT(2,7)
REAL*8  AIPSA(2,7),BPF(7,7),S(7,7),S(7,7),S(7,7),S(7,7),S(7,7),S(7,7)
REAL*8  R(2,2),RINV(2,2),Z(7,2),XS(7,1,201),F(2,7)
REAL*8  FG(2,2),BFG(7,1),EBFG(7,1),GS(7,1),EIG(7,1)
REAL*8  Q(2,2),ATSG(7,1),AX(7,1),BU(7,1),EIG(7,1)
REAL*8  P(7,7),PS(7,7),AYO,UGN(2,1),UG(2,1),UL(2,1)
REAL*8  YO,XC,ZO,VXO,VYO,VZO,ATXO,YS(201),ZS(201)
REAL*8  X(7,1),U(2,1),EI(7,1),G(1,1),EG(7,1),UN(2,1)
REAL*8  ABFX(7,1),KP(201),ACD(201),PCD(201),PHI
REAL*8  A3(7,7,201),FD12(201),FD13(201),FD14(201),FG3(7,1,201)
REAL*8  AT3(7,7,201),b3(7,2,7,201)
REAL*8  FD15(201),FD16(201),FD17(201),EBFGG(7,1),UC(2,1)

REAL*8  FD21(201),FD22(201),FD23(201),FD24(201)
REAL*8  FD25(201),FD26(201),FD27(201)

INTEGER  I,J,K,N,L,K1,COUNT,CCOUNT,M,KN,KL,NN
REAL*8  PHI,PCO,PH(201)
REAL*8  AC(201),KPS(201),PC(201),YM(201),ZM(201),CGS(201)
REAL*8  FS11(201),FS12(201),FS13(201),FS14(201)
REAL*8  FS15(201),FS16(201),FS17(201),DPH(201)

REAL*8  FS21(201),FS22(201),FS23(201),FS24(201)
REAL*8  FS25(201),FS26(201),FS27(201)

REAL*8  FGD1(201),FGD2(201),FGD3(201),FGD4(201)
REAL*8  FGD5(201),FGD6(201),FGD7(201)

AMIN=-19.6
PHI=0.0
PHIC=0.0
COUNT=0.0
TI=5.0
ACO=26.7
GI(1,1)=-s.8

```

S000490  
 TES00500  
 TES00510  
 TES00520  
 TES00530  
 TES00540  
 TES00550  
 TES00560  
 TES00570  
 TES00580  
 TES00590  
 TES00600  
 TES00610  
 TES00620  
 TES00630  
 TES00640  
 TES00650  
 TES00660  
 TES00670  
 TES00680  
 TES00690  
 TES00700  
 TES00710  
 TES00720  
 TES00730  
 TES00740  
 TES00750  
 TES00760  
 TES00770  
 TES00780  
 TES00790  
 TES00800  
 TES00810  
 TES00820  
 TES00830  
 TES00840  
 TES00850  
 TES00860  
 TES00870  
 TES00880  
 TES00890  
 TES00900  
 TES00910  
 TES00920  
 TES00930  
 TES00940  
 TES00950  
 TES00960

```

C C C
1 IF(COUNT.EG.101)GC TC 50
C C C
K=COUNT+1
C C C
INITIALIZE MATRIX W
DO 3 I=1,7
DO 2 J=1,7
W11(I,J)=0.
CONTINUE
3 CCNTINUE
W11(1,1)=1.
W11(4,4)=1.
DO 5 I=1,7
SG(I,1)=C.
DO 4 J=1,7
S(I,J)=W11(I,J)
CONTINUE
5 CCNTINUE
WRITE(6,25)
YT0=0.0
YMO=0.
XT0=250C.
XMO=0.
ZTC=100.
ZMU=0.
VYT0=0.
VYMC=0.
VXTC=500.
VXMC=1000.
VZTC=0.0C.
VZMO=0.
C
YO=YT0-YMO
XO=XT0-XMO
ZO=ZT0-ZMO
VXO=VXTC-VXMO
VYO=VYT0-VYMO
VZO=VZTC-VZMO
C
ATX0=0
ATY0=-4.*S.8
ATZ0=0.0
DELPHO=C.

```

TESS00970  
 TESS00980  
 TESS00990  
 TESS01000  
 TESS01010  
 TESS01020  
 TESS01030  
 TESS01040  
 TESS01050  
 TESS01060  
 TESS01070  
 TESS01080  
 TESS01090  
 TESS01100  
 TESS01110  
 TESS01120  
 TESS01130  
 TESS01140  
 TESS01150  
 TESS01160  
 TESS01170  
 TESS01180  
 TESS01190  
 TESS01200  
 TESS01210  
 TESS01220  
 TESS01230  
 TESS01240  
 TESS01250  
 TESS01260  
 TESS01270  
 TESS01280  
 TESS01290  
 TESS01300  
 TESS01310  
 TESS01320  
 TESS01330  
 TESS01340  
 TESS01350  
 TESS01360  
 TESS01370  
 TESS01380  
 TESS01390  
 TESS01400  
 TESS01410  
 TESS01420  
 TESS01430  
 TESS01440

```

C COSTET=1.0
C DELPHO=C.0
C INITIAL IZATION OF STATE VECTOR X(K)
C X(1,1)=VC
C X(2,1)=VVO
C X(3,1)=AIVO
C X(4,1)=ZC
C X(5,1)=VZO
C X(6,1)=AIZO
C X(7,1)=DELPHO
C *****
C DC 6 I=1,7
C XS(I,1)=X(I,1)
C 6 CCNTINUE
C DC 7 I=1,7
C X(I,1)=XS(I,1,K)
C 7 CCNTINUE
C PHIO=PHI
C L=101
C CCOUNT=CCOUNT+1
C DC 19 N=K,L
C KI=N-1
C DC 9 I=1,7
C DO 8 J=1,7
C A(I,J)=0.
C 8 CCNTINUE
C TAU=20.
C DELT=.05C
C E=2.7187
C ACO=26.7
C TI=5.0-KI*T
C COSTET=1.0
C A(1,1)=1.
C A(1,2)=DELT
C A(2,2)=1.
C A(4,4)=1.
C A(5,5)=1.

```

TESO1450  
 TESO1460  
 TESO1470  
 TESO1480  
 TESO1490  
 TESO1500  
 TESO1510  
 TESO1520  
 TESO1530  
 TESO1540  
 TESO1550  
 TESO1560  
 TESO1570  
 TESO1580  
 TESO1590  
 TESO1600  
 TESO1610  
 TESO1620  
 TESO1630  
 TESO1640  
 TESO1650  
 TESO1660  
 TESO1670  
 TESO1680  
 TESO1690  
 TESO1700  
 TESO1710  
 TESO1720  
 TESO1730  
 TESO1740  
 TESO1750  
 TESO1760  
 TESO1770  
 TESO1780  
 TESO1790  
 TESO1800  
 TESO1810  
 TESO1820  
 TESO1830  
 TESO1840  
 TESO1850  
 TESO1860  
 TESO1870  
 TESO1880  
 TESO1890  
 TESO1900  
 TESO1910  
 TESO1920

```

A(7,7) = 1. * DELT / TAU
A(3,3) = DEXP(-1. * DELT / TAU)
A(6,6) = DELT
A(4,5) = TAU * DELT - TAU ** 2 * (1. - DEXP(-DELT / TAU))
A(1,3) = A(1,3)
A(4,6) = A(1,3)
A(2,3) = TAU * (1. - DEXP(-DELT / TAU))
A(5,6) = A(2,3)
A(1,7) = ACO * DCOS(PHIO) * (DELT ** 2 - ((2 * K1 + 1.) / (2 * TI)) * DELT *
A(2,7) = ACO * DCOS(PHIO) * (DELT - ((2 * K1 + 1.) / (2 * TI)) * DELT ** 2)
A(4,7) = ACO * DSIN(PHIO) * (DELT ** 2 - ((2 * K1 + 1.) / (2 * TI)) * DELT *
A(5,7) = ACO * DSIN(PHIO) * (DELT - ((2 * K1 + 1.) / (2 * TI)) * DELT ** 2)
DO 11 I = 1, 7
DO 10 J = 1, 7
A3(I, J, N) = A(I, J)
CONTINUE
11 CONTINUE
C
CALL GMTRA(A, AT, 7, 7)
C
INITIALIZE MATRIX B
C
B12V = DELT ** 3 / 2. - ((2. * K1 + 1.) / (4. * TI)) * DELT ** 4
C
B22V = DELT ** 2 / 2. - ((K1 * DELT + DELT) ** 3 / (3. * TI))
1+ ((K1 * DELT + DELT) ** 2) * K1 * DELT / (2. * TI) - ((K1 * DELT) ** 3) / (6. * TI)
C
B(1,1) = DSIN(PHIO) * DELT ** 2 / 2.
B(1,2) = ACO * DCOS(PHIO) * (B12V)
B(2,1) = DELT * DSIN(PHIO)
B(2,2) = ACO * DCOS(PHIO) * (B22V)
B(3,1) = 0.
B(3,2) = C.
B(4,1) = -CCOS(PHIO) * DELT ** 2 / 2.
B(4,2) = ACO * DSIN(PHIO) * (B12V)
B(5,1) = -DELT * DCOS(PHIO)
B(5,2) = ACO * DSIN(PHIO) * (B22V)
B(6,1) = C.
B(6,2) = C.
B(7,1) = C.
B(7,2) = DELT
C
DO 13 I = 1, 7
DO 12 J = 1, 2
B3(I, J, N) = B(I, J)
CONTINUE
12 CONTINUE
C
  
```

TESO1930  
 TESO1940  
 TESO1950  
 TESO1960  
 TESO1970  
 TESO1980  
 TESO1990  
 TESO2000  
 TESO2010  
 TESO2020  
 TESO2030  
 TESO2040  
 TESO2050  
 TESO2060  
 TESO2070  
 TESO2080  
 TESO2090  
 TESO2100  
 TESO2110  
 TESO2120  
 TESO2130  
 TESO2140  
 TESO2150  
 TESO2160  
 TESO2170  
 TESO2180  
 TESO2190  
 TESO2200  
 TESO2210  
 TESO2220  
 TESO2230  
 TESO2240  
 TESO2250  
 TESO2260  
 TESO2270  
 TESO2280  
 TESO2290  
 TESO2300  
 TESO2310  
 TESO2320  
 TESO2330  
 TESO2340  
 TESO2350  
 TESO2360  
 TESO2370  
 TESO2380  
 TESO2390  
 TESO2400

```

13 CONTINUE
   CALL GMTRA(B,BT,7,2)
   DO 15 I=1,7
     DO 14 J=1,7
       AT3(I,J,N)=AT(I,J)
     CONTINUE
   CONTINUE
14 CONTINUE
15 DO 17 I=1,2
     DO 16 J=1,7
       BT3(I,J,N)=BT(I,J)
     CONTINUE
   CONTINUE
16 INITIALIZE MATRIX E
17 DO 18 I=1,7
     EI(I,1)=0.
   CONTINUE
18 EI(4,1)=-DELT**2/2.*COSTET
   EI(5,1)=-DELT*COSTET
19 CONTINUE
   INITIALIZE MATRIX Q
   Q(1,1)=.C0578
   Q(1,2)=C.
   Q(2,1)=C.
   Q(2,2)=5.
   C
   C INITIALIZE MATRIX P
   DC 21 I=1,7
   DO 20 J=1,7
     P(I,J)=0.
   CONTINUE
20 CONTINUE
21 C
   C
   C *****
   C SOLUTION OF RICCATI EQUATION *****
   C *****
   C *****
   M=101
22 IF(M.LI.1.)GO TO 31
   DC 24 I=1,7
   DO 23 J=1,7
     A(I,I,J)=A3(I,J,M)
     AT(I,I,J)=AT3(I,J,M)
   CONTINUE
23 CONTINUE
24 CCNTINUE
  
```



TESO2890  
 TESO2900  
 TESO2910  
 TESO2920  
 TESO2930  
 TESO2940  
 TESO2950  
 TESO2960  
 TESO2970  
 TESO2980  
 TESO2990  
 TESO3000  
 TESO3010  
 TESO3020  
 TESO3030  
 TESO3040  
 TESO3050  
 TESO3060  
 TESO3070  
 TESO3080  
 TESO3090  
 TESO3100  
 TESO3110  
 TESO3120  
 TESO3130  
 TESO3140  
 TESO3150  
 TESO3160  
 TESO3170  
 TESO3180  
 TESO3190  
 TESO3200  
 TESO3210  
 TESO3220  
 TESO3230  
 TESO3240  
 TESO3250  
 TESO3260  
 TESO3270  
 TESO3280  
 TESO3290  
 TESO3300  
 TESO3310  
 TESO3320  
 TESO3330  
 TESO3340  
 TESO3350  
 TESO3360

```

C      G(I,1)=-5.8
C
C      X(K+1)=(A-EF)X(K)+EG(K)
C
C      K=CCUNT+1
C      KP(K)=K-1
C      KN=K-1
C      32 IF(KN.EQ.K)GO TO 42
C
C      CC 34 I=1,2
C      FG(I,1)=FG3(I,1,KN+1)
C      DO 33 J=1,7
C      F(I,J)=F3(I,J,KN+1)
C      33 CONTINUE
C      34 CONTINUE
C      *****
C
C      CALL GMPRC(F,X,UN,2,7,1)
C      CALL GMPRC(FG,G,UGN,2,1,1)
C      DO 35 I=1,2
C      U(I,1)=-1.*UN(I,1)
C      UG(I,1)=-1.*UGN(I,1)
C      CONTINUE
C      UG(1,1)=14.70
C      UG(2,1)=0.0
C      CONTINUE
C      CALL GMADD(U1,UG,U,2,1)
C      DO 37 I=1,7
C      J=1,7
C      AT(I,J)=AT3(I,J,KN+1)
C      A(I,J)=A3(I,J,KN+1)
C      CONTINUE
C      CONTINUE
C      DO 39 I=1,7
C      J=1,2
C      B(I,J)=B3(I,J,KN+1)
C      CONTINUE
C      CONTINUE
C      DO 41 I=1,2
C      FG(I,1)=FG3(I,1,KN+1)
C      DO 40 J=1,7
C      BT(I,J)=BT3(I,J,KN+1)
C      F(I,J)=F3(I,J,KN+1)
  
```

```

TESO 3370
TESO 3380
TESO 3390
TESO 3400
TESO 3410
TESO 3420
TESO 3430
TESO 3440
TESO 3450
TESO 3460
TESO 3470
TESO 3480
TESO 3490
TESO 3500
TESO 3510
TESO 3520
TESO 3530
TESO 3540
TESO 3550
TESO 3560
TESO 3570
TESO 3580
TESO 3590
TESO 3600
TESO 3610
TESO 3620
TESO 3630
TESO 3640
TESO 3650
TESO 3660
TESO 3670
TESO 3680
TESO 3690
TESO 3700
TESO 3710
TESO 3720
TESO 3730
TESO 3740
TESO 3750
TESO 3760
TESO 3770
TESO 3780
TESO 3790
TESO 3800
TESO 3810
TESO 3820
TESO 3830
TESO 3840

```

```

C
40 CONTINUE
41 CONTINUE
   CALL GMPRD(B,F,BF,7,2,7)
   CALL GMSLB(A,BF,7,7)
   CALL GMPRD(ABF,X,ABFX,7,7,1)
   CALL GMPRD(B,F,FG,7,2,1)
   CALL GMSLB(EL,FG,EBFG,7,1)
   CALL GMPRD(EBFG,G,EBFGG,7,1,1)
   CALL GMACD(ABFX,EBFG,X,7,1)
      KN=KN+1
   GO TO 32
42 CCNTINUE
   *****
   LIMIT IN COMANDEL ACCELERATION *****
   IF(U(1,1).LT.AMIN)U(1,1)=AMIN
   CCNTINUE
   *****
   ***** MISSILE MISSILE MISSILE *****
   ***** MISSILE MISSILE MISSILE *****
   INITIALIZATION OF STATE VECTOR X(K)
   INITIALIZE MATRIX A
   KI=COUNT
   DC 44 I=1,7
   DO 43 J=1,7
     A(I,J)=0.
   CCNTINUE
43 CONTINUE
44 CONTINUE
   TAU=20.05C
   DELT=.718
   E=2.718
   ACO=U(1,1)
   COSTET=1.0
   DO 45 I=1,7
     X(I,1)=XS(I,1,K)
   CCNTINUE
   A(7,7)=0.
45 CONTINUE
   A(1,1)=1.0
   A(1,2)=1.0
   A(2,2)=1.0
   A(4,4)=1.0
   A(5,5)=1.0
   A(7,7)=1.0
   A(3,3)=DEXP(-1.0)
   A(6,6)=DEXP(-1.0)

```

IES03850  
 IES03860  
 IES03870  
 IES03880  
 IES03890  
 IES03900  
 IES03910  
 IES03920  
 IES03930  
 IES03940  
 IES03950  
 IES03960  
 IES03970  
 IES03980  
 IES03990  
 IES04000  
 IES04010  
 IES04020  
 IES04030  
 IES04040  
 IES04050  
 IES04060  
 IES04070  
 IES04080  
 IES04090  
 IES04100  
 IES04110  
 IES04120  
 IES04130  
 IES04140  
 IES04150  
 IES04160  
 IES04170  
 IES04180  
 IES04190  
 IES04200  
 IES04210  
 IES04220  
 IES04230  
 IES04240  
 IES04250  
 IES04260  
 IES04270  
 IES04280  
 IES04290  
 IES04300  
 IES04310  
 IES04320

```

A(4,5)=CELT
A(1,3)=TAU*DEL T-TAU**2*(1.-DEXP(-DEL T/TAU))
A(4,6)=A(1,3)
A(2,3)=TAU*(1.-DEXP(-DEL T/TAU))
A(5,6)=A(2,3)
A(1,7)=ACO*DCOS(PHIO)*DELT**2/2.
A(2,7)=ACO*DCOS(PHIO)*DELT
A(4,7)=ACO*DSIN(PHIO)*DELT**2/2.
A(5,7)=ACO*DSIN(PHIO)*DELT
CONTINUE
INITIALIZE MATRIX B
B(1,1)=DSIN(PHIO)*DELT**2/2.
B(1,2)=ACO*DCOS(PHIO)*DELT**3/6.
B(2,2)=C.0
B(2,1)=CELT*DSIN(PHIO)
B(3,1)=C.
B(3,2)=C.
B(4,1)=C.
B(4,2)=ACO*DSIN(PHIO)*DELT**3/6.
B(5,1)=-DEL T*DCOS(PHIO)
B(5,2)=ACO*DSIN(PHIO)*DELT**2/2.
B(6,1)=C.
B(6,2)=C.
B(7,1)=C.
B(7,2)=CELT
IF(K.EQ.1.)GO TO 46
CONTINUE
PH(K)=PHIO
PYS(K)=X(1,1)
ZS(K)=X(4,1)
CONTINUE
CALL GMFPRD(A,X,AX,7,7,1)
CALL GMFPRD(B,U,BU,7,2,1)
CALL GMFPRD(EI,GI,EIG,7,1,1)
CALL GMADD(AX,BU,AXB,7,1)
CALL GMADD(AXB,EIG,AXB,7,1)
PHIO=PHIC+X(7,1)
DO 48 I=1,7
  XS(I,1,K+1)=X(I,1)
CONTINUE
46
47
48
C
C
C
C
C
C
C
  
```



TESO4810  
 TESO4820  
 TESO4830  
 TESO4840  
 TESO4850  
 TESO4860  
 TESO4870  
 TESO4880  
 TESO4890  
 TESO4900  
 TESO4910  
 TESO4920  
 TESO4930  
 TESO4940  
 TESO4950  
 TESO4960  
 TESO4970  
 TESO4980  
 TESO4990  
 TESO5000  
 TESO5010  
 TESO5020  
 TESO5030  
 TESO5040  
 TESO5050  
 TESO5060  
 TESO5070  
 TESO5080  
 TESO5090  
 TESO5100  
 TESO5110  
 TESO5120  
 TESO5130  
 TESO5140  
 TESO5150  
 TESO5160  
 TESO5170  
 TESO5180  
 TESO5190  
 TESO5200  
 TESO5210  
 TESO5220  
 TESO5230  
 TESO5240  
 TESO5250  
 TESO5260  
 TESO5270  
 TESO5280

CALL CURVE (KPS, YM, 101, -1)  
 CALL LINESP (2, 0)  
 CALL LINES (MISS, DIST: 7 DIRECTION\$, IPAK, 1)  
 CALL LINES (MISS, DIST: 7 DIRECTION\$, IPAK, 2)  
 CALL LEGENC (IPAK, 2, 3, 5, 0, 5)  
 CALL BLREC (3, 3, 0, 3, 3, 5, 1, 2, .03)  
 CALL DASH (1, 1)  
 CALL GRID (1, 1, DASH)  
 CALL RESET (C)  
 CALL ENDPL (C)  
 CALL HPROT (MOVIE)  
 CALL AREA2D (7, 0, 9, 0)  
 CALL XNAME (K\$, 1, CO)  
 CALL YNAME (ACCELERATION - METERS/SQ.SEC\$, 100)  
 CALL HEADIN (4TH CASE\$, 100, 1, 4)  
 CALL HEADIN (INITIAL TARGET ACCELERATION= -4. G\$, 100, 1, 4)  
 CALL HEADIN (INITIAL TARGET POSITION= -600 M\$, 100, 1, 4)  
 CALL HEADIN (SAMPLE PERIOD= 0.05 SEC\$, 100, 1, 4)  
 CALL CROS  
 CALL GRAF (C, SCALE, 100, -25, SCALE, 110)  
 CALL CURVE (KPS, AC, 101, -1)  
 CALL FRAME  
 CALL DASH (1, 1)  
 CALL GRID (1, 1, DASH)  
 CALL RESET (C)  
 CALL ENDPL (C)  
 CALL HPROT (MOVIE)  
 CALL AREA2D (7, 0, 9, 0)  
 CALL XNAME (K\$, 1, CO)  
 CALL YNAME (ROLL RATE - RDS/SEC\$, 100)  
 CALL HEADIN (4TH CASE\$, 100, 1, 4)  
 CALL HEADIN (INITIAL TARGET ACCELERATION= -4. G\$, 100, 1, 4)  
 CALL HEADIN (INITIAL TARGET POSITION= -600 M\$, 100, 1, 4)  
 CALL HEADIN (SAMPLE PERIOD= 0.05 SEC\$, 100, 1, 4)  
 CALL CROS  
 CALL GRAF (C, SCALE, 100, 0, SCALE, 8)  
 CALL CURVE (KPS, PC, 101, -1)  
 CALL FRAME  
 CALL DASH (1, 1, DASH)  
 CALL GRID (1, 1, DASH)  
 CALL RESET (C)  
 CALL ENDPL (C)  
 CALL HPROT (MOVIE)  
 CALL AREA2D (7, 0, 9, 0)  
 CALL XNAME (K\$, 1, CO)  
 CALL YNAME (ROLL ANGLE - RDS\$, 100)  
 CALL HEADIN (4TH CASE\$, 100, 1, 4)  
 CALL HEADIN (INITIAL TARGET ACCELERATION= -4. G\$, 100, 1, 4)

TESO5250  
 TESO5300  
 TESO5310  
 TESO5320  
 TESO5330  
 TESO5340  
 TESO5350  
 TESO5360  
 TESO5370  
 TESO5380  
 TESO5390  
 TESO5400  
 TESO5410  
 TESO5420  
 TESO5430  
 TESO5440  
 TESO5450  
 TESO5460  
 TESO5470  
 TESO5480  
 TESO5490  
 TESO5500  
 TESO5510  
 TESO5520  
 TESO5530  
 TESO5540  
 TESO5550  
 TESO5560  
 TESO5570  
 TESO5580  
 TESO5590  
 TESO5600  
 TESO5610  
 TESO5620  
 TESO5630  
 TESO5640  
 TESO5650  
 TESO5660  
 TESO5670  
 TESO5680  
 TESO5690  
 TESO5700  
 TESO5710  
 TESO5720  
 TESO5730  
 TESO5740  
 TESO5750  
 TESO5760

```

CALL HEADIN('INITIAL TARGET POSITION=-600 M$',100,1.,4)
CALL HEADIN('SAMPLE PERIOD=0.05 SEC$',100,1.,4)
CALL CROSS
CALL FRAME
CALL GRAF(C.,SCALE,100.,0.,SCALE,4.)
CALL DASH
CALL GRID(1,1)
CALL RESET('CASH')
CALL CURVE(KPS,DPH,101,-1)
CALL ENDPL(C)
CALL DCNEPL

C *****
C   FORMAT('1')
25 FCRMAT(1X//5X,4X,'AC',9X,'PC',9X,'YM',9X,'ZM',9X,'DPH'
31 FORMAT(1X//5X,6(F9.4,3X)//)
35 FORMAT(1X//)
C   STOP
C   END
C   SUBROUTINE GMTRA
C   SUBROUTINE GMTRA(A,R,N,M)
C   DIMENSION A(1),R(1)
C   DOUBLE PRECISION A,R
C
C   IR=0
C   DO 10 I=1,N
C   IJ=I-N
C   DO 10 J=1,M
C   IJ=IJ+1
C   IR=IR+1
C   R(IR)=A(IJ)
C   10 RETURN
C   END
C *****
C   SUBROUTINE GMPRD
C   PURPOSE
C   MULTIPLY TWO GENERAL MATRICES TO FORM A RESULTANT GE
C   MATRIX
C   USAGE
C   CALL GMPRD(A,B,R,N,M,L)
C   DESCRIPTION OF PARAMETERS
C   A - NAME OF FIRST INPUT MATRIX
  
```

```

TESO5770
TESO5780
TESO5790
TESO5800
TESO5810
TESO5820
TESO5830
TESO5840
TESO5850
TESO5860
TESO5870
TESO5880
TESO5890
TESO5900
TESO5910
TESO5920
TESO5930
TESO5940
TESO5950
TESO5960
TESO5970
TESO5980
TESO5990
TESO6000
TESO6010
TESO6020
TESO6030
TESO6040
TESO6050
TESO6060
TESO6070
TESO6080
TESO6090
TESO6100
TESO6110
TESO6120
TESO6130
TESO6140
TESO6150
TESO6160
TESO6170
TESO6180
TESO6190
TESO6200
TESO6210
TESO6220
TESO6230
TESO6240

```

```

B - NAME OF SECOND INPUT MATRIX
R - NAME OF OUTPUT MATRIX
M - NUMBER OF ROWS IN A
L - NUMBER OF COLUMNS IN A AND ROWS IN B
    NUMBER OF COLUMNS IN B

```

```

REMARKS
ALL MATRICES MUST BE STORED AS GENERAL MATRICES
MATRIX R CANNOT BE IN THE SAME LOCATION AS MATRIX A
MATRIX R CANNOT BE IN THE SAME LOCATION AS MATRIX B
NUMBER OF COLUMNS OF MATRIX A MUST BE EQUAL TO NUMBER
OF MATRIX B

```

```

SUBROUTINES AND FUNCTION SUBPROGRAMS REQUIRED
NONE

```

```

METHOD
THE M BY L MATRIX B IS PREMULTIPLIED BY THE N BY M M
AND THE RESULT IS STORED IN THE N BY L MATRIX R.

```

```

.....
SUBROUTINE GMPRO(A,B,R,N,M,L)
DIMENSION A(L),B(L),R(L)
DOUBLE PRECISION A,B,R

```

```

IR=0
IK=-M
DO 10 K=1,L
IK=IK+M
DO 10 J=1,N
IR=IR+I
JI=J-N
IB=IK
R(IR)=0
DC 10 I=1,M
JI=JI+A
IB=IB+1
R(IR)=R(IR)+A(JI)*B(IB)
RETURN
END

```

```

.....
SUBROUTINE GMSUB
PURPOSE
SUBTRACT ONE GENERAL MATRIX FROM ANOTHER TO FORM RES

```

```

CCCCCCCCCCCCCCCCCCCCCCCCCCCCCCCCCCCCCCCCCCCCCCCCCCCCCCCCCCCC
C

```

TESO6250  
 TESO6260  
 TESO6270  
 TESO6280  
 TESO6290  
 TESO6300  
 TESO6310  
 TESO6320  
 TESO6330  
 TESO6340  
 TESO6350  
 TESO6360  
 TESO6370  
 TESO6380  
 TESO6390  
 TESO6400  
 TESO6410  
 TESO6420  
 TESO6430  
 TESO6440  
 TESO6450  
 TESO6460  
 TESO6470  
 TESO6480  
 TESO6490  
 TESO6500  
 TESO6510  
 TESO6520  
 TESO6530  
 TESO6540  
 TESO6550  
 TESO6560  
 TESO6570  
 TESO6580  
 TESO6590  
 TESO6600  
 TESO6610  
 TESO6620  
 TESO6630  
 TESO6640  
 TESO6650  
 TESO6660  
 TESO6670  
 TESO6680  
 TESO6690  
 TESO6700  
 TESO6710  
 TESO6720

```

CCCCCCCCCCCCCCCCCCCCCCCCCCCCCCCCCCCC
MATRIX
USAGE  CALL  GMSUB(A,B,R,N,M)
DESCRIPTION OF PARAMETERS
A - NAME OF FIRST INPUT MATRIX
B - NAME OF SECOND INPUT MATRIX
R - NAME OF OUTPUT MATRIX
N - NUMBER OF ROWS IN A,B,R
M - NUMBER OF COLUMNS IN A,B,R
REMARKS
ALL MATRICES MUST BE STORED AS GENERAL MATRICES
SUBROUTINES AND FUNCTION SUBPROGRAMS REQUIRED
NONE
METHOD
MATRIX B ELEMENTS ARE SUBTRACTED FROM CORRESPONDING
ELEMENTS
.....
SUBROUTINE GMSUB(A,B,R,N,M)
DIMENSION A(I),B(I),R(I)
DOUBLE PRECISION A,B,R
CALCULATE NUMBER OF ELEMENTS
NM=N*M
SUBTRACT MATRICES
DO 10 I=1,NM
R(I)=A(I)-E(I)
10 RETURN
END
.....
SUBROUTINE GMADD
PURPOSE
ADD TWO GENERAL MATRICES TO FORM RESULTANT GENERAL M
USAGE
CALL GMADD(A,B,R,N,M)
CCCCCCCCCCCCCCCCCCCCCCCCCCCCCCCCCCCC

```

```

TES06730
TES06740
TES06750
TES06760
TES06770
TES06780
TES06790
TES06800
TES06810
TES06820
TES06830
TES06840
TES06850
TES06860
TES06870
TES06880
TES06890
TES06900
TES06910
TES06920
TES06930
TES06940
TES06950
TES06960
TES06970
TES06980
TES06990
TES07000
TES07010
TES07020
TES07030
TES07040
TES07050
TES07060
TES07070
TES07080
TES07090
TES07100
TES07110
TES07120
TES07130
TES07140
TES07150
TES07160
TES07170
TES07180
TES07190
TES07200

DESCRIPTION OF PARAMETERS
A - NAME OF FIRST INPUT MATRIX
B - NAME OF SECOND INPUT MATRIX
R - NAME OF OUTPUT MATRIX
N - NUMBER OF ROWS IN A,B,R
M - NUMBER OF COLUMNS IN A,B,R

REMARKS
ALL MATRICES MUST BE STORED AS GENERAL MATRICES

SUBROUTINES AND FUNCTION SUBPROGRAMS REQUIRED
NONE

METHOD
ADDITION IS PERFORMED ELEMENT BY ELEMENT
.....
SUBROUTINE GMADD(A,B,R,N,M)
DIMENSION A(I),B(I),R(I)
DOUBLE PRECISION A,B,R
CALCULATE NUMBER OF ELEMENTS
NM=N*M
ADD MATRICES
DO I=1,NM
R(I)=A(I)+B(I)
RETURN
END

SUBROUTINE GAUSS?
PURPOSE
INVERT A DOUBLE PRECISION MATRIX BY THE GAUSS-JORDAN M
THIS ROUTINE IS A DOUBLE PRECISION VERSION OF SSP ROUT
MINV USING FL-NPGS-GAUSS3 (F-63) CALLING SEQUENCE
USAGE
CALL GAUSS3(N,EPS,A,X,KER,K)
DESCRIPTION OF PARAMETERS
N: ORDER OF MATRIX

```

TESO 7210  
 TESO 7220  
 TESO 7230  
 TESO 7240  
 TESO 7250  
 TESO 7260  
 TESO 7270  
 TESO 7280  
 TESO 7290  
 TESO 7300  
 TESO 7310  
 TESO 7320  
 TESO 7330  
 TESO 7340  
 TESO 7350  
 TESO 7360  
 TESO 7370  
 TESO 7380  
 TESO 7390  
 TESO 7400  
 TESO 7410  
 TESO 7420  
 TESO 7430  
 TESO 7440  
 TESO 7450  
 TESO 7460  
 TESO 7470  
 TESO 7480  
 TESO 7490  
 TESO 7500  
 TESO 7510  
 TESO 7520  
 TESO 7530  
 TESO 7540  
 TESO 7550  
 TESO 7560  
 TESO 7570  
 TESO 7580  
 TESO 7590  
 TESO 7600  
 TESO 7610  
 TESO 7620  
 TESO 7630  
 TESO 7640  
 TESO 7650  
 TESO 7660  
 TESO 7670  
 TESO 7680

EPS: DUMMY PARAMETER NOT USED BY GAUSS3  
 A: TWO-DIMENSIONAL ARRAY CONTAINING MATRIX TO BE INV  
 X: ERROR FLAG  
 KER: =1 INDICATES NO ERRORS  
 =2 INDICATES MATRIX IS SINGULAR OR NEARLY SINGUL  
 K: ROW AND COLUMN DIMENSION OF A AND X IN USER'S PRO  
 (ACTUAL NUMBER APPEARING IN USER'S DIMENSION STAT

REMARKS  
 ALL FLOATING POINT VARIABLES ARE DOUBLE PRECISION (REA  
 IF N IS GREATER THAN 50, THE DIMENSIONS OF ARRAYS L,M,  
 MUST BE CHANGED TO BE GREATER THAN OR EQUAL TO N.

```

SUBROUTINE GAUSS3 (N, EPS, A, X, KER, K)
REAL*8 A, X, Y, D
DIMENSION A(1), X(1), L(50), M(50), Y(50,50)
CC 1 I=1, N
DC 1 J=1, N
IND=(I-1)*K+J
Y(I, J)=A(I, INC)
KER=1
N2=2*N
CALL AMINV(Y, N, J, L, M)
CALL ARRAY(1, N, N, 50, 50, Y, Y)
IF(D.EQ.0.) KER=2
DC 2 I=1, N
DC 2 J=1, N
IND=(I-1)*K+J
X(IND)=Y(I, J)
RETURN
END
SUBROUTINE ARRAY(MODE, I, J, N, M, S, D)
DIMENSION S(1), D(1)
REAL*8 S, D
NI=N-I
IF(MODE=1) 100, 100, 120
IJ=I*J+1
NM=N*J+1
DC 110 K=1, J
NM=NM-NI
CC 110 L=1, I
IJ=IJ-1
NM=NM-1
110 D(NM)=S(I, J)
  
```

CCCCCCCCCCCCCCCC



```

08170
08180
08190
08200
08210
08220
08230
08240
08250
08260
08270
08280
08290
08300
08310
08320
08330
08340
08350
08360
08370
08380
08390
08400
08410
08420
08430
08440
08450
08460
08470
08480
08490
08500
08510
08520
08530
08540
08550
08560
08570
08580
08590
08600
08610
08620
08630
08640

```

```

C .....
C SEARCH FCR LARGEST ELEMENT
C .....
L=1.0D0
NK=-N K=1,N
DC 80 NK=NK+N
L(K)=K
M(K)=K
KK=NK+K
BIGA=A(KK)
DC 20 J=K,N
IZ=N*(J-1)
DC 20 I=K,N
IJ=IZ+1
IF(DABS(BIGA)-DABS(A(IJ))) 15,20,20
10 IF(BIGA=A(IJ))
15 L(K)=I
M(K)=J
20 CONTINUE

C INTERCHANGE ROWS
C .....
J=L(K)
IF(J-K) 35,35,25
25 KI=K-N I=1,N
DC 30 I=KI+N
KI=KI+N
FCLD=-A(KI)
I=KI-K+J
A(KI)=A(JI)
30 A(JI)=HOLL

C INTERCHANGE COLUMNS
C .....
35 I=M(K)
IF(I-K) 45,45,38
38 JF=N*(I-1)
DC 40 J=I,N
JK=NK+J
JI=JP+J
HOLD=-A(JK)
A(JK)=A(JI)
40 A(JI)=HOLL

C DIVIDE CCLUMN BY MINUS PIVOT (VALUE OF PIVOT ELEMENT IS
C CONTAINED IN BIGA)

```

TES08650  
 TES08660  
 TES08670  
 TES08680  
 TES08690  
 TES08700  
 TES08710  
 TES08720  
 TES08730  
 TES08740  
 TES08750  
 TES08760  
 TES08770  
 TES08780  
 TES08790  
 TES08800  
 TES08810  
 TES08820  
 TES08830  
 TES08840  
 TES08850  
 TES08860  
 TES08870  
 TES08880  
 TES08890  
 TES08900  
 TES08910  
 TES08920  
 TES08930  
 TES08940  
 TES08950  
 TES08960  
 TES08970  
 TES08980  
 TES08990  
 TES09000  
 TES09010  
 TES09020  
 TES09030  
 TES09040  
 TES09050  
 TES09060  
 TES09070  
 TES09080  
 TES09090  
 TES09100  
 TES09110  
 TES09120

```

C      45 IF(BIGA) 48,46,48
      46 D=0.000
      RETURN
      48 DC 55 I=1,N
      IF(I-K) 50,55,50
      50 IK=NK+I
      55 A(IK)=A(IK)/(-BIGA)
      CCNT INUE
C      REDUCE MATRIX
      DC 65 I=1,N
      IK=NK+I
      HCLD=A(IK)
      IJ=I-N
      DC 65 J=1,N
      IJ=IJ+N
      IF(I-K) 60,65,60
      IF(J-K) 62,65,62
      60 KJ=IJ-I+K
      62 A(IJ)=HOLD*A(KJ)+A(IJ)
      65 CCNT INUE
C      DIVIDE FCW BY PIVCT
      KJ=K-N
      DC 75 J=1,N
      KJ=KJ+N
      IF(J-K) 70,75,70
      70 A(KJ)=A(KJ)/BIGA
      75 CCNT INUE
C      PRODUCT CF PIVCTS
      C=D*BIGA
C      REPLACE PIVOT BY RECIPROCAL
      A(KK)=1.0/BIGA
      80 CCNT INUE
C      FINAL ROW AND CCLUMN INTERCHANGE
      K=N
      100 K=(K-1)
      105 IF(K) 150,150,105
      I=L(K)
  
```

```

108 IF(I-K) 12C,120,1C8
    IC=N*(K-1)
    JR=N*(I-1)
    DO 110 J=1,N
    JK=JQ+J
    HLLD=A(JK)
    JI=JR+J
    A(JK)=-A(JI)
    A(JI) =HOLD
110 J=M(K)
120 IF(J-K) 10C,100,125
125 KI=K-N I=1,N
    KI=KI+A
    HCLD=A(KI)
    JI=KI-K+J
    A(KI)=-A(JI)
130 A(JI) =HOLD
150 GC TO 100
15C RETURN
    CENIFY

```

```

TESO9130
TESO9140
TESO9150
TESO9160
TESO9170
TESO9180
TESO9190
TESO9200
TESO9210
TESO9220
TESO9230
TESO9240
TESO9250
TESO9260
TESO9270
TESO9280
TESO9290
TESO9300
TESO9310
TESO9320
TESO9330
TESO9340

```

## LIST OF REFERENCES

1. Stallard, D. V., "An Approach to Optimal Guidance for a Bank-to-Turn Missile," Proceedings of AIAA Guidance and Control Conference, Danvers, Mass., August 1980.
2. Kwakernaak, H. and Sivan, R. Linear Optimal Control Systems, Wiley-Interscience, 1972.
3. Bryson, A. E. and Ho, Y. C. Applied Optimal Control, Halsted Press, 1975.

## INITIAL DISTRIBUTION LIST

		No. Copies
1.	Defense Technical Information Center Cameron Station Alexandria, Virginia 22314	2
2.	Library, Code 0142 Naval Postgraduate School Monterey, California 93943	2
3.	Department Chairman, Code 67 Department of Aeronautical Engineering Naval Postgraduate School Monterey, California 93943	1
4.	Professor D.J. Collins, Code 67Co Department of Aeronautical Engineering Naval Postgraduate School Monterey, California 93943	3
5.	Professor H. A. Titus, Code 62Ts Department of Electrical Engineering Naval Postgraduate School Monterey, California 93943	1
6.	Office of The Air Attache Brazilian Embassy 3006 Massachusetts Av NW Washington DC 20008	3
7.	Centro Tecnico Aeroespacial Rua Paraibuna S/N 12200 Sao Jose dos Campos - SP Sao Paulo, BRAZIL	1
8.	Centro Tecnico Aeroespacial Instituto de Atividades Espaciais Rua Paraibuna S/N 12200 Sao Jose dos Campos - SP Sao Paulo, BRAZIL	2
9.	Centro Tecnico Aeroespacial Instituto de Atividades Espaciais Divisao de Sistemas Belicos Rua Paraibuna S/N 12200 Sao Jose dos Campos - SP Sao Paulo, BRAZIL	2
10.	MAJ Carlos A. L. Velloso Centro Tecnico Aeroespacial Instituto de Atividades Espaciais Rua Paraibuna S/N 12200 Sao Jose dos Campos - SP Sao Paulo, BRAZIL	3

LAND

FILMED

DTIC